Development of a bead-in-matrix delivery system for insulin

C Strydom

orcid.org/ 0000-0002-4012-4820

B.Pharm

Dissertation submitted in partial fulfilment of the requirements for the degree Magister Scientiae in Pharmaceutics at the North-West University

Supervisor: Prof JH Steenekamp

Co-supervisor: Prof JH Hamman

Graduation May 2018

Student number: 22793372

ACKNOWLEDGEMENTS

To the **Lord, our Saviour**, thank you for the strength and determination to complete this dissertation to the best of my ability.

Jos Strydom, my father, **Mariana Strydom**, my mother and **Bernice Strydom**, my sister, thank you for your loving support and encouragement throughout all of my studies. I wouldn't be able to complete my studies without you. I love you.

JP Annandale, my husband, thank you for your unwavering love and support during this journey and also trying to help, even if only to listen to me ranting. "Ek is bitter baie lief vir jou". Thank you for being my number one cheerleader.

Prof. Jan H. Steenekamp, my supervisor, thank you for your guidance throughout this journey. Thank you for always being prepared to listen even if it is not work related. I truly couldn't ask for a better supervisor and mentor.

Prof. Josias H. Hamman, my co-supervisor, thank you for your time, effort and advice. It was a privilege to work with you.

Prof. Jan du Preez, thank you for assisting me with the HPLC.

Dr. Liezl Badenhorst, thank you for always having an ear willing to listening. Thank you for motivating me whenever I needed motivation.

My friends, Anja, Corneli, Nita and Zenobia to name a few, thank you for being the best friends anyone could ask for, for your support and for making this journey one to remember. Thank you for making life colourful.

My colleagues, Alandi, Chantelle and Mandi, thank you for your support and always willing to help.

To the **North-West University** for the financial contribution towards my studies.

ABSTRACT

The oral route remains the most convenient and popular route for drug administration. However, for therapeutic peptide drugs, parenteral administration remains the most used route of administration as the use of the oral route for protein and peptide drugs being hindered by pre-systemic enzymatic degradation and low intestinal epithelial permeability. To overcome the low intestinal epithelial permeability, a safe and effective absorption enhancing agent can be included in the dosage form. Previous studies found that *Aloe vera* gel, sodium deoxycholate and *N*-trimethyl chitosan chloride (TMC) had the ability to increase drug transport across *in vitro* intestinal epithelial models.

The aim of this study was to prepare a bead-in-matrix delivery system comprising of micro-beads containing insulin loaded into macro-beads containing an absorption enhancer. Three different absorption enhancers, namely *A. vera* gel, sodium deoxycholate and TMC at two different concentration levels (0.5% and 1% w/w) were investigated. Based on the experimental variables, 18 bead-in-matrix formulations were prepared in total. The bead-in-matrix delivery systems were designed in such a way that the absorption enhancer in the macro-beads could reach the site of absorption first, in order to open the tight junctions to facilitate the paracellular transport of insulin contained in the micro-beads.

The bead-in-matrix delivery systems were characterised in terms of insulin content (assay), weight variation, particle size, dissolution behaviour and the ability to deliver insulin across porcine intestinal tissue. Electron microscopy indicated that micro-beads could be successfully enclosed within macro-beads resulting in a bead-in-matrix delivery system. In an effort to investigate the possibility to limit insulin release and in effect protect it from an acidic environment, the bead-in-matrix delivery systems were successfully coated with a mixture of Eudragit® L100 and Eudragit® S100 to produce enteric coated delivery systems. Dissolution studies indicated that the enteric coating limited insulin release in an acidic environment and complete insulin release was illustrated at a pH of 6.8 within 150 min for all bead-in-matrix delivery systems. All the bead-in-matrix delivery systems exhibited similar drug release patterns. Transport data indicated that the absorption enhancers (i.e. *A. vera* gel, sodium deoxycholate and TMC) in all bead-in-matrix formulations successfully facilitated the paracellular transport of insulin. The most effective absorption enhancer in this study was *A. vera* gel.

Key words: absorption enhancer, *Aloe vera* gel, extrusion-spheronisation, insulin, oral route sodium deoxycholate, TMC

TABLE OF CONTENTS

LIST OF TABLES (HEADING 0)

LIST OF FIGURES (HEADING 0)

LIST OF ABBREVIATIONS

%RSD	Percentage relative standard deviation
3D	Three dimensional
BCS	Biopharmaceutics Classification System
BP	British Pharmacopoeia
FDA	Food and Drug Administration
GI	Gastro-intestinal
HCl	Hydrochloric acid
HPLC	High performance liquid chromatography
KRB	Krebs-Ringer bicarbonate
LOD	Limit of detection
LOQ	Limit of quantification
LY	Lucifer yellow
NaOH	Sodium hydroxide
NWU-RERC	North-West University Research Ethics Regulatory Commitee
P_{app}	Apparent permeability coefficient
PEG	Polyethylene glycolation
P-gp	P-glycoprotein
R^2	correlation coefficient
RME	Receptor-mediated endocytosis
RSD	Relative standard deviation
SD	Standard deviation
SEM	Scanning electron microscopy

TEER	Transepithelial electrical resistance
USP	United States Pharmacopoeia
UV	Ultra violet

CHAPTER 1: INTRODUCTION

1.1 Background and justification

1.1.1 Absorption enhancement of protein and peptide drugs

Therapeutic proteins and peptides such as insulin, growth hormone, interferons, interleukins, blood factors, anticoagulants, and thrombolytics need frequent doses over long periods of time, for the management of chronic diseases (Buchanan & Revell, 2015:172; Lee, 2002:572). The oral administration of therapeutic proteins and peptides is challenging due to their high molecular weight, hydrophilicity and susceptibility to enzymatic inactivation in the gastrointestinal tract (Salamat-Miller & Johnston, 2005:201). Commercially available protein formulations are delivered via the parenteral route (such as injections) due to poor bioavailability, poor stability and short-plasma half-life (Hassani *et al*., 2015:12; Renukuntla *et al*., 2013:76).

The oral route is considered by most as the preferred route to administer medication. Oral administration presents many advantages over the parenteral route of administration. These advantages include better patient comfort, ease of administration and decreased medical costs (Kristensen 2013:365; Lee, 2002:572). Manufacturing and administering advantages include no need for sterile manufacturing conditions with reduced production costs and the avoidance of discomfort, pain and infections normally associated with injections (Fasano, 1998:1351).

For the successful delivery of protein and peptides via the oral route, there are many barriers that have to be overcome. These barriers include enzymatic and chemical degradation, hydrophilic characteristics and poor permeability across intestinal mucosa (Chen *et al*., 2009:587; Hamman *et al.,* 2005:167). To reduce the impact of the intestinal barriers, different pharmaceutical strategies have been recommended to maximize bioavailability of protein and peptide drugs. These strategies include chemical modification of the proteins and peptides, special drug delivery systems, targeted delivery, co-administration of enzyme inhibitors and absorption enhancers (Hamman *et al.,* 2005:167; Whitehead *et al.,* 2004:37).

The oral delivery of protein and peptide drugs is hampered by a number of barriers. These barriers include enzymatic and chemical degradation, poor aqueous solubility, low intrinsic membrane permeability (Chen *et al.,* 2009:587). A major problem associated with drug absorption enhancing agents is the damage to the intestinal epithelium. However, certain absorption enhancing agents have the ability to increase the intestinal absorption in a reversible way without causing serious or lasting toxic effects. This has sparked renewed interest in safe and effective oral drug absorption enhancement (Whitehead *et al.,* 2008:128).

1.1.2 *Aloe vera* leaf material as an absorption enhancers

Aloe vera (*A. vera*) (L.) Burm.f (*Aloe barbadenis Miller*) leaf gel contains different phytochemical substances, which include minerals, enzymes, polysaccharides, water- and fat soluble vitamins, organic acids and phenolic compounds. The *A vera* gel has some therapeutic properties attributed to polysaccharides. These properties include the promotion of radiation damage repair, anti-bacterial, anti-viral, anti-fungal, anti-diabetic, anti-neoplastic, immuno-stimulating, anti-inflammatory and anti-oxidant effects. With regard to drug absorption, *A vera* gel and whole leaf liquid preparations significantly increased the overall extend of absorption of both vitamins C and E in humans after oral administration (Beneke *et al.*, 2012:476; Vinson *et al.,* 2005: 761).

In vitro studies on *A vera* have shown that both the gel and whole leaf extract were able to significantly reduce the transepithelial electrical resistance (TEER) of Caco-2 cell monolayers and thereby showed the ability to open tight junctions (Radha & Laxmipriya, 2015:23; Chen *et al.*, 2009:592). The TEER is a measurement of tight junction integrity between adjacent intestinal cells. Opening of tight junctions will reduce the TEER of the intestinal epithelium, because of the increasing flow of ions through the intercellular spaces (Beneke *et al.*, 2012:479).

1.1.3 Bile salt as absorption enhancer

The amphipathic steroidal bio-surfactants, also known as bile salts, are derived from cholesterol in the liver. They have been widely used as absorption enhancers to increase drug transport across biological barriers such as the intestinal membrane (Moghimipour *et al.*, 2015:14451). Bile salts enhance drug permeation through biological membranes by interacting with the phospholipids in cell membranes (Moghimipour *et al.*, 2015:14457).

Sodium deoxycholate (bile salt) has been used as an absorption enhancer for drugs administered via different routes, including the oral route. It is generally considered that bile salts act as absorption enhancers due to the membrane destabilising activities of these agents (Li, 2016:2). It has been postulated that the formation of calcium complexes by bile salts may be linked to the increase in paracellular drug movement (Lillienau *et al*., 1992:421). It was shown in a previous study that lowering the concentration of free calcium in the extracellular environment may affect the integrity of intercellular tight junctions (Michael *et al*., 2000:139). Notable disadvantages of bile salts are that they cause irreversible damage to the mucosa and are ciliotoxic. It has been reported that dihydroxy bile salts are more toxic than trihydroxy bile salts (Moghimipour *et al.,* 2015:14463).

1.1.4 Chitosan as absorption enhancer

The non-toxic, biocompatible and biodegradable features of chitosan render it as a good candidate as an absorption enhancer in the development of novel gastrointestinal (GI) drug delivery systems (Hejazi & Amiji, 2003:151; Tozaki *et al.*, 1997:1016). Chitosan is soluble in an acidic environment, due to protonation, but exhibits poor solubility in neutral and alkaline environments (Hejazi & Amiji, 2003:160). The mechanism by which chitosan act as an absorption enhancer, is linked to the opening the tight junctions between epithelial cells and allowing the paracellular transport of hydrophilic and macromolecular compounds (Jonker *et al.*, 2002:206). Chitosan has long been used to improve the uptake of proteins across the epithelial tissue, mainly because of its muco-adhesive and tight junction modulating properties and because of its low toxicity (Wallis *et al.*, 2014:1092).

1.1.5 *N*-trimethyl chitosan chloride as absorption enhancer

N-trimethyl chitosan chloride (TMC) was synthesised to overcome the insoluble nature of chitosan in alkaline environments (Hejazi & Amiji, 2003:160). *N*-trimethyl chitosan chloride shows a higher solubility over a wider pH range and has been shown to open the paracellular pathway without causing damage to the cell membranes (Caeamella *et al.,* 2010:7). It reversibly interacts with components of tight junctions; this interaction leads to the opening of the paracellular route. The mechanism of enhancing intestinal permeability is similar to that of protonated chitosan (Thanou *et al.,* 2001:S91). *N*-trimethyl chitosan chloride can increase the absorption of hydrophilic and macromolecular drugs such as insulin (Jonker *et al.*, 2002:206).

1.1.6 Beads in multiple-unit dosage forms

Multiple-unit dosage forms contain a number of sub-units, each containing a certain portion of the total drug dose. Multiple-unit dosage forms have several advantages over single-unit dosage forms such as a more predictable and reproducible GI transit time, more consistent blood levels and improved bioavailability, less GI disturbances and greater product safety (Patwekar & Baramade, 2012:578; Atyabi *et al*., 2005:40). The more predictable and reproducible GI transit time of multiparticulate drug delivery systems are related to the fact that gastric emptying of multiparticulates are less variable compared to conventional single-unit dosage forms. If sub-units have a diameter of less than 2 mm, they are able to leave the stomach continuously; even if the pylorus is closed (Dey *et al*., 2008:1068). Beads are spherical pellets used in multiple-unit oral dosage forms such as filled hard-gelatine capsules or tablets. Different techniques may be used to manufacture beads such hot melt extrusion, granulation, layer-by-layer techniques and extrusion-spheronisation of which extrusion spheronisation is one of the most popular methods (Mallipeddi *et al*., 2010:54).

1.2 Problem statement

Peptide/protein therapeutics are potent drugs, however, administration is currently limited to the parenteral route despite the fact that these therapeutics are frequently used for chronic therapy. These therapeutics are usually administered by the parenteral route as a consequence of their low oral bioavailability, which is partly due to poor membrane permeation. The problem to be solved is to find an effective solid oral dosage form that can deliver peptide drugs such as insulin across the intestinal epithelium after oral administration. Combination of peptide drugs such as insulin with an absorption enhancer within a multiple-unit dosage form offers an attractive possibility with potential to improve the oral bioavailability of peptide/protein drugs.

1.3 Aims and objectives

1.3.1 General aim

The aim of this study is to develop and evaluate a multiple-unit bead-in-matrix dosage form containing an absorption enhancer (see Figure 1.1 for schematic illustration) for the delivery of a peptide drug. The multiple-unit dosage form consisted of micro-beads loaded into macro-beads, which were loaded into hard gelatine capsules. The micro-beads contained the active ingredient (i.e. insulin) and the macro-beads contained the micro-beads together with an absorption enhancer (i.e. *A. vera* gel or sodium deoxycholate or TMC). The dosage form was designed in such a way to release the drug absorption enhancer immediately after administration from the macro-beads to open the tight junctions followed by a delayed release of the insulin from the micro-beads.

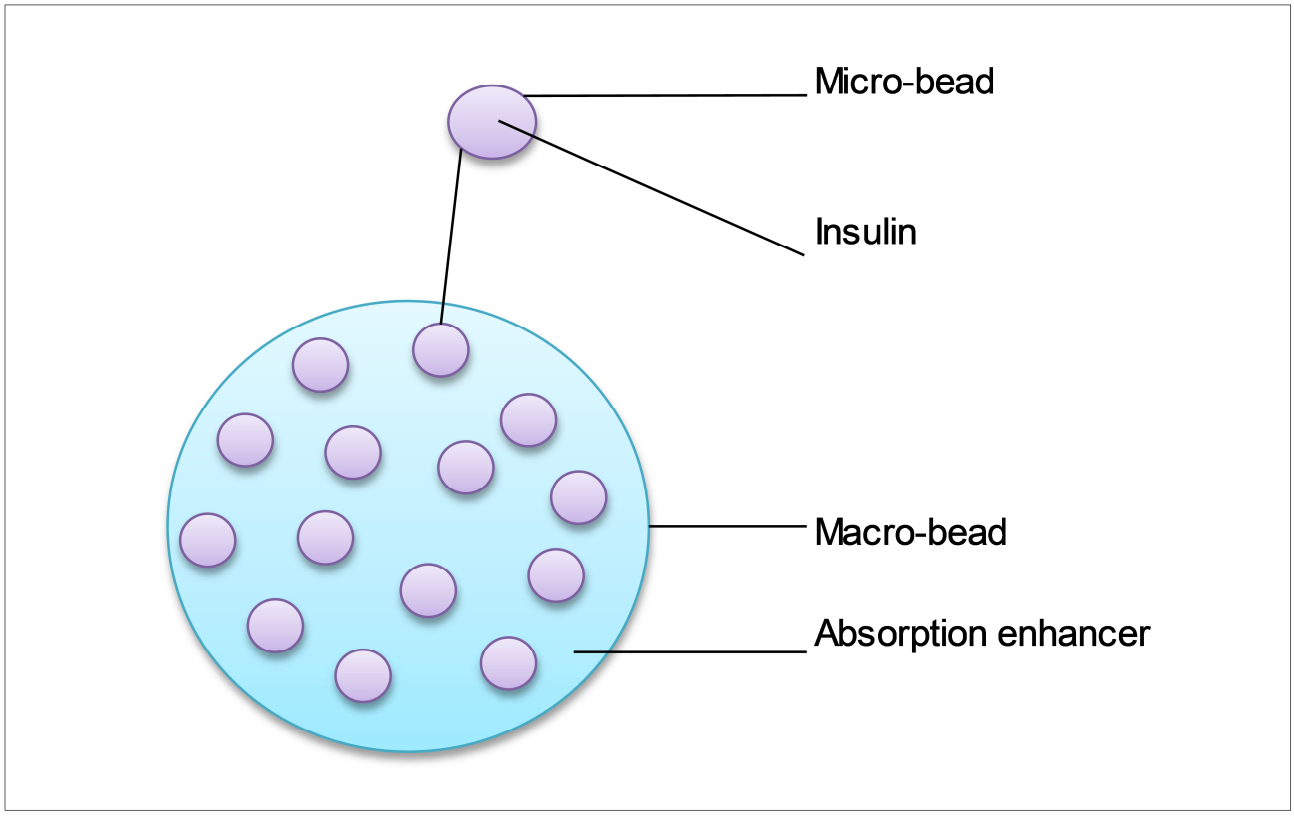

Figure 1.1: Schematic illustration of the bead-in-matrix delivery system to be developed in this study

1.3.2 Specific objective

The following objectives were set for the study:

- To prepare micro-beads (0.5 mm diameter) by means of extrusion-spheronisation containing insulin (0.01%) as active ingredient and a filler (Pharmacel®).
- To prepare macro-beads (2.5 mm) containing the micro-beads (in different concentrations) and an absorption enhancer (*A. vera* gel, TMC or sodium deoxycholate).
- To characterise the bead-in-matrix delivery system in terms of size, size distribution, morphology, drug content, and drug release.
- Conduct *ex vivo* drug transport studies to evaluate the bead-in-matrix delivery system's ability to deliver insulin across excised intestinal pig tissue in a Sweetana-Grass diffusion model.

- To validate a high performance liquid chromatography method to analyse samples for insulin content.

1.4 Design of the study

In this study, the permeation of a model drug (i.e. insulin) was manipulated by formulation of chemical absorption enhancers in bead-in-matrix solid oral dosage forms. Control groups were included to eliminate the effect of chance interferences. The bead formulations containing different selected absorption enhancers were each be combined with beads containing different amounts of insulin to prepare bead-in-matrix drug delivery systems as outlined in Table 1.1.

Table 1.1: Composition of bead-in-matrix drug delivery systems

		Absorption enhancer and concentration					
		Aloe vera		Sodium deoxycholate		TMC	
		Concentration (% w/w)		Concentration (% w/w)		Concentration (% w/w)	
		0.5	1	0.5	1	0.5	1
Conc. of micro-beads (%)	20	A	B	C	D	E	F
	40	G	H	I	J	K	L
	60	M	N	O	P	Q	R

Each bead-in-matrix formulation were evaluated not only in terms of physical properties, but also in terms of insulin delivery performance across excised pig intestinal tissues in an *in vitro* diffusion model.

1.5 Layout of dissertation

Chapter 1 delivers a brief overview of the background, the research problem and a summary of the motivation for the research undertaken in this study. Chapter 2 is a review of related and applicable literature, placing the research project in the context of oral protein and peptide drug delivery. Chapter 3 outlines the experimental and statistical methods used. Chapter 4 conveys the results and discussions. Chapter 5 details the final conclusions and is discussed along with recommendations for future studies.

CHAPTER 2: LITERATURE STUDY

2.1 Introduction

Peptides with a wide range of applications in medicine and biotechnology have emerged during the past few decades. There are currently more than 60 Food and Drug Administration (FDA) approved therapeutic peptides on the market (e.g. vasopressin, somatostatin, calcitonin and growth factors (Renukuntla *et al.,* 2013:75)). The number of peptide containing medicinal products is expected to grow remarkably, with approximately 140 therapeutic peptides under investigation in clinical trials and more than 500 therapeutic peptides in pre-clinical development. Given their attractive pharmacological profile and intrinsic properties, peptides represent an interesting starting point for the design of novel drugs. The interest in peptide therapeutics may be attributed to their specificity that translates to excellent safety, tolerability and efficacy profiles in humans (Fosgerau & Hoffman, 2015: 122).

Clinical use of peptides as therapeutic agents is hampered by their high molecular weight and hydrophilic characteristics, which lead to relatively low oral bioavailability. This is also the basis for the class III classification for this group of therapeutic agents by the Biopharmaceutics Classification System (BCS) (Wallis *et al.,* 2014:1087; Brayden & Maher, 2010:5). The oral bioavailability of peptide drugs rarely exceeds 1 – 2% (Renukuntla *et al.,* 2013:75; Carino & Mathiowitz, 1999:250). This is one of the main reasons why around 75% of all peptide drugs are formulated in injectable dosage forms (Fosgerau & Hoffman, 2015: 122). However, patients find injections both unpleasant and difficult to self-administer (Hamman *et al.,* 2005:166), leading to a need for less invasive treatment options.

Oral administration of therapeutic proteins or peptides such as insulin, represent one of the greatest challenges in modern pharmaceutical technology (Niu *et al.,* 2014:119). Poor absorption after oral administration can be attributed to extensive hydrolysis by the proteolytic enzymes in the GI tract and/or poor membrane permeability characteristics (Tozaki *et al*., 1997:1016). Oral delivery of insulin will mimic the natural physiological release pattern more closely and will improve patient compliance as well as patient acceptability. It will also exclude pain, discomfort and infections associated with injections (Mansuri *et al.,* 2016:161; Soarse *et al.,* 2012:122; Lee 2002:572).

Different approaches have been followed in an attempt to overcome the obstacles associated with poor oral peptide delivery. These approaches include the use of absorption enhancers, enzyme inhibitors, hydrogels, muco-adhesive systems, liposomes, nanoparticles, microparticles, chemical modification, pro-drug development, targeting of membrane transporters and cell penetrating peptides (Renukuntla *et al.,* 2013:85-89).

2.2 Drug absorption from the GI tract

The GI tract is designed to prevent the entry of toxins, pathogens and undigested macromolecules, while concurrently digesting and absorbing nutrients like amino acids, sugars, vitamins and co-factors. The intestinal mucosa uses biochemical and physiological mechanisms to complement the physical barrier against protein absorption resulting in poor bioavailability (Renukuntla *et al.,* 2013:75; Daugherty & Mrsny, 1999a:144). Furthermore, the large molecular size and hydrophilic nature of peptide and protein drugs increase the bioavailability problems (Zhou & Li Wan Po, 1991a:97-98; Banga & Chein, 1988:19-20).

Drug molecules can move across the intestinal epithelium by using one of two main pathways namely transcellular transport (see Figure 2.1), which involves the transport of molecules through the cell membranes and paracellular transport (see Figure 2.1), which involves the passive transport of molecules through the intercellular spaces between adjacent cells of the intestinal epithelium (Lemmer & Hamman, 2013:103; Widmaier *et al.,* 2008:114; Salama *et al.,* 2006:16). The predominant pathway for drug transport or absorption depends on the physicochemical characteristics of the drug as well as the membrane features. Generally, lipophilic drugs cross the intestinal epithelium by means of the transcellular pathway, while hydrophilic drugs cross the intestinal epithelium via the paracellular transport pathway (Salama *et al.,* 2006:16).

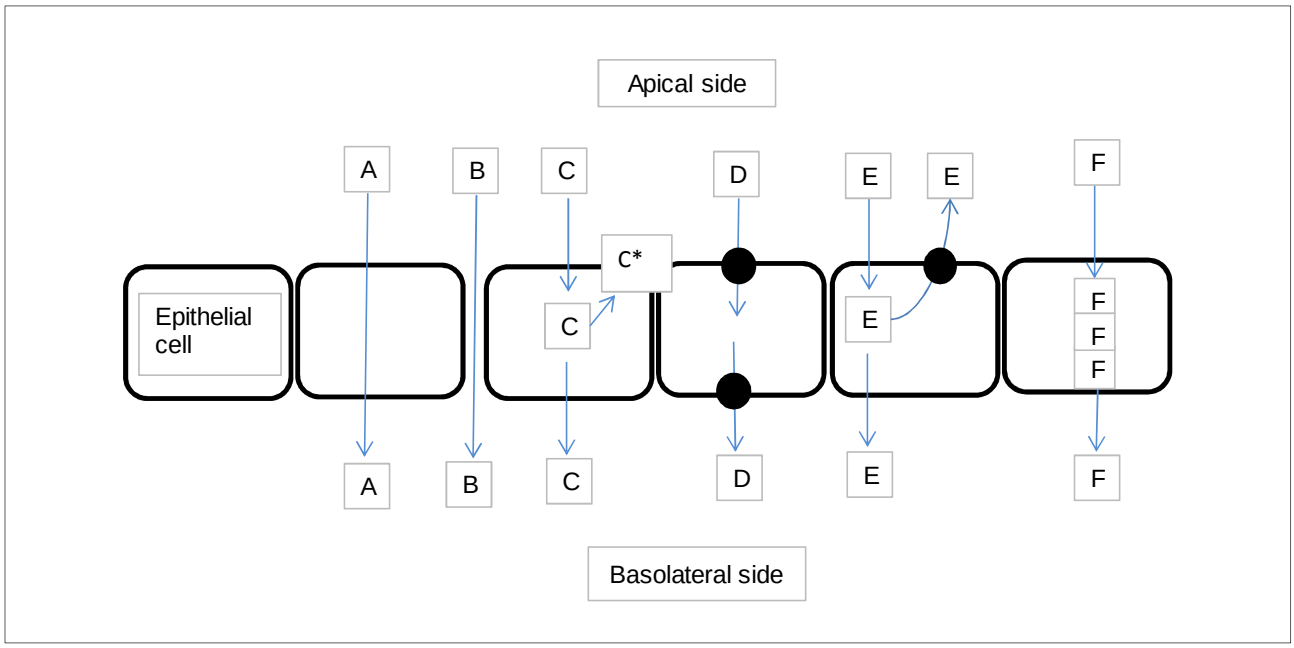

Figure 2.1: Pathways of intestinal drug absorption. **A** transcellular diffusion (e.g. thyrotropin-releasing hormone); **B** paracellular diffusion enhanced by a modulator of the tight junctions; **C** transcellular passive diffusion with intracellular metabolism (C*); **D** carrier-mediated transcellular transport (e.g.

captopril); **E** transcellular diffusion modified by an apically polarized efflux mechanism (e.g. cyclosporin); **F** transcellular vesicular transport (including non-specific fluid-phase endocytosis or receptor-mediated transcytosis) [reproduced from Hamman *et al.,* 2005:167]

2.2.1 Transcellular pathway

Transcellular transport is the movement of molecules across the epithelia by moving through the cells (see Figure 2.1). Transcellular transport needs a distinct interaction between the drug and the membrane. This transport depends on the molecule's interaction with the lipid bilayer and the interaction with different integral and peripheral membrane proteins (Pauletti *et al.,* 1996:8). This absorption or uptake can take place through diffusion, pinocytosis or carrier mediation (Lui *et al.,* 2009:267).

2.2.1.1 Passive diffusion

Passive diffusion is the process by which drug molecules move from an area of high concentration on one side of the biological membrane, through the lipid bilayer, to an area of low concentration on the other side of the biological membrane. Diffusion is concentration-and temperature dependent (Backes 2007:1; Shagel *et al.,* 2005:252). Passive diffusion can be described by Fick's law of diffusion (Equation 2.1).

$$\frac{dQ}{dt} = \frac{DAK}{h}(C_{gi}\text{-}C_p) \qquad \text{Equation 2.1}$$

where: $\frac{dQ}{dt}$ = rate of diffusion

D = diffusion coefficient

K = lipid-water partition coefficient

A = surface area of membrane

h = membrane thickness

C_{gi}-C_p = difference between concentrations of the drug in the GI tract and blood, respectively.

From Equation 2.1 it is clear that there are several factors that influence the diffusion of drugs. One of these factors is lipid solubility. The partition coefficient represents the lipid-water

partitioning of a drug. More lipid-soluble drugs will have a higher K-value. Lipid soluble molecules cross cell membrane more easily than water soluble molecules (Shargel *et al.,* 2005:253; Shargel & Yu, 1999:101-103).

2.2.1.2 Carrier-mediated transport

Certain drug molecules and many nutrients are absorbed through the transcellular pathway by a carrier-mediated mechanism (the carrier/transporter is responsible for binding a drug molecule and transporting it across the membrane) of which there are two primary types namely, active transport and facilitated transport. On the surface of the apical cell membrane of a columnar absorption cell, the drug molecule forms a complex with the carrier. The drug-carrier complex then moves across the membrane and liberates the drug on the other side of the membrane. The carrier returns to the initial position on the apical surface of the cell membrane adjacent to the gastro-intestinal tract lumen to await the arrival of another drug molecule to be transported (Aulton 2007:281; Shargel *et al.,* 2005:379).

2.2.1.2.1 Active transport

Active transport is a carrier-mediated movement of molecules across the membrane of a cell requiring energy, that allows the cell to admit otherwise impermeable molecules against a concentration gradient. Furthermore, this transport process is saturable and subject to competitive inhibition (Brooker, 2010:30, Aulton 2007:282, Shargel *et al.,* 2005:379-380). Protein and peptide drugs are usually not recognised by an active transport system; an exception is drugs that are recognized by the di-peptide (e.g. carnosine, anserine) or tri-peptide (e.g. leupeptin, melanostatin) transporter system in the GI tract (Rekukuntla *et al.,* 2013:78).

2.2.1.2.2 Facilitated diffusion or transport

Facilitated diffusion or transport, similar to active transport, is a carrier-mediated process. However, it differs from active transport in that it does not involve the transfer of drug molecules against a concentration gradient. This transport, therefore, does not require energy to take place. When substances are transported by facilitated diffusion, they are transported down the concentration gradient but at a much faster rate than would be anticipated based on the molecular size and polarity of the molecule. This process is saturable and is subject to competitive inhibition (Grassl, 2012:154; Aulton 2007:282; Shargel *et al*., 2005:380).

2.2.1.3 Endocytosis

Endocytosis can be defined as the uptake of material by a cell from the environment by invagination of the cell's plasma membrane, which can happen through either phagocytosis or

pinocytosis (Brooker, 2010:635, Aulton 2007:283). Endocytosis depends on energy to help the uptake process where the invaginated material is transferred to lysosomes or vesicles. The contents of some vesicles bypass enzymatic digestion and are transferred to the basolateral membrane of the cell, where the material then undergoes exocytosis (discharge of particles from a cell that are too large to diffuse through the wall (Brooker 2010:681, Aulton 2007:283)). Endocytosis can further be arranged into receptor-mediated endocytosis, transcytosis and phagocytosis (Silverstein *et al*., 1977:673).

2.2.1.3.1 Receptor-mediated endocytosis

Receptor-mediated endocytosis (RME) is a common mechanism by which animal cells internalize a variety of selected extracellular materials associated with their specific receptors. Materials include peptide hormones, growth factors, cytokines, plasma glycoproteins, lysosomal enzymes, toxins and viruses (Sato *et al.,* 1996:446). Receptor-mediated endocytosis is activated by the binding of a specific macromolecule to a surface receptor on the cell membrane (Washington *et al*., 2001:16). The ligand-bound receptors cluster in discrete regions called coated pits, which invaginate into the cell to form endocytotic vesicles or endosomes. The ligand and receptor dissociate at an acidic pH (pH 5 – 5.5) within the endosomes. The internalized receptors commonly recycle back to the cell surface for more binding, while the internalized ligand is sorted and delivered to lysosomes for degradation, for the most part (Aulton 2007:283; Sato *et al.,* 1996:446).

2.2.1.3.2 Pinocytosis

Pinocytosis (also known as fluid-phase endocytosis) can be described as the immersion of small droplets of extracellular fluid by the membrane vesicles. Molecules absorbed by pinocytosis include the fat-soluble vitamins A, D, E and K, small particles (such as lipoproteins, colloids and immune complexes), low molecular weight solutes, fluids, and soluble macromolecules (such as antibodies, enzymes and hormones) (Aulton 2007:283; Washington *et al.,* 2001:15; Shargel Yu, 1999:107 and Silverstein *et al*., 1977:673).

2.2.1.3.3 Phagocytosis

Phagocytosis can be defined as the engulfment (of particles larger than 500 nm) by the cell membrane (extensions of the plasma membrane called pseudopodia fold) of certain cells (Widmaier *et al.,* 2008:112; Aulton, 2007:283; Ball, 2004:76). Most cells undergo pinocytosis, and only a few special types of cells, such as those of the immune system, carry out phagocytosis (Widmaier *et al.,* 2008:112). Phagocytosis explains the process that facilitates the absorption of some vaccines, including the polio vaccine, from the GI tract (Ashford, 2007a:283; Silverstein *et al*., 1977:673).

2.2.1.3.4 Transcytosis

Transcytosis can be defined as the active process that allow materials such as vitamins, macromolecules and ions to be transported in a vesicle through the cell and secreted on the opposite side (Aulton, 2007:283; Di Paquale & Chiorini, 2006:506). This transport represents a potential useful pathway for the mucosal transport of protein and peptide drugs as this route avoids the enzymatic breakdown of the molecules (Hamman, 2007:101; Baker *et al.,* 1991:371). Transcytosis is likely to be discriminatively receptor-mediated, but in the fluid stage of the vesicles it may many times be non-discriminative (Di Paquale & Chiorini, 2006:506).

2.2.2 Paracellular pathway

Unlike lipophilic drug molecules, the passive transcellular pathway is not the primary transport pathway for most polar compounds as their lack of lipophilic properties restricts transport via passive diffusion across the cell membrane. However, polar compounds may be transported via the intercellular spaces and tight junctions between cells (Shargel *et al.,* 2005:373). This movement between adjacent cells through the intercellular spaces represents the paracellular pathway. Paracellular permeability is regulated by intercellular junctional complexes (Lemmer & Hamman, 2013:103). The paracellular route is the favoured route of transport by compounds with low molecular weight and hydrophilic characteristics. Although protein and peptide molecules are hydrophilic in nature with a LogP value < 0, they are also relatively large molecules (Renukuntla *et al.,* 2013:77; Morishita & Peppas, 2006:905).

The paracellular pathway represents an aqueous extracellular space separating adjacent cells in the GI tract. To use the paracellular pathway substances need to be transferred across a region of packed, hydrophobic intracellular proteins in between intestinal epithelial cells under the brush border that forms a continuous absorption barrier known as the ‘tight junction’ complex (Hamman *et al*., 2005:167; Lappierre, 2000:255). Tight junctions form an intercellular border (otherwise known as the fence mechanism) reducing or hindering paracellular movement of solutes through the epithelial monolayer (Van Itallie & Anderson, 2014:157; Artursson & Palm*,* 2012:282).

Several strategies to enhance the passage of protein and peptide drug molecules through the GI tract epithelium have been investigated. A study of such strategies groups them into two categories, namely controlling the tight junctions associated with the paracellular pathway and physio-chemical transformation of the drug molecules (Salamat-Miller & Johnston, 2005:203).

2.2.2.1 Tight junctions

The epithelial cells of the GI tract are clustered together by intercellular junctional complexes that are classified as the tight junctions (zonula occludens), the adherence junctions (zonula adherens) and the desmosomes (macula adherens) that are located the closest to the basolateral side (Van Itallie & Anderson, 2014:157; Salamat-Miller & Johnston, 2005:203). As mentioned before, the tight junctions form a network that simulates a continuous belt around the epithelial cells that seals the intercellular spaces and regulates paracellular movement of solutes (Salamat-Miller & Johnston, 2005:203).

Tight junctions are selectively permeable for certain small hydrophilic molecules (e.g. ions, nutrients and certain drugs) and function as both 'gate' and 'fence'. The gate function controls the passive diffusion of fluid, electrolytes, macromolecules and cells through the paracellular route. The fence function maintains the polar distribution of the plasma membrane proteins in the apical and basolateral domain (Hamman *et al.,* 2005:167; Thanou *et al.,* 2001:S93). The separation between the apical and basolateral surfaces maintains the functional asymmetry needed to transport material in only one direction across the membrane. It is important to mention that tight junctions are dynamic structures that can be regulated by substances to increase paracellular permeability (Hamman *et al.,* 2005:167).

The change of ion movement across the epithelium through the intercellular spaces can be determined by means of the measurement known as the TEER. TEER demonstrates the level of permeability (leakiness of the tight junctions) of the space between adjacent epithelial cells (Salama *et al.,* 2006:15).

2.3 Limitation to oral bioavailability of peptide drugs

The primary function of the GI tract is to ensure the proper digestion and absorption of nutrients, fluids and electrolytes, which requires a complex of enzymes (e.g. proteases for protein digestion) and unique environments (e.g. from the harsh acidic environment in the stomach to the more basic environment in the intestine, with its villous design to maximise the absorption surface for nutrients). The GI tract epithelium serves as a physical barrier, which protects the body from toxins, antigens and pathogens (Hamman *et al.,* 2005:166). Another important barrier presented by the GI tract is a biochemical barrier namely the first-pass metabolism. First-pass metabolism has a great effect on the bioavailability of certain orally administered drugs (Urbanska *et al.,* 2016:49). Barriers (e.g. physical and biochemical) that may limit the uptake of drugs are illustrated in Figure 2.2. In the development of oral dosage forms for protein or peptide drugs it is important to overcome these obstacles and/or barriers to ensure successful systemic drug delivery (Park *et al.,* 2011:280).

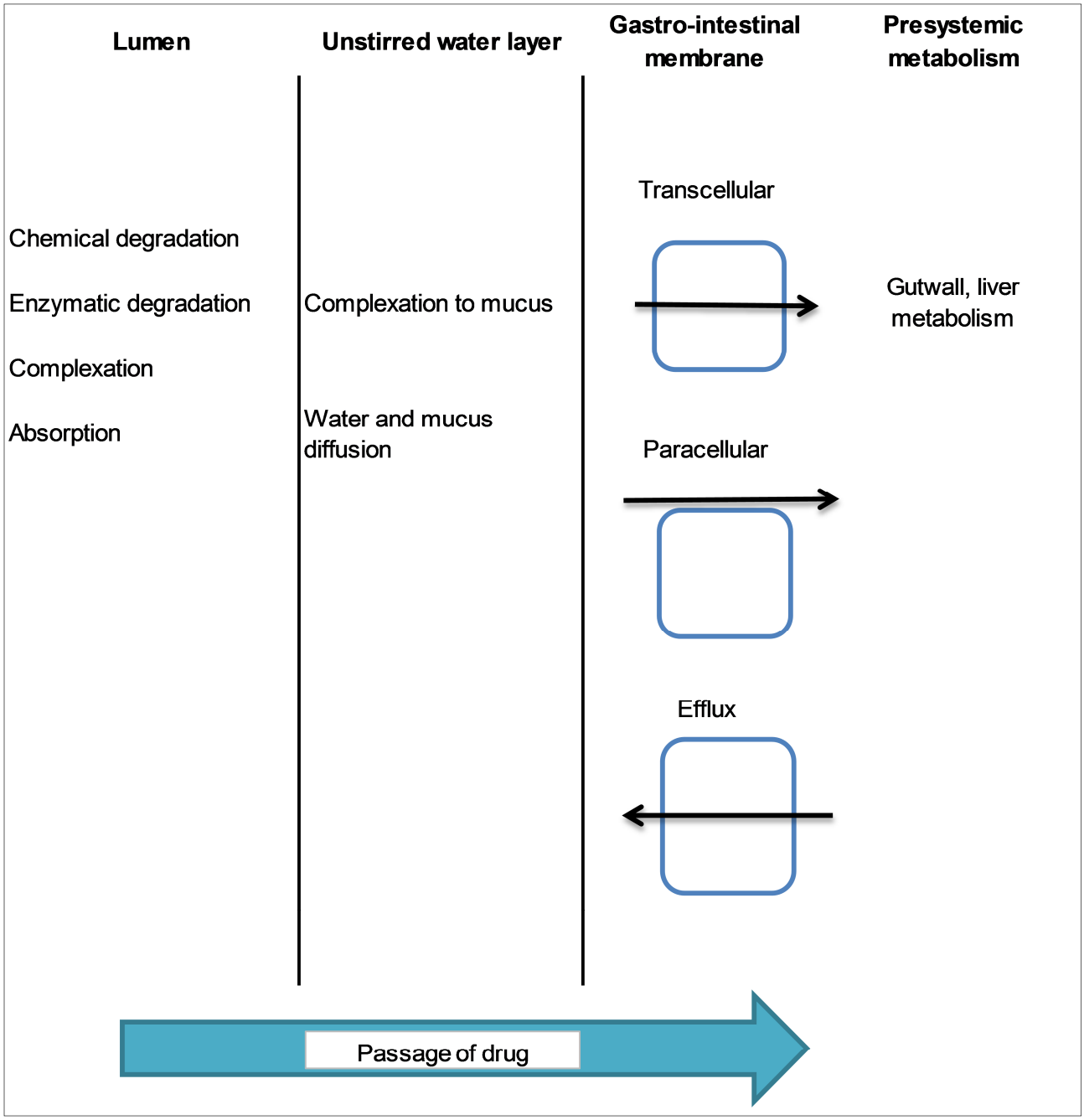

Figure 2.2: Diagram illustrating the barriers to drug absorption from the gastro-intestinal tract (Aulton, 2007:276)

2.3.1 Physical barriers

The physical barriers to absorption and bioavailability include the unstirred water layer, epithelial cell membrane (for transcellular uptake), and the tight junctions (for paracellular uptake) that are positioned between epithelial cells. The efflux transporter systems may also have a role in regulating the absorption of certain substances (Hamman *et al.*, 2005:166).

2.3.1.1 Unstirred water or mucus layer

The surface of the living epithelia is covered with mucus and glycocalyx (see Figure 2.3) to protect the mucosal epithelium (Ensign *et al.,* 2012:559). The main components of the mucous layers include water (up to 95% by weight), mucin (no more than 5% by weight), inorganic salts (about 1% by weight), carbohydrates and lipids (Peppas & Huang, 2004:1676). This gel-like aqueous matrix or mucus layer forms an unstirred water layer creating an aqueous diffusion barrier that may hamper drug permeation. Mucin is released from the goblet cells (representing the second largest population of intestinal epithelium cells), which give rise to a viscous mucous layer on the gut wall (Günther *et al.,* 2014:41; Zhang & Wu 2014:902).

The unstirred water layer is a main drug permeation barrier for actively and passively absorbed solutes (Loftsson, 2012:363; Hamman *et al.,* 2005:167). The access of large molecules such as peptides and proteins to the epithelial surface is restricted by the mucus layer (Hamman *et al.,* 2005:167).

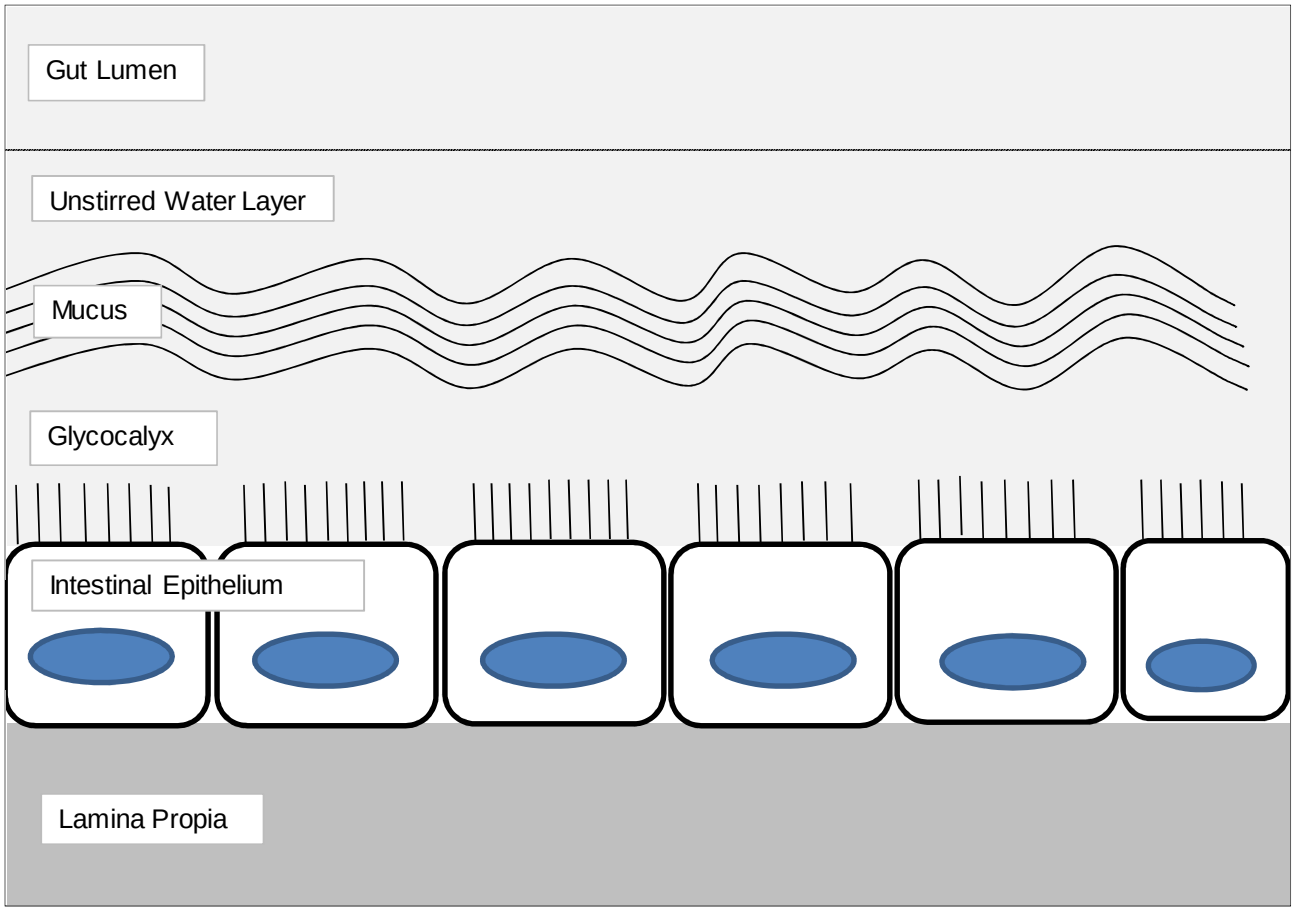

Figure 2.3: Diagram illustrating the mucus layer and glycocalyx (Daugherty & Mrsny, 1999a:146)

2.3.1.2 Epithelial barrier

The gastro-intestinal first line of defence is represented by a single cell layer of intestinal epithelial cells. These epithelial cells are of importance in the host defence by providing a physical barrier with highly specialized innate immune functions (Günther *et al.,* 2014:41).

2.3.1.2.1 Apical cell membrane

The apical epithelial cell membrane consists of a double phospholipid layer. The major lipid elements are phosphatidylcholine, phosphatedylethanolamine, phosphatedylserine, phosphatedylinositol, phosphatidic acid, cholesterol and glycolipids (Washington *et al*., 2006:3-4; Van Hoogdalem *et al.,* 1989:410).

The transport of molecules across the phospholipid bilayer has generally been correlated with their lipophilicity. To cross the phospholipid bilayer, molecules need a certain degree of lipophilicity and a low molecular size (Aulton, 2007:294). Certain hydrophilic molecules like water, ions, di- and tripeptides cross the plasma membrane by other means (e.g. carrier-mediated transport or pores) (Renukuntla *et al.,* 2013:78). For transcellular transport, drugs need to be recognized by a carrier if carrier-mediated transport is to be used or the drugs need to possess the necessary size and lipophilicity to support passive transport (Renukuntla *et al.,* 2013:78). The apical membrane therefore acts as a well regulated barrier to the absorption of large, hydrophilic molecules like peptides and proteins.

2.3.1.2.2 Basal cell membrane

The basal membrane of absorptive cells is about 7 nm thick. The lipid composition of the basal membrane substantially differs from the composition of the apical microvillus membrane. This difference may be the cause for the higher fluidity of the basal cell membrane compared to the apical membrane (Madara & Treir, 1987:1218-1220). A less pronounce barrier function compared to the apical membrane might be caused by the higher fluidity (Van Hoogdalem *et al.,* 1989:411).

2.3.1.3 Capillary wall

Capillaries are directly beneath the intestinal epithelium. The capillaries of the intestinal villi are fenestrated and possess a characteristic asymmetry. Solutes and water can exchange across the cell membrane of the capillary endothelium via small perforations, known as fenestrae, intercellular junctions, pinocytosis and transendothelial channels (Granger *et al.,* 1987:1673-1674). The walls of the intestinal capillaries are not considered as an important barrier to drug absorption (Van Hoogdalem *et al.,* 1989:411).

2.3.1.4 Efflux transporter system

Poor bioavailability of certain drugs, including peptides can be aggravated by efflux transporter systems such as P-glycoprotein (P-gp) in combination with intracellular metabolism (Hamman *et al.,* 2005:167-168). Illustrated in Figure 2.1 E, P-gp is located in the apical surface of the columnar cells (brush border membrane) in the jejunum and actively pumps compounds from within the cell back into the intestinal lumen, thus limiting the absorption of drugs (Aulton 2007:283; Hamman *et al.,* 2005:168; Burton *et al*., 1997:143 and Hunter & Hirst, 1997:129).

2.3.2 Biochemical barriers

Proteolytic enzymes (e.g. pepsin, trypsin and chymotrypsin) throughout the GI tract can deactivate protein and peptide drugs (Dane & Hänninen, 2015:47; Hamman *et al.,* 2005:168). The biochemical barrier is still one of the most important absorption barriers for protein and peptide drugs. Furthermore, enzymatic degradation is very challenging and therefore complex to overcome. This is because of the fact that enzymes are unambiguous and their degradation action takes place at numerous sites (Krishna & Yu, 2007:256).

2.3.2.1 Luminal enzymes

Luminal enzymes are the enzymes present in the gastro-intestinal fluids and include enzymes from pancreatic and intestinal secretions. The principal proteolytic enzyme found in the gastric juice is pepsin. Pepsin and proteases are mainly responsible for the degradation of protein and peptide drugs (e.g. insulin, thyrotropin releasing hormone and phenyl alanine) in the lumen (Gavhane & Yadav, 2012:334; Aulton 2007:277).

Proteolysis starts in the stomach in the presence of pepsin and continues throughout the intestine. Luminal degradation of peptides is due to exposure to enzymes released from the pancreas into the intestine. The most relevant pancreatic proteases are the serine endopeptidases trypsin, alpha chymotrypsin, elastase, and the exopeptidases carboxypeptidase A and B (Hamman & Steenekamp, 2011:76)

2.3.2.2 Brush border membrane bound enzymes and intracellular enzymes

Contact with enzymes associated with the enterocytes such as those in the brush border membrane, cytoplasm and lysosomes also contributes to the pre-systemic degradation of peptides (Hamman *et al.,* 2005:168). The brush border is the collective term for the layer of epithelial cell membranes that covers the surface of each villus (Widmaier *et al.,* 2008:536). The final degradation of peptides will occur upon contact with the brush border or following entry into the cell (Lee & Yamamoto, 1990:188-190; Alpers, 1987:1476). Brush border enzymes

include aminopeptidase A, P and W, endopeptidases, carboxy-exopeptidases P and M, alkaline phosphatase and dipeptidyl dipeptidase (Langguth *et al.,* 1997:41-43; Basson & Hong 1996:155).

Following endocytosis intracellular peptide degradation can occur in the lysosomes. The proteolytic degradation in the lysosomes is catalyzed by catephsins and may involve endo- and exopeptidase activity. Proteolytic activity at the brush border seems to be more dominant than in the lysosomes (Langguth *et al.,* 1997:41).

2.4 Strategies to improve bioavailabilty

It is evident from the previous sections, that the oral bioavailability of protein and peptide drugs is hampered by the absorption barriers, resulting in a relatively poor oral bioavailability of between 1-2% (Renukuntla *et al.,* 2013:75; Carino & Mathiowitz, 1999:250). Strategies to improve the oral bioavailability can be divided into two main groups including formulation approaches and chemical modification. Low bioavailability can be addressed by the formulation of novel dosage forms that include the incorporation of absorption enhancers and/or enzyme inhibitors into drug delivery systems (Park *et al.*, 2010:72; Liu *et al*., 2009:267). Chemical modification may be achieved through the synthesis of pro-drugs; structural transformations that target particular receptors, transporters or the preparation of peptidomimetics (Brady, 2006:314).

2.4.1 Formulation approaches

2.4.1.1 Absorption enhancers

The use of absorption enhancers to improve drug absorption is an active research field (Moghimipour *et al.,* 2015:14451; Renukunta *et al.,* 2013:79). According to Muranishi (1990:2) absorption enhancers are compounds that reversibly remove or temporarily disrupt the intestinal barrier with minimum tissue damage, thus allowing a drug to penetrate the epithelial cells and enter the blood and/or lymph circulation. There are a number of mechanisms by which absorption enhancers can act: (a) temporarily disrupting the structural integrity of the intestinal barrier, (b) opening of tight junctions, (c) decreasing mucus viscosity and (d) increasing membrane fluidity (Choonara *et al*., 2014:1269; Renukuntla *et al.*, 2013:79; Hamman *et al*., 2005:168).

Highly effective absorption enhancers often cause damage and irritate the intestinal mucosal membrane. There is therefore a need for the development of more effective and less toxic drug absorption enhancers (Takizawa *et al.*, 2013:664). The fundamental consideration of effective drug uptake facilitation by chemical permeation/absorption enhancers is ensuring that the drug

permeability is predictable, reversible and reproducible. Absorption enhancers should further promote intestinal permeability without risking toxic outcomes (Legen *et al*., 2005: 184).

2.4.1.1.1 *Aloe* leaf materials

A. vera (L.) Burm.f. (*Aloe barbadensis* Miller) is a plant distinguished by leaves containing water storage tissue in order to survive in dry areas (such as North Africa, Central America and southern USA). The inner translucent pulp of the leaves consists of a soft tissue with large thin-walled parenchyma cells that contains a viscous mucilage or gel (Hamman, 2008:1600). The gel is composed of water (98%) and polysaccharides (such as pectin, mannose derivatives, hemicelluloses, cellulose, acemannan and glucomannan). The foremost biologically functional molecule of the *A. vera* leaf gel is thought to be acemannan. The structure of acemannan can be described as an extended chain of acetylated polymannose (de Bruyn, 2015:18; Chen *et al*., 2009:588).

In vivo studies on *A. vera* gel and whole leaf extract showed an increase in the bioavailability of vitamins C and E in humans (Vinston *et al.,* 2005:760). *In vitro* studies on *A. vera* has shown that both the gel and whole leaf extract were able to significantly reduce the TEER of Caco-2 cell monolayers and thereby showed the ability to open tight junctions. *A. vera* gel and whole leaf materials showed potential to enhance the permeability of poorly permeable drugs across the intestinal epithelium (Radha & Laxmipriya, 2015:23; Beneke *et al.*, 2012:476; Chen *et al*., 2009:592).

2.4.1.1.2 Chitosan

Chitosan is a ß-(1,4) connected carbohydrate polymer of 2-amino-2-deoxy-D-glucose and is developed through the deacetylation of chitin, the most copious natural polymer after cellulose (Thanou *et al.,* 2001:117; Thanou *et al.,* 1999:74). Chitosan is a natural polymer that is non-toxic, biocompatible and biodegradable (Hejazi & Amiji, 2003:151; Thanou *et al.,* 2001:117; Thanou *et al.,* 1999:74 and Tozaki *et al.*, 1997:1016). These characteristics render chitosan a good candidate for the development of novel GI drug delivery systems (Hejazi & Amiji, 2003:151). Chitosan is soluble in an acidic environment due to protonation; and as a consequence is able to act as an absorption enhancer of hydrophilic macromolecular compounds such as buserelin and insulin (Hejazi & Amiji, 2003:160; Thanou *et al*., 2001:117; Thanou *et al*., 1999:74).

Chitosan's mechanism of action as an absorption enhancer is linked to the opening of the tight junctions between epithelial cells and allowing the paracellular transport of hydrophilic and macromolecular compounds (Jonker *et al.*, 2002:206). Chitosan has long been used to improve the uptake of proteins across the epithelial tissue mainly because of its muco-adhesive and tight

junction modulating properties and because of its low toxicity (Wallis *et al.*, 2014:1092). However, chitosan exhibits poor solubility in neutral and alkaline environments. Due to the limitation as absorption enhancer due to solubility problems in alkaline environments, the synthesis of chitosan derivatives, including TMC has been triggered (Thanou *et al.*, 2001:117).

2.4.1.1.3 *N*-trimethyl chitosan chloride (TMC)

A partially quaternised chitosan derivative, TMC, has a higher water solubility compared to chitosan due to an increase in the positive charges on the polymer chain causes the molecular expansion in solution (Boonyo *et al.,* 2007:169). TMC showed a higher solubility in a wider pH range than chitosan and was proved to open tight junctions to make the paracellular pathway available for macromolecular drug transport without damage to cell membranes (Caramella *et al.,* 2010:7; Thanou *et al.,* 2001:S91).

2.4.1.1.4 Bile salt

The amphipathic steroidal bio-surfactants, also known as bile salts, are derived from cholesterol in the liver. They have been widely used as absorption enhancers to increase drug transport across biological barriers such as the intestinal membrane. Bile salts enhance drug permeation through biological membranes by interacting with the phospholipids in cell membranes (Moghimipour *et al.*, 2015:14457). A notable disadvantage of bile salts is the irreversible damage to the mucosa and ciliotoxicity. It has been reported that dihydroxy bile salts are more toxic than trihydroxy bile salts (Moghimipour *et al.,* 2015:14463).

2.4.1.2 Polymeric hydrogels

Hydrogels are three-dimensional (3D), hydrophilic, polymeric networks capable of consuming large amounts of water or biological fluids. Hydrogels exhibit a thermodynamic compatibility with water which allows them to swell in an aqueous environment. According to the mechanical and structural (based on the nature of the side groups) characteristics of hydrogels, they can be classified as neutral or ionic. The swelling behaviour of hydrogels is dependent on the external environment (Peppas *et al.,* 2000:27-28). In low pH values (corresponding to gastric juice) the network forms complexes and thereby do not swell to a high degree. Thus, drugs incorporated in hydrogels can be protected from degradation by the digestive enzymes present in the stomach (Ichikawa & Peppas, 2003:609).

2.4.1.3 Muco-adhesive systems

Bio-adhesion describes the extended connection between drug delivery systems and the gastro-intestinal mucosa. Terms that are commonly used to describe bio-adhesion include

"cyto-adhesion" (connection between the drug delivery system and the surface of the cell) and "muco-adhesion" (connection between the drug delivery system and the mucus layer) (Rekha & Sharma, 2013:54). The formulation of bio-adhesive drug delivery systems aims at prolonging the intestinal transit time by slowing the movement of the delivery system through the gastro-intestinal tract by adhering to the mucosa (Aulton, 2007:498; Peppas, 2004:11). These attributes can enhance the bioavailability of drugs, especially for peptide and protein delivery (Peppas & Huang, 2004:1676).

In a previous study, a muco-adhesive hydrogel shuttle drug delivery system was formulated for effective gastro-intestinal delivery of peptide and protein drugs. Absorption enhancers as well as enzyme inhibitors were included in this system, which were intended to be released first (first phase) followed by the protein drug (second phase) as illustrated in Figure 2.4. The system was designed to swell and attach to the wall of the small intestine after which the double phase release was supposed to occur. The drug delivery system managed to protect the drug from proteolytic enzymes, while being dependent on the environmental pH for drug release (de Bruyn, 2015:20; Dorkoosh *et al.,* 2001:11).

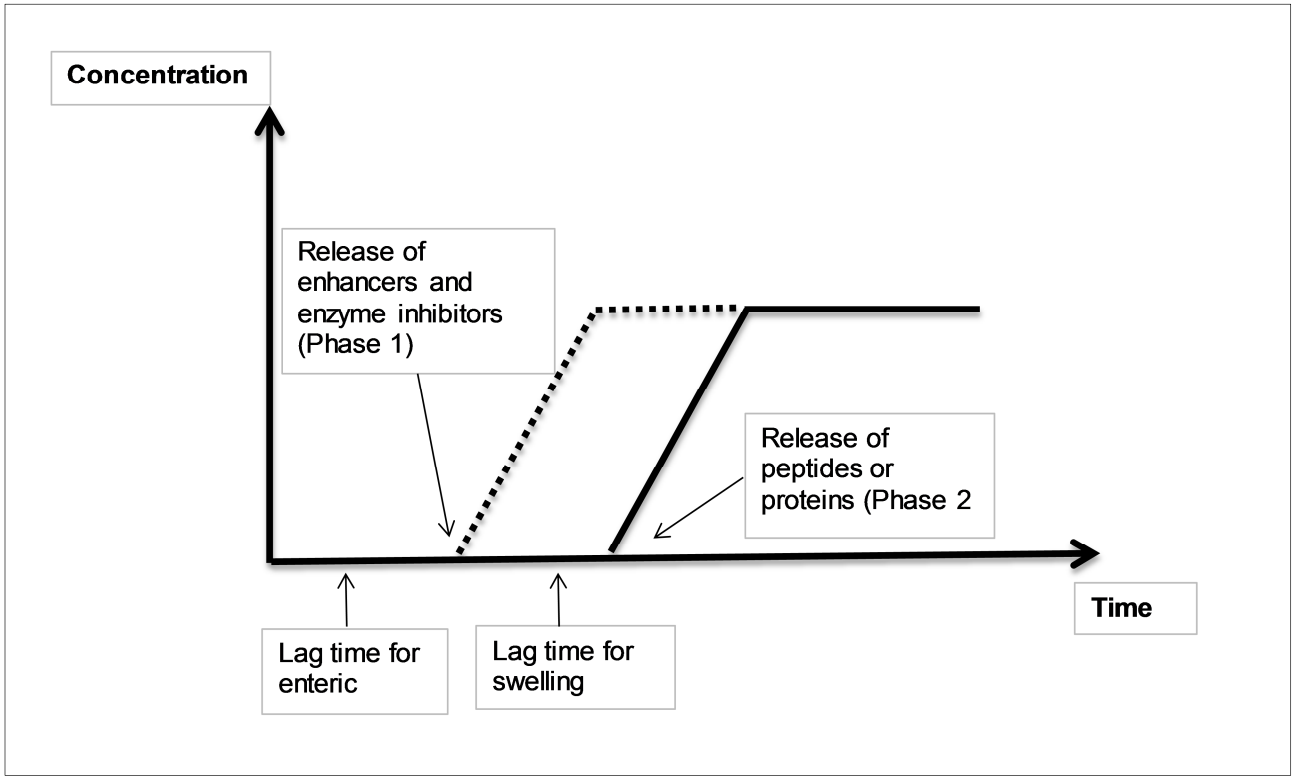

Figure 2.4: Graph illustrating a double phase time controlled release profile as theoretically expected from a polymeric hydrogel shuttle system (Dorkoosh et al., 2001:11)

2.4.1.4 Nano-scale technologies

Application of colloidal polymeric particulate drug delivery systems have demonstrated the potential to reduce the challenges associated with the oral delivery of protein and peptide drugs. A majority of particulate carrier systems for peptide and protein drug uptake such as nanoparticles, emulsions, liposomes and microspheres have been applied to protect peptides and proteins against the enzymes and the acidic medium found in the GI tract and controlling the rate of drug release (Hildalgo, 2001:388). Nanoparticle-based oral drug delivery systems for peptide and protein drugs have proved to be useful in the efforts to enhance bioavailabilty, because they can provide a protecting effect against biochemical degradation (Mukhopadhyay *et al.,* 2012:1462; Vllasaliu *et al.,* 2010:184; Chen *et al.,* 2008:226).

2.4.1.5 Enzyme inhibitors

Enzyme inhibitors can influence protein and peptide drug bioavailability by decreasing the activities of the protein degradation enzymes. Examples of enzyme inhibitors and the enzymes they inhibit can be seen in Tabel 2.1. The deployment of enzyme inhibitors, unfortunately, remains questionable bearing in mind the possible feedback-controlled protease secretion, adverse outcomes, the breakdown of dietary proteins and intestinal mucosal damage. The possibility to address these undesirable outcomes include the application of delivery systems that offer simultaneous discharge of the inhibitor and the peptide while limiting their concentration in a small and localized area, controlling the movement of the inhibitor out of the delivery system or ensuring that a close contact exists between the mucosa and the delivery system (de Bruyn, 2015:21; Náray-Szabó, 2014:254, Kerns & Di, 2008:86; Tillement, 2006:695 and Park & Mrsny, 2000:32).

Table 2.1: Table of the enzyme inhibitors and the enzymes that are inhibited

Enzyme inhibitors	Inhibiting
Aprotinin	Chymotrypsin and trypsin
FK448	Chy-381 motrypsin
Soybean trypsin	Pancreatic endopeptidases
Chicken ovomucoid	Trypsin

2.4.1.6 Multi-particular dosage forms

Multi-particulate drug delivery systems can be described as oral dosage forms consisting of multiple small discrete units each containing a part of the total drug dose. These drug delivery systems are divided in sub-units, typically consisting of spherical particles with a diameter that can range from 0.05 to 2.00 mm. To administer the recommended dose, these sub-units can be filled in a sachet or encapsulated in a hard gelatine capsule or compressed into a tablet (Patwekar & Baramade, 2012:758; Dey *et al.,* 2008:1068).

Advantages of multi-particulate drug delivery systems include increased bioavailability, predictable and short gastric residence time, reduced risk of systemic toxicity, less inter- and intra-subject variability, no risk of dose dumping and reduced risk of local irritation (Patwekar & Baramade, 2012:758; Dey *et al.,* 2008:1068; Zhang *et al.,* 2002:198). Disadvantages of multi-particulate drug delivery systems include low, limited drug loading, a higher need for excipients compared to single-unit dosage forms, lack of manufacturing reproducibility and efficacy, a large number of process variables, a multiple of formulation steps, higher costs of production, the need for advanced technology and trained personal needed for manufacturing (Patwekar & Baramade, 2012:758; Dey *et al.,* 2008:1069).

Despite the disadvantages associated with multi-particulate dosage forms, benefits include ease of disintegration in the stomach, provision of a convenient, fast disintegrating tablet that dissolves in water before swallowing, which improves compliance in geriatric and paediatric patients. After disintegration, the individual sub-unit particles pass quickly through the GI tract. Sub-units with diameters of less than 2 mm are able to leave the stomach continuously, even if the pylorus is closed (Dey *et al.,* 2008:1068). Multi-particulate drug release can occur through different mechanisms, which include diffusion, osmosis and erosion (Patwekar & Baramade, 2012:758; Dey *et al.,* 2008:1069).

Diffusion: This takes place on contact with aqueous fluid in the GI tract after which the water diffuses into the core of each particle. Drug dissolution occurs and the drug molecules diffuse to the exterior.

Osmosis: Water is allowed to enter the particle through a semi-permeable coating membrane, after which an osmotic pressure is created inside the particle. Due to the osmotic pressure the drug is expelled out of the particle to the outside through the coating.

Erosion: In some cases the coating/matrix can be designed to wear away gradually with time, thus delivering the drug contained within the particle.

2.4.2 Chemical modifications

Chemical modifications that can improve the bioavailability of protein and peptide drugs include the usage of pro-drugs, structural transformations, peptidomimetics, lipidisation, PEGylation, amino acid substitution and targeting membrane receptors and transporters (Anderle, 2009:23).

2.4.2.1 Pro-drugs

Pro-drugs entail synthesis of a pharmacological inert compound that needs biotransformation to turn into a pharmacologically active entity (Krishna & Yu, 2007:256). Pro-drugs are therefore administered as the inactive form that are activated in a number of ways, e.g. by intestinal bacteria, in the brain or by liver enzymes (see Figure 2.5). Pro-drugs are used for a variety of reasons such as to improve drug stability, increase systemic drug absorption, to reduce gastro-intestinal side-effects, crossing the blood-brain barrier or to prolong the duration of activity (Shargel *et al.,* 2005:321)

The majority of methods used for pro-drug synthesis focused on changing one functional group in the molecule (Anderle, 2009:23). Pro-drugs that target membrane transporters are chemically designed to become substrates for membrane transporters, which facilitates their uptake (Krishna & Yu, 2007:256). Pro-drugs get transferred across the epithelial membrane and reach the systemic circulation in its original state after which the pro-drug can undergo biotransformation to the active drug form, or can instantly be subjected to the enzymatic hydrolysis in the intracellular surrounding after which it is released as an active drug in the systemic circulation as illustrated in Figure 2.5 (de Bruyn, 2015:21-22; Brady, 2006:314; Herkenne, 2005:268).

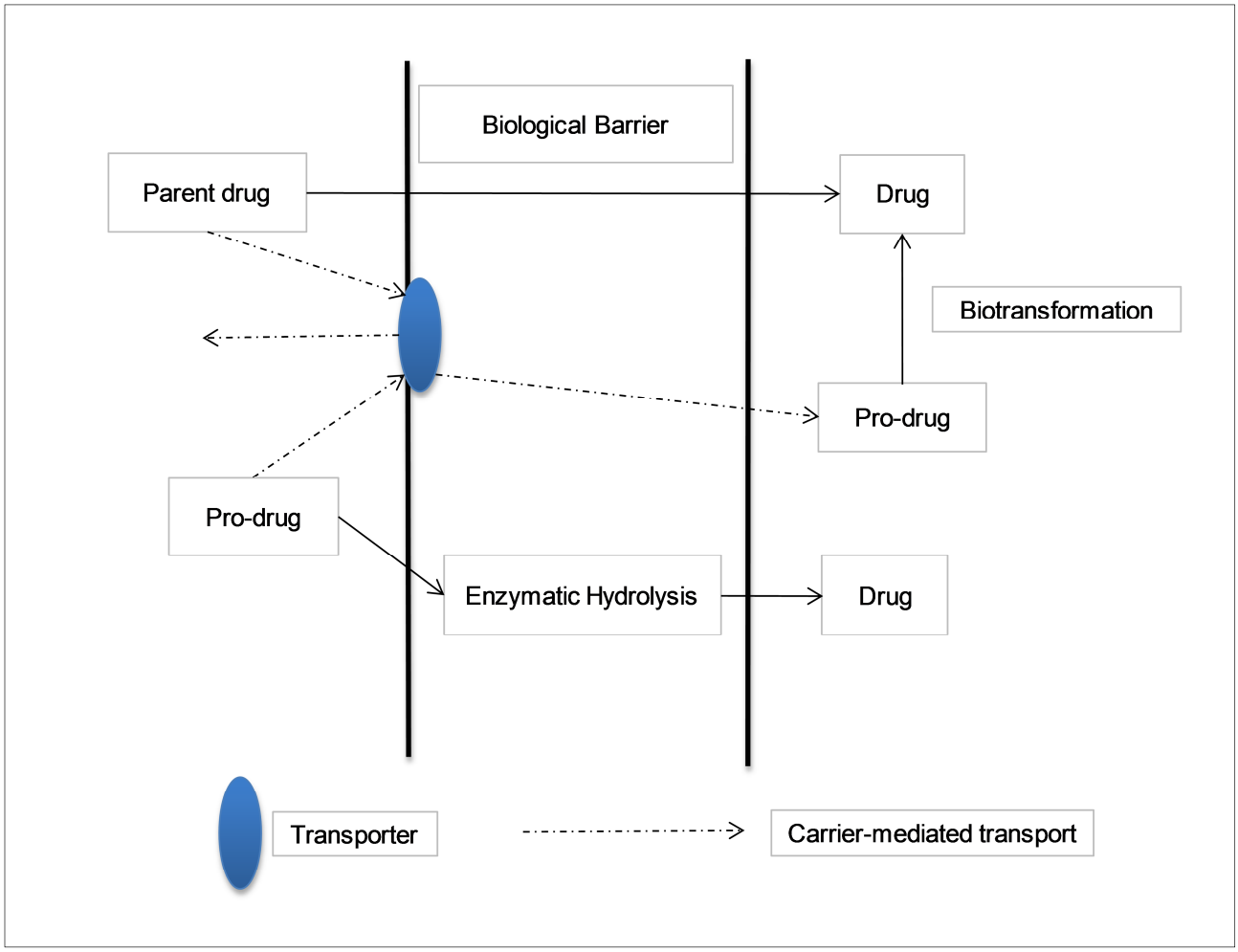

Figure 2.5: Schematic illustration of the pro-drug approach (Majumdar *et al.,* 2004:1439)

2.4.2.2 Amino acid substitution

The chemical transformation of protein and peptide drugs that depend on amino acid substitution can be achieved by using an alternative amino acid or replacing the D-amino acid with the L-amino acid or by changing the sequence of amino acids (Krishna & Yu, 2007:256).

2.4.2.3 Lipidisation

Lipidisation takes place by conjugating a fatty acid onto a protein or peptide molecule, which improves the bioavailability of the macromolecule by enhancing its lipophilicity and therefore also its diffusion across biological membranes (Anderle, 2009:23).

2.4.2.4 Polyethylene glycolation (PEGylation)

PEG refers to a biocompatible and non-toxic polymer which can be dissolved in an aqueous and organic solvent. The pharmacokinetic properties of protein and peptide drugs can be enhanced through covalent linking to PEG, also known as PEGylation (Mathiowitz *et al.,*

2009:53, Chitchumroonchokchai, 2004:23). PEGylation is well known for its benefits in boosting the *in vivo* circulation half-life of proteins and peptides by intercepting their breakdown, reducing their renal disposal and enhancing their physico-chemical properties (Chitchumroonchokchai, 2004:23). PEGylation has become an advanced field of chemical modifications of peptide molecules and multifaceted strategies exist to link PEG to a macromolecule.

2.5 Summary

The oral route is the most acceptable route for the administration of drugs. When formulating an oral dosage form for protein and peptide drugs, important challenges such as poor bioavailability and pre-systemic degradation should be overcome. After oral administration, protein and peptide drugs encounter physical barriers (i.e. the unstirred water layer, epithelial cell membranes, tight junctions and efflux transporter systems) and biochemical degradation (i.e. luminal enzymes and brush border enzymes) present in the gastro-intestinal tract.

Different approaches have been used to overcome the above mentioned obstacles associated with oral protein and peptide delivery. These strategies include the use of absorption enhancers, enzyme inhibitors, hydrogels, muco-adhesive systems, liposomes, nanoparticles, microparticles, chemical modification, pro-drug development, targeting of membrane transporters and cell penetrating peptides. The bead-in-matrix drug delivery system was aimed to release the drug absorption enhancer first to overcome the absorption barrier and thereafter the peptide drug was released and subsequently absorbed.

CHAPTER 3: MATERIALS AND METHODS

3.1 Introduction

To achieve the aim of this study, two types of beads were formulated. The first type consisted of micro-beads, which contained insulin as an active ingredient and Pharmacel® as a filler. The second type consisted of macro-beads forming the matrix of the delivery system, which contained both the micro-beads and an absorption enhancing agent (i.e. *A vera* gel, sodium deoxycholate and TMC) (see Figure 1.1 in Section 1.3.1). The macro-beads were film coated and then loaded into hard gelatin capsules. The hard gelatin capsules filled with the macro-beads formed the bead-in-matrix (double phase) delivery systems (see Figure 3.1), which were specifically designed for effective oral delivery of insulin.

The rationale behind the concept of this delivery system was that the macro-beads will release their content first after administration upon reaching the small intestine (due to the enteric film coating); after which the absorption enhancing agent will act to open the tight junctions between epithelial cells. The micro-beads will consequently release the insulin at a slower rate due to the design of the formulation. Once the micro-beads reached the site of absorption, the drug delivery of insulin into the blood stream would be facilitated via the paracellular route due to the already opened tight junctions.

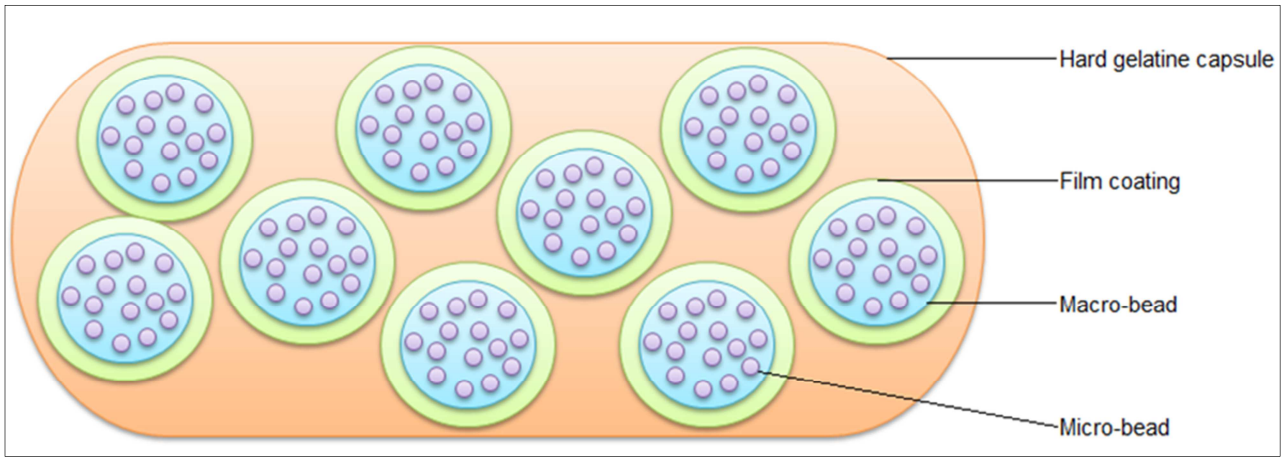

Figure 3.1: Schematic illustration of the bead-in-matrix delivery system

In order to test the drug delivery potential of this bead-in-matrix dosage form, an *in vitro* permeation technique was used where excised porcine intestinal tissue was mounted on a diffusion apparatus. The bead-in-matrix delivery system was applied to the excised porcine intestinal tissues to mimic the *in vivo* situation more realistically. The *in vitro* technique also faced limitations in the sense that only uncoated beads could be tested, since coated beads would delay the release of insulin beyond the limited viability period (approximately 2 h) of the

excised tissue after removal from the animal. Besides the permeation studies, the different bead-in-matrix formulations were evaluated in terms of physical properties namely, mass variation, particle size distribution and dissolution behaviour. This chapter contains all the materials and methods which were used during this study.

3.2 Materials

The materials and their batch numbers used in the formulation of the beads are listed in Table 3.1.

Table 3.1: Materials used in the formulation of the beads

Material	Batch Number
Ac-di-sol® (Crosscarmellose Sodium) was obtained from BASF (Midrand, South Africa)	T017C
Aloe vera gel	*No batch number
Ethanol was purchased from Rochelle Chemicals (Johannesburg, South Africa)	1044255
Kollidon®VA 64	93520356VO
Insulin (Human Recombinant) was purchased from Sigma Aldrich (Johannesburg, South Africa)	15L255-G
N-trimethyl chitosan chloride (TMC)	*No batch number
Pharmacel® was sourced from Warren Chem Pharmaceuticals (Pty) (LTD) (Cape Town, South Africa)	100043
Sodium deoxycholate was purchased from Sigma Aldrich (Johannesburg, South Africa)	SLBQ1228V

* Was available in house

The materials and their batch numbers used during the film coating process are listed in Table 3.2.

Table 3.2: Materials used in the film coating process

Material	Batch Number
Eudragit® S100	B120705005
Eudragit® L100	B12603009
Triethyl citrate	BCBH5668V
Talc	
Acetone	1035162
Isopropanol	31853

The materials and their batch numbers used during the transport studies across excised porcine intestinal tissue are listed in Table 3.3.

Table 3.3: Materials used in transepithelial electrical resistance and transport studies

Material	Batch Number
Krebs-Ringer bicarbonate (KRB) buffer was purchased from Sigma-Aldrich (Johannesburg, South Africa)	Multiple batches were used during the study
Sodium bicarbonate was purchased from Sigma Aldrich (Johannesburg, South Africa)	021M01014V
Porcine proximal jejunum tissue was collected from the local abattoir (Potchefstroom, South Africa)	N/A

The materials and their batch numbers used during the dissolution studies are listed in Table 3.4.

Table 3.4: Materials used in dissolution studies

Material	Batch Number
Hydrochloric acid was purchased from Associated Chemical Enterprises (Johannesburg, South Africa)	H1116CC02500
Potassium phosphate buffer was purchased from	

3.3 Formulation and preparation of beads

3.3.1 Preparation of micro-beads containing insulin

Micro-beads were prepared using extrusion-spheronisation. Weighed amounts of the dry powders namely 0.1% w/w insulin and Pharmacel® (qs) were mixed in a Turbula® mixer (Willy A. Bachofen, Switzerland) for 10 min at 69 rpm for each bead formulation. The total weight of the powder mixture for each micro-bead formulation was 50 g. A volume of 70 ml of distilled water was slowly added to the powder mixture of the micro-bead formulation while blending the powder mass in a Kenwood® KM300 chef mixer. The wetted powder mass was passed through a 0.5 mm extrusion screen (Type 20 Caleva® extruder, Caleva Process Solutions, England) at a speed of 35 rpm to form spaghetti-like extrudates. This process was followed by spheronisation of the extrudate using a Caleva® spheronising apparatus (Caleva Process Solutions, England) at 2080 rpm for 10 min to form spherical beads. The beads were lyophilised by first freezing the beads in a -80℃ freezer and then drying them under vacuum (Virtis, Gardiner N.Y. USA) for up to 48 hours (de Bruyn 2015:28).

3.3.2 Preparation of macro-bead containing micro-beads and an absorption enhancer

Macro-beads were prepared in a similar manner as described for micro-beads containing insulin. In this case, different bead formulations (in total 18 formulations) were prepared, each containing a different absorption enhancing agent as shown Table 1.1 (Chapter 1, Section 1.4). For the macro-bead formulation, weighed amounts of the dry powder ingredients (0.5% w/w or 1% w/w absorption enhancer together with 0.5% w/w Ac-di-sol®, 1% w/w Kollidon®VA 64 and (qs) Pharmacel®) were mixed with different concentrations of micro-beads (20%, 40% an 60% w/w respectively) to make a total of 50 g and mixed in the Turbula® mixer (Willy. A. Bachofen, Switzerland) at 69 rpm for 10 min.

A mixture of distilled water (40 ml) and ethanol (2 ml) was added to these powder mixtures, while blending in a Kenwood® KM300 planetary mixer. The wetted powder mass was passed through a 2.5 mm extrusion screen (Type 20 Caleva® extruder, Caleva Process Solutions, England) at a speed of 30 rpm followed by spheronisation of the extrudate (Caleva® spheroniser, Caleva Process Solutions, England) at 1200, 1300 and 1400 rpm for the 60, 40 and 20% micro-bead concentration respectively for 5 min to form spherical beads. The beads were lyophilised by first freezing the beads at -80℃ and then drying them under vacuum (Virtis, Gardiner N.Y. USA) for up to 24 hours.

3.3.3 Film coating of insulin-containing beads

3.3.3.1 Coating formulation

The bead-in-matrix formulations were film coated by using a suspension formulation as shown in Table 3.5. The Eudragit® L100 and Eudragit® S100 powders were added slowly into half of the diluent mixture consisting of acetone, isopropanol and water; this mixture was stirred with a Heidolph RZR-2000® overhead stirrer until the polymers were completely dissolved. Triethyl citrate was added to the remaining half of the diluent mixture, which was stirred for 10 min with a high shear mixer. This mixture was slowly poured into the Eudragit® solution while stirring with a high shear mixer. The coating suspension was passed through a 0.5 mm sieve under vacuum. Talc was added to the sieved solution and stirred with the high shear mixer, before it was sprayed onto the bead-in-matrix formulation in a coating pan.

Table 3.5: Ingredients used to prepare the suspension for film coating of the beads

Ingredient	Function	Quantity (g)	% w/w
Eudragit® S100	Polymer	7.83	3.13
Eudragit® L100	Polymer	7.83	3.13
Triethyl citrate	Plasticiser	1.58	0.63
Talc	Anti-tacking	7.83	3.13
Acetone	Diluent	85.75	34.3
Isopropanol	Diluent	128.50	51.4
Water	Diluent	10.70	4.28
Total		250	100

3.3.3.2 Spray coating process

The macro-beads (bead-in-matrix formulations) were coated with the Eudragit® suspension using a pan-coater (Associated Electrical Industries Pty Ltd, SA). The macro-beads (±5 g) were added to the drum of the pan-coater which was rotated at a speed of 8 rpm and then sprayed with the coating suspension using a hand spray bottle at a distance of 15 cm from the beads, while simultaneously drying the beads by means of an air stream with an inlet air temperature of approximately 40℃. Different coating times (i.e 1 5, 20, 25, 30 min) were employed to determine the influence of the coating time on the coating layer thickness on placebo macro-beads. To evaluate the coating process, scanning electron micrographs (SEM) micrographs were captured of the coated beads. In preparation for the SEM imaging, the coated placebo bead-in-matrix beads were sliced (using a scalpel blade) in half. This was done to obtain a better indication of the thickness of the film coating.

3.4 Evaluation of the bead formulations

3.4.1 Assay

The insulin content of a sample (1 g) bead-in-matrix formulation was determined by means of high performance liquid chromatography (HPLC). The bead sample was placed into a volumetric flask, which was made up to volume (100 ml) with KRB buffer. The mixture was placed onto a Labcon® MSH10 magnetic stirrer (Labcon laboratory equipment Pty Ltd, SA) and was stirred for 12 h. The insulin quantity that was present in the solution was used to obtain the experimental value of the insulin content in the bead-in-matrix delivery system (de Bruyn, 2015:29-30). The experimental value was compared to that of the theoretical value in order to express the insulin content as a percentage of the dose that was intended to be contained in the dosage form. The percentage insulin content was calculated with the following equation:

$$\% \text{ Content} = \frac{(\text{experimental value of insulin content})}{(\text{theoretical value of insulin content})} \times 100 \qquad \text{(Equation 3.1)}$$

3.4.2 Mass variation

Ten hard gelatin capsules (size 0) were individually filled by hand with beads taken from each bead-in-matrix formulation and the content of each capsule was weighed. The mass of the beads in each capsule was compared to that of the average mass. The mass variation of capsules containing beads (uncoated, single–dose) weighing more than 300 mg should not have a percentage deviation of more than ± 7.5% from the average (USP, 2014:492). An acceptable variation in mass of the capsules may be used as an indication of an acceptable variation in drug content under conditions that would ensure mixture homogeneity.

3.4.3 Particle size analysis

One technique that can be used to determine the particle size distribution of solid particles is laser light diffraction. A representative sample is dispersed at an adequate concentration in a suitable liquid, which is passed through a beam of monochromatic light. A multi-element detector then measures the light scattering caused by the particles (e.g. beads) at various angles. Further analysis is done on the numerical values collected by the detectors through the use of mathematical algorithms and an appropriate optical model. These calculations provide the proportion of total volume to a number of size ranges, which forms a volumetric particle size distribution (BP, 2018: XVII).

Size distribution and the size of the different bead-in-matrix formulations were analysed by a Malvern® Mastersizer 2000 (Malvern Instruments Ltd. Worcestershire, UK) fitted with a Hydro 2000MU sample dispersion unit. A volume of 600 ml ethanol was used to flush the system and to align the optics within the apparatus and it was also used as the liquid dispersant for each bead-in-matrix sample. The Mastersizer® software was used to capture and process the data to obtain the mean particle size and particle size distribution.

3.4.4 Drug release from the bead formulation

The oral delivery of protein and peptide drugs (i.e. insulin) is hindered due to enzymatic degradation in the stomach (Kristensen *et al.,* 2013:366; Hassani *et al.,* 2015:12). One of the solutions to overcome the enzymatic degradation is to film coat the dosage form with a polymer or mixture of polymers that exhibit a pH-dependent solubility. Eudragit®L and S polymers are the preferred choice of coating polymers, due to their dissolution properties in mediums with a pH of 6-7 (Evonik 2017:4; Khan *et al.,* 2000:550; Khan *et al.,* 1999:216). Thus the main objective of the dissolution studies was to ensure that the film coating was successful in protecting the beads (insulin) from a low pH environment as well as to confirm insulin release in an environment with a pH >6.

Dissolution behaviour of insulin from the coated bead-in-matrix formulations were evaluated in triplicate by means of placing one capsule of each formulation in three individual dissolution vessels, respectively. Samples (2 ml) were withdrawn from each dissolution vessel using a syringe at time intervals of 120, 130, 137, 146, 155, 185, 215, 245 min, which were each immediately replaced with 2 ml of fresh dissolution medium. The samples obtained from the dissolution study were analysed with an HPLC method to determine the amount of insulin in the dissolution medium at each time point.

3.4.4.1 Preparation of hydrochloric acid media

Dissolution of insulin from the different bead-in-matrix formulations were conducted in a 0.1 M HCl at pH 1.2 with the paddle method in a six vessel dissolution apparatus (Distek 2500 dissolution apparatus, North Brunswick, NJ, USA) for the first 2 h of the dissolution studies. The dissolution medium was set at 600 ml with a stirring rate of 150 rpm and the temperature was kept at 37 ± 0.5ºC.

The preparation of the HCl media with a pH 1.2 was prepared as follows: 29.4 ml of a 32% w/w HCl solution was made up to volume (3000 ml) with distilled water. The pH was checked and adjusted by adding sufficient volumes of either 0.1 M HCl or 0.1 M NaOH.

3.4.4.2 Preparation of potassium phosphate buffer

Immediately after the 2 h acid stage of dissolution, the dissolution medium was changed to render a dissolution medium with a pH adjusted to 6.8. The acid dissolution stage was therefore followed by a dissolution stage in a higher pH medium to determine whether the polymer coating on the bead-in-matrix formulations was able to dissolve thereby enabling dissolution of the insulin within the formulations. To achieve the correct medium for the buffer stage, a 0.2 M trisodium phosphate dodecahydrate ($Na_3PO_4.12H_2O$) solution (300 ml) was added to the acid medium ensuring a pH of 6.8. The stirring rate was kept at 150 rpm and the temperature at 37 ± 0.5ºC for 2 h.

The trisodium phosphate dodecahydrate ($Na_3PO_4.12H_2O$) buffer solution was prepared by dissolving 32.79 g trisodium orthophosphate (anhydrous) in distilled water (1000 ml), adjusting the pH by adding sufficient volumes of 0.1 M HCl or 0.1 M NaOH.

3.5 Trans-epithelial electrical resistance and transport studies

3.5.1 Preparation and mounting of excised porcine intestinal tissue on half-cells of the Sweetana-Grass diffusion apparatus

Approval from the Research Ethics Regulatory Committee (NWU-RERC) at the North-West University was obtained for the use of porcine intestinal tissue (ethics approval number: NWU-00025-15-A5). Directly after pigs were slaughtered (Potch Abattoir, Potchefstroom, South Africa), a piece of approximately 30 cm of the proximal jejunum tissue was collected from the GI tract. The intestinal tissue was rinsed with ice cold KRB buffer and transported for approximately 15 min in cold KRB buffer in a cooler box from the abattoir to the laboratory.

In the laboratory, the jejunum was pulled onto a glass tube (Figure 3.2, A) where it was kept moist by applying KRB buffer. The serosa was removed by blunt dissection (Figure 3.2, B) and

the tissue was cut along the mesenteric border with a scalpel blade. A piece of heavy duty filter paper was placed on a Perspex® plate positioned on ice. The tissue was washed using cold KRB buffer from the glass rod onto the filter paper (Figure 3.2, C & D). The tissue and filter paper were cut into approximately 2 cm pieces (Figure 3.2, E), taking special care avoiding Peyer's patches (Figure 3.3) (Peyer's patches are small masses of lymphatic tissue in the ileum close to the epithelial surface (Aulton, 2007:273)), while keeping the tissue moist with KRB buffer. These segments of tissue were mounted onto the half-cells of the Sweetana-Grass diffusion apparatus and the filter paper was removed (Figure 3.2, F). The two half-cells were clamped together with metal rings (Figure 3.2, G) and these combined chambers were placed into a heating block and filled with 7 ml pre-heated (37℃) KRB buffer. The half-cells of the chambers were connected to parallel gas flow (5% CO_2; 95% O_2) with a flow rate of 15-20 ml/min (Figure 3.2, H).

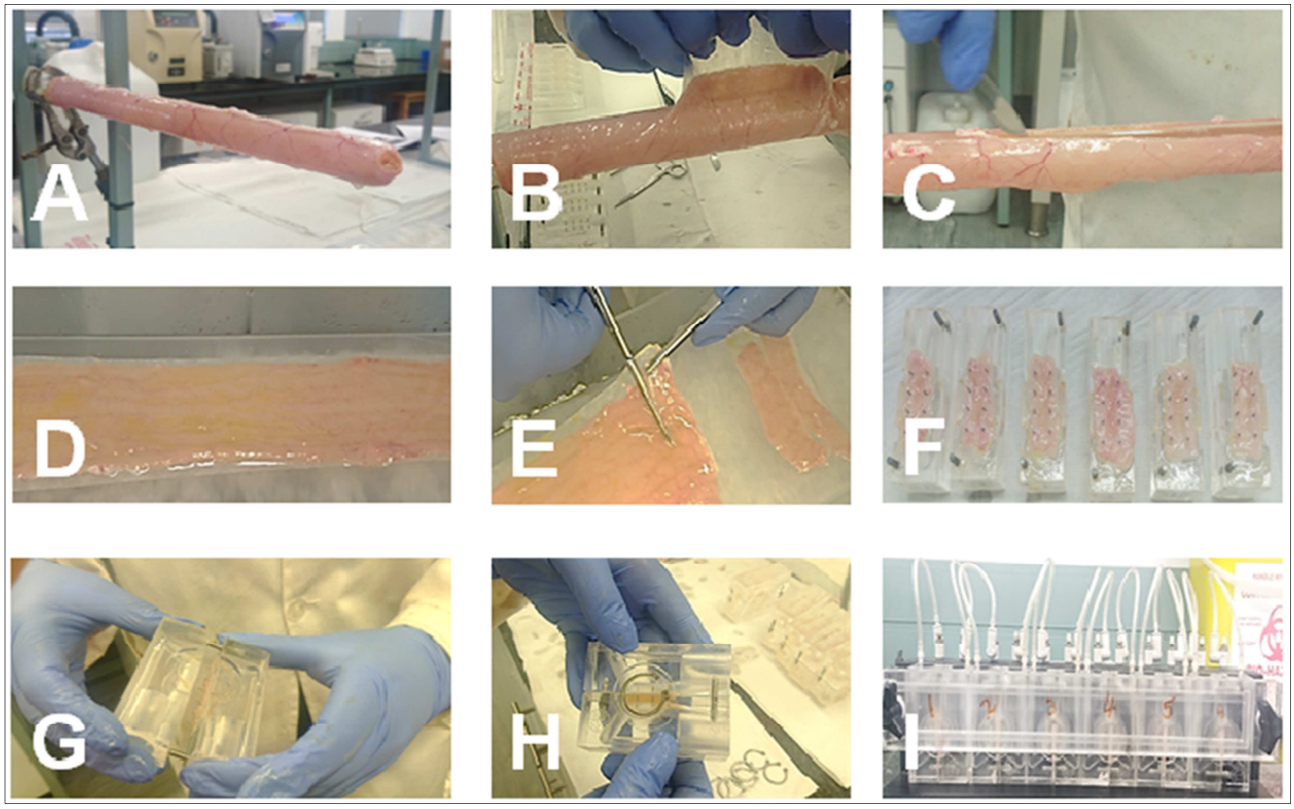

Figure 3.2: Images (A-I) illustrating the preparation and mounting of the porcine jejunum on the Sweetana-Grass diffusion chamber. **A:** excised porcine jejunum on glass rod, **B:** removal of serosa, **C:** jejunum cut open, **D:** jejunum tissue placed on Perspex® plate, **E:** jejunum together with filter paper cut into rectangular pieces, **F:** jejunum mounted on half-cell, **G:** half-cells clamped together, **H:** clamped chambers kept in place with metal ring, **I:** chambers in heat block.

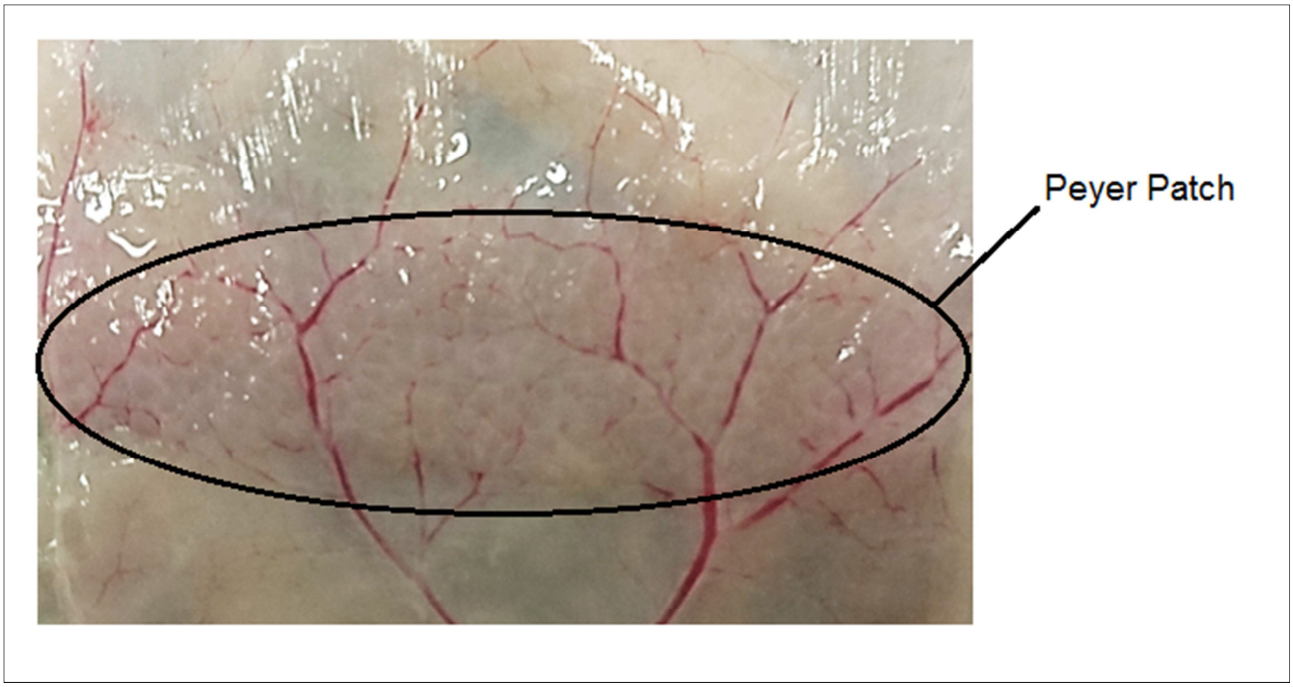

Figure 3.3: Image illustrating what a peyer's patch look like on porcine intestinal tissue

The assembled cells were left for 15 min to acquaint the tissues with the environment before transport studies commenced.

3.5.2 *In vitro* transport studies

3.5.2.1 *In vitro* transport control studies

Lucifer yellow (LY) was used to assess the integrity (Buyukozturk *et al.,* 2010:24) of the porcine intestinal tissues. A concentration of 54.18 µg/ml LY was applied to the apical chamber. Samples (180 µl) were withdrawn from the basolateral chamber every 20 min over a 2 h period and replaced immediately after every withdrawal with 180 µl pre-heated (37℃) KRB buffer. The concentration of LY in the transport samples was determined by means of a validated fluorescence spectroscopy method. The percentage LY transported was plotted as a function of time.

A transport control study consisted of beads containing insulin only, which was used to show that insulin does not cross the tissue in significant quantities without the addition of an absorption enhancer. A sufficient quantity (1.178 g) of the bead-in-matrix formulation containing insulin only was added to the apical chamber to provide an approximate concentration of 0.1 mg/ml insulin. Samples (200 µl) were withdrawn from the basolateral chamber every 20 min over a 2 h period and replaced immediately after every withdrawal with 200 µl pre-heated (37℃) KRB buffer. The insulin concentration in the transport samples was determined by means of a validated HPLC method.

3.5.2.2 Insulin transport across excised porcine tissue

The transport of insulin across excised porcine intestinal tissue was determined after exposure to the bead-in-matrix formulation. The formulation was suspended in the transport medium (KRB buffer) on the apical side for 120 min. A sufficient quantity (1.178 g) of the bead-in-matrix formulation was added to the apical chamber to provide an approximate concentration of 0.1 mg/ml insulin. Samples (200 µl) were withdrawn from the basolateral chamber every 20 min over a 2 h period and replaced immediately after every withdrawal with 200 µl pre-heated (37℃) KRB buffer. The insulin concentration in the transport samples was determined by means of a validated HPLC method.

The percentage insulin transported across the excised intestinal tissue was plotted as a function of time. Apparent permeability coefficient (P_{app}) values were calculated from these graphs using the following equation (Hellum & Nilsen, 2008:468; Hansen & Nilsen, 2009:88):

$$P_{app} = \frac{dQ}{dt} \times \frac{1}{A.Co.60} \quad \text{(Equation 3.3)}$$

Where P_{app} represents the apparent permeability coefficient ($cm.s^{-1}$), dQ/dt ($\mu g.s^{-1}$) represents the increase in the amount of drug in the receiver chamber within a given time period, which is equivalent to the slope of the plot of drug concentration transported versus time. A represents the effective surface area (cm^2) of the excised pig intestinal tissue between the apical and basolateral chambers and C_o is the initial insulin concentration in the apical chamber ($\mu g.cm^{-3}$).

3.5.3 Validation of the analytical method for Lucifer yellow (LY)

The analytical method that was used to quantify the LY concentration in the transport samples from the LY study was validated prior to use. Excitation and emission wavelengths of 485 nm and 535 nm were employed respectively (Buyukozturk *et al.,* 2010:23). LY samples were prepared at three different concentrations using the following method. The first concentration (50 µg/ml) was prepared by weighing 2.485 mg of LY powder accurately and made up to volume (50 ml) with KRB solution. The second concentration (25 µg/ml) was prepared by accurately taking 25 ml of the 50 µg/ml LY solution and made up to volume (50 ml) with KRB solution. The third concentration (12.5 µg/ml) was prepared by accurately taking 25 ml of the 25 µg/ml LY solution and made up to volume (50 ml) with KRB solution. The method was validated with respect to linearity, precision, limit of detection and limit of quantification.

3.5.3.1 Linearity

The linearity of an analytical technique refers to the direct correlation between the analysis measurement (e.g. fluorensence value) and the analyte concentration (µg/ml) (BP, 2018:III). For an analytical method to be considered acceptable in terms of linearity, a correlation coefficient (R^2) of more than 0.995 should be achieved. The R^2 should be determined by a series of three to six tests over a minimum of five concentrations (Singh 2013:29). For LY a stock solution of 50 µg/ml was prepared and from the stock solution a serial of dilutions was prepared (i.e. 50 µg/ml; 16.667 µg/ml; 5.556 µg/ml; 1.852 µg/ml; 0.617 µg/ml; 0.206 µg/ml; 0.069 µg/ml; 0.023 µg/ml; 0.008 µg/ml; 0.003 µg/ml; 0.001 µg/ml and 0.0003 µg/ml). The fluoroscence values were used to plot the standard curve (fluorenscence value as a function of concentration) in order to perform a regression analysis to obtain the R^2 value.

3.5.3.2 Precision

According to the BP (2018), the precision of an analytical procedure indicates the closeness of agreement between a series of measurements obtained from multiple sampling of the same sample under prescribed conditions. Customarily precision is measured as the relative standard deviation (RSD) of a set of replicates (Patel *et al.,* 2017:251). Precision can be divided into intra-day and inter-day precision.

3.5.3.2.1 Intra-day precision

Repeatability expresses the precision under the same operating conditions over a short interval of time. In this study all three different concentration LY solutions were evaluated on the same day three hours apart, to obtain the intra-day precision. Intra-day precision is specified to have a RSD lower than 2% (Shabir, 2003:62).

3.5.3.2.2 Inter-day precision

Inter-day precision was determined by analysing the samples of three different concentrations on three successive days (24 hours apart), to determine the inter-day consistency of the method. %RSD value of ≤2% for inter-day precision is considered acceptable (Shabir, 2003:62).

3.5.3.3 Limit of detection (LOD) and limit of quantification (LOQ)

LOD is the lowest concentration at which an analyte in a sample is detected, but not quantified with acceptable accuracy (BP, 2018:III; USP, Patel *et al.,* 2017:252, 2014:1160). LOD was determined with visual inspection using equation 3.4.

3.3 x SD/S (Equation 3.4)

LOQ is the lowest concentration at which an analyte in the sample can be determined with the accuracy and precision necessary for the method in question (BP, 2018:III; Patel et al., 2017:252, USP, 2014:1160). LOQ was determined using equation 3.5.

10 x SD/S (Equation 3.5)

Where SD represents the standard deviation of the KRB solution and S represents the slope of the calibration curve of LY (Rambla-Alegre *et al.,* 2012:107).

3.5.4 Statistical analysis

Data analysis on the transport results were performed with STATISTICA Ver 12. Tukey's significant post-hoc tests were performed and statistically significant differences were accepted when $p < 0.05$.

3.5.5 High-performance liquid chromatography analysis of insulin

An HPLC analytical method (previously developed in the Analytical Technology Laboratory of Pharmacen, North-West University, Potchefstroom, South Africa) was validated as described below and used to analyse the dissolution and transport samples for insulin content.

3.5.5.1 Chromatographic conditions

High performance liquid chromatography is a multi-stage separation method where molecules of the analyte in solution are distributed between a stationary and a mobile phase and the analyte molecules that are eluded can be detected by a variety of techniques such as ultra violet (UV) light absorbance. The stationary phase is packed in a column and the mobile phase is a liquid forced through the column under high pressure (USP, 2014:6378-6379). The chromatographic conditions used to analyse the insulin in this study are summarised in Table 3.7.

Table 3.6: Summary of the chromatographic conditions used to analyse the dissolution and transport study samples

Parameters	Description
Analytical instrument	HP1100 series HPLC equipped with a pump, auto-sampler, UV detector and Chemstation Rev. A.10.01 data acquisition and analysis software.
Column	Vydac C18 Protein and peptide column, 218TP54, 300 Å, 250 x 4.6 mm (Grace Vydac, Hesperia, CA).
Mobile phase	**Phase A:** Degassed mixture of HPLC grade water and 0.1% orthophosphoric acid. **Phase B:** Acetonitrile
Flow rate	1.0 ml/min
Injection volume	50 µl
Detection	UV absorbance at 210 nm
Retention time	±6.14 min
Stop time	12 min
Solvent	HPLC grade water

The mobile phase consisted of two components and was applied by means of a gradient, as shown in Table 3.8

Table 3.7: Gradient conditions for the mobile phase used in the analytical method

Time (min)	Mobile Phase A	Mobile Phase B
0	80	20
6	40	60
8	40	60
8.2	80	20
12	80	20

3.5.5.2 Standard solution preparation

Approximately 5 mg of human recombinant insulin was precisely weighed and dissolved in 50 ml KRB buffer. This standard insulin solution was transferred to a HPLC vial and volumes of 10, 20, 30, 40 and 50 µl were injected into the HPLC, to from a standard curve. This process was repeated every time an HPLC analysis of dissolution and transport samples were conducted to create a standard curve, which was used to calculate the insulin concentration from the peak areas of the insulin peaks on the chromatograms by using linear regression using Equation 3.4.

$$\text{Concentration in sample (µl/ml)} = \frac{\text{(peak area of sample - y-intercept)}}{\text{slope}} \qquad \text{(Equation 3.4)}$$

3.6 Validation of chromatographic analytical method

3.6.1 Introduction

The HPLC method used in this study was previously developed and validated (Kleynhans, 2015:37-41), thus it was only necessary to determine the LOD, LOQ, specificity and linearity.

3.6.2 Linearity

The linearity of an analytical technique refers to the relationship between the analysis measurement and the analyte concentration (e.g. peak area) (BP, 2018:III; USP, 2014:1160; Singh, 2013:29). A standard solution of 0.1 mg/ml was prepared in a KRB buffer of which 2.5, 5, 10, 20, 30, 40, and 50 µl were injected in duplicate into the chromatograph. The peak areas on the chromatograms were plotted as a function of insulin concentration and a linear regression of the curve was done by using Microsoft Excel® software from which the R^2 was obtained. An R^2 value ≥ 0.99 was required for the analytical method to be acceptable.

3.6.3 Limit of detection (LOD) and limit of quantification (LOQ)

LOD is the lowest concentration at which an analyte in a sample is detected (BP, 2018:III; USP, 2014:1160). LOD was taken as an insulin peak on the chromatogram equal to three times the average baseline noise (Rambla-Alegre *et al.,* 2012:106-107).

LOQ is the lowest concentration at which an analyte in the sample can be determined with the accuracy and precision necessary for the method in question (BP, 2018:III; USP, 2014:1160). This value may be the lowest concentration in the standard curve. The LOQ was taken as the lowest concentration of insulin that could be determined with a RSD of ≤ 15% for six replicates.

3.6.4 Specificity

Specificity is the ability of an analytical method to detect an analyte in the presence of other substances, which may interfere with the detection of the analyte (BP, 2018:III; USP, 2014:1159). Samples of 0.1% w/w insulin solutions in the presence of *A. vera* gel, sodium deoxycholate, TMC, Pharmacel®, Ac-di-sol®, Kollidon VA 64®, ethanol and KRB were analysed with the HPLC method, which represented the solutions used during the *in vitro* transport studies. The chromatograms were inspected to ensure the insulin peak was completely separated from those of the other components for the analytical method to be acceptable.

3.7 Summary

In order to design a bead-in-matrix dosage form, two different types of beads were prepared (micro-beads and macro-beads). The micro-beads were incorporated into the macro-beads at three different concentrations, film coated and then loaded into hard gelatin capsules. The micro-bead formulation contained insulin as the active ingredient and Pharmacel® as the filler. The macro-bead formulations contained one of three different concentrations of micro-beads (20%, 40% and 60% w/w), Ac-di-sol® as disintegrant, Kollidon VA 64® as binder and Pharmacel® as the filler and one of three different absorption enhancers (*A. vera* gel, sodium deoxycholate or TMC) at two different concentration (0.5% and 1% w/w). The rationale was to develop a dosage form that after administration will allow the absorption enhancing agent to release first in the small intestine to open the tight junctions. The insulin will then be released from the micro-beads once they are released from the matrix (macro-beads) in the small intestine. The insulin will then be delivered across the intestinal tissue via the paracellular route (i.e. through the opened tight junctions) into the bloodstream.

CHAPTER 4: RESULTS AND DISCUSSION

4.1 Introduction

In this study a bead-in-matrix delivery system was developed, consisting of micro-bead-in-macro-bead formulations loaded into hard gelatin capsules for oral peptide delivery. The bead-in-matrix delivery system was evaluated with regard to the insulin content (i.e. assay), mass variation, particle size distribution, drug release and transport across excised porcine intestinal tissue. Insulin content of the delivery system was determined by means of a previously developed HPLC method. This method was validated in terms of linearity, limit of detection (LOD), limit of quantification (LOQ) and specificity.

To indicate that the mounting technique of the excised porcine intestinal tissue on the diffusion chambers did not compromise its integrity, a Lucifer yellow (LY) permeation study was done before starting with the bead-in-matrix transport studies. The potential paracellular transport enhancing effect of the uncoated bead-in-matrix formulations containing three different absorption enhancing agents (i.e. *A. vera* gel, sodium deoxycholate and TMC) was investigated by studying their ability to enhance the transport of insulin over excised porcine intestinal tissue, as an indication of their ability to manipulate the tight junctions in the intestine. This ability to enhance membrane permeation of insulin was compared to the control group (micro-beads containing only insulin and Pharmacel®).

4.2 Formulation of the bead-in-matrix delivery system

In principle, the bead-in-matrix delivery system entailed the preparation of micro-beads (passed through a 0.5 mm sieve) loaded into macro-beads (passed through a 2.5 mm). To prove the concept that a bead-in-bead delivery system could be prepared successfully, SEM micrographs (Figure 4.1) were taken of three different bead-in-bead formulations. This was done to proof the concept of a bead-in-matrix formulation, these formulations were prepared without any insulin. The bead-in-bead formulations of which the SEM micrographs were taken differed in terms of the micro-bead content (20, 40 and 60% w/w) as explained in the legend of Figure 4.1.

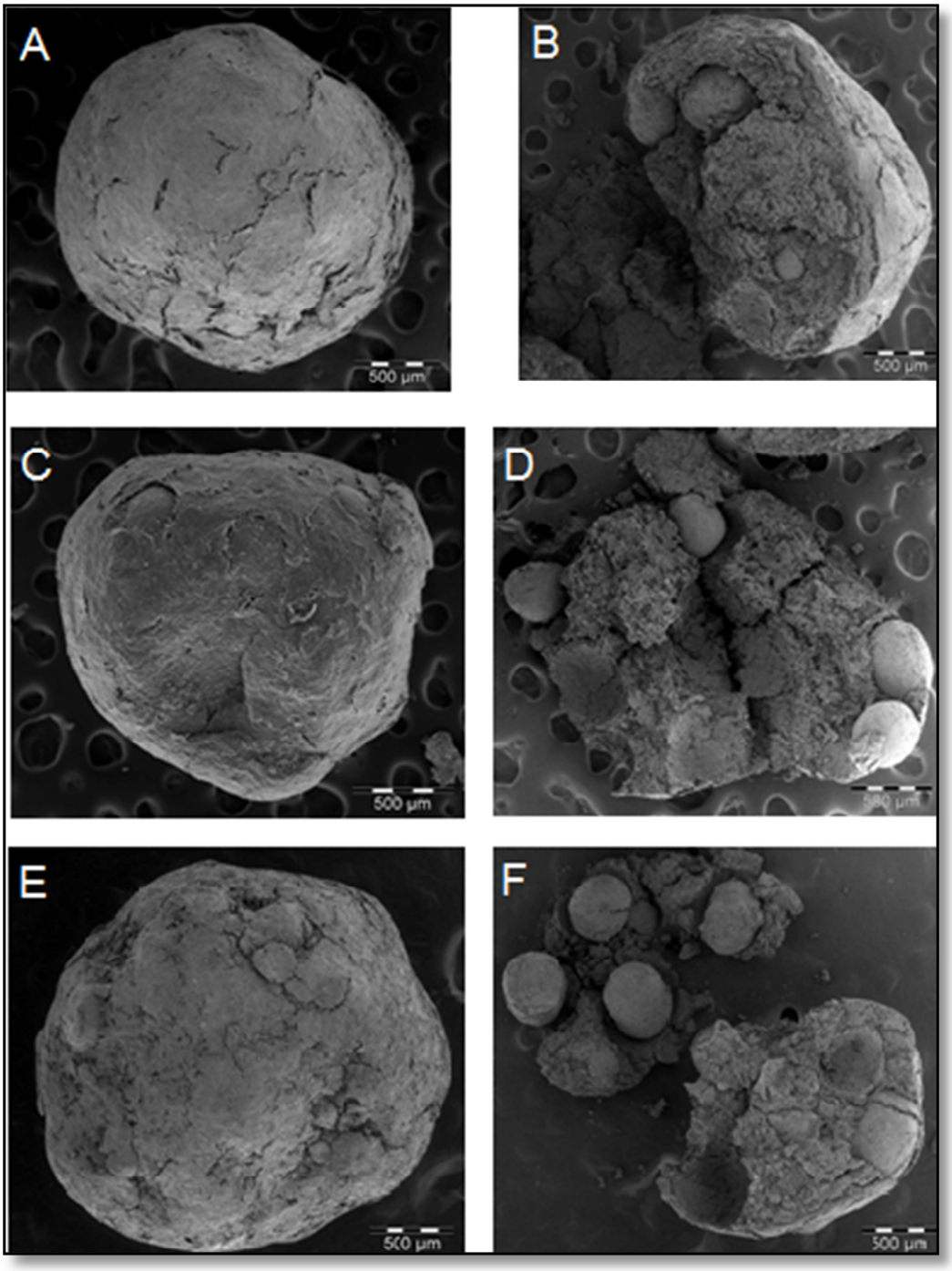

Figure 4.1: SEM micrographs of the bead-in-matrix drug delivery systems with different concentrations of micro-beads. **A & B:** Bead-in-matrix formulation containing 20% w/w micro-beads. **C & D:** Bead-in-matrix formulation containing 40% w/w micro-beads. **E & F:** Bead-in-matrix formulation containing 60% w/w micro-beads

The SEM micrographs in Figure 4.1 clearly indicate that micro-beads could successfully be loaded into macro-beads. The images also indicate that the shape of the bead-in-matrix formulations were dependent on the micro-bead concentration. A higher micro-bead concentration resulted in a slight deviation in the spherical shape of the beads. Based on these results, formulation and preparation of insulin containing bead-in-bead matrix delivery systems (18 formulations as outlined in Table 1.1 in Chapter 1) were done.

4.2.1 Film coating of the bead-in-matrix drug delivery system

Insulin is susceptible to enzymatic and chemical degradation (Buchanan & Revell, 2015:172), a problem that can be overcome to some extent with an enteric coating of the bead-in-matrix delivery system. To evaluate the time needed for spray coating to reach the optimum thickness, different batches of placebo bead-in-matrix formulations were coated for different time periods (i.e 15, 20, 25, 30 min). The thickness of the coating on the beads was investigated by means of SEM micrographs and the formulation with the most appropriate film coating was selected and the time period of coat spraying (i.e. 30 min) was applied to all 18 bead-in-matrix formulations.

Figure 4.2 depicts typical SEM micrographs taken at two different magnifications from placebo bead-in-matrix formulations coated with a mixture of Eudragit® L 100 and Eudragit® S 100.

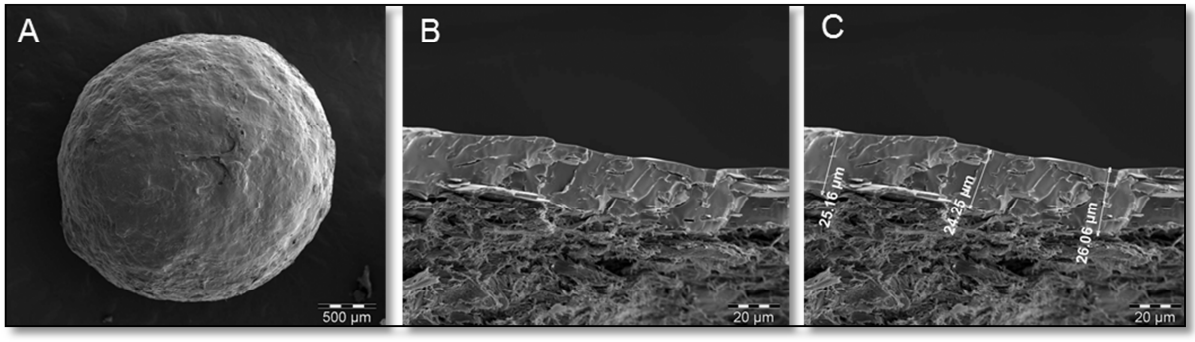

Figure 4.2: Scanning electron microscopy micrographs indicating the film coating on a macro-bead of a typical bead-in-matrix delivery system

The coating was soft and flexible as the blade smeared the film coating when the beads were cut into half (Figure 4.2.B & C), which was also observed by Bashaiwoldu *et al.*, 2011:345. Table 4.2 depicts the coating layer thickness range for the placebo bead-in-matrix formulations for different coating times.

Table 4.1: Coating thickness results for the different coating times

Coating time (min)	Coating thickness range (μm)
15	4.92 – 20.67
20	6.23 – 45.04
25	8.27 – 38.00
30	24.25 – 26.06

From the results in Table 4.2, a coating time of 30 min was selected, due to the small range (24.25 – 26.06 μm) in coating thickness when compared to the other coating thickness ranges. According to Lehmann *et al.* (2001:10) an impermeable coating thickness range is between 20 – 40 μm. The effectiveness of the coating to limit insulin release in an acidic environment was assessed during the dissolution studies.

4.3 Evaluation of bead formulations

In total, 18 different bead formulations were prepared based on the compositions as indicated in Table 1.1 (Chapter 1). These bead formulations were evaluated and the results are discussed in the following sections.

4.3.1 Assay of micro-beads

An assay was performed to determine the quantity of insulin within the micro-bead formulation. Theoretically, a 1 g sample of the micro-bead formulation contained 1 mg of insulin. As the 1 g sample of micro-beads was dispersed in 100 ml of dispersant (KRB solution), the resulting suspension had a theoretical concentration of 0.1 mg/ml. The experimental concentration of insulin in this suspension was determined by means of HPLC using linear regression.

The percentage insulin content in the micro-bead formulation was 59.42%. The percentage was calculated by dividing the experimentally determined insulin content (assay result) with the theoretical insulin content (weighed and included into the mixture during formulation). The loss of insulin can perhaps be explained through physical loss and/or chemical degradation during the production of the micro-bead formulation, freeze drying, handling and storing of the micro-bead formulation. In future studies, the cause for the loss of the active ingredient should be investigated.

4.3.2 Mass variation

An important attribute in pharmaceutical products is a constant dose of active ingredient between individual dosing units within the same batch. Mass variation can be used as an indication of the magnitude in the variation in the dose between individual units within the same batch. The results for mass variation of 10 hard gelatin capsules (size 0) hand filled with the different bead-in-matrix formulations (see Table 1.1) are shown in Table 4.2.

Table 4.2: Mass variation results for hard gelatine capsules filled with different bead-in-matrix formulations

Formulation	Absorption enhancer	Concentration absorption enhancer (% w/w)	Concentration micro-beads (% w/w)	Average mass with standard deviation (g)
A	*A. vera* gel	0.5	20	0.3532 ± 0.0091
B	*A. vera* gel	1	20	0.3802 ± 0.0120
C	*A. vera* gel	0.5	20	0.3806 ± 0.0096
D	*A. vera* gel	1	20	0.3888 ± 0.0137
E	*A. vera* gel	0.5	20	0.4443 ± 0.0167
F	*A. vera* gel	1	20	0.4590 ± 0.0078
G	Sodium deoxycholate	0.5	40	0.4070 ± 0.0146
H	Sodium deoxycholate	1	40	0.4202 ± 0.0092
I	Sodium deoxycholate	0.5	40	0.4029 ± 0.0165
J	Sodium deoxycholate	1	40	0.3975 ± 0.0097
K	Sodium deoxycholate	0.5	40	0.4163 ± 0.121
L	Sodium deoxycholate	1	40	0.4169 ± 0.0150
M	TMC	0.5	60	0.4156 ± 0.0127
N	TMC	1	60	0.4200 ± 0.0131
O	TMC	0.5	60	0.4118 ± 0.0097
P	TMC	1	60	0.4542 ± 0.0194
Q	TMC	0.5	60	0.4258 ± 0.0169
R	TMC	1	60	0.4273 ± 0.0095

According to the USP (2014:492), the weight of an individual bead filled capsule (for each type of bead-in-matrix formulation) must not deviate from the average mass of the bead filled capsule by more than ± 7.5%. The bead-in-matrix formulations prepared in this study complied with this USP specification.

4.3.3 Particle size analysis

4.3.3.1 Bead-in-matrix formulations containing *A. vera* gel

The particle size distributions of the bead-in-matrix formulations for the 0.5% w/w *A. vera* gel formulations (i.e. 20, 40 and 60% w/w micro-bead containing formulations) are shown in Figure 4.3 A, B and C, respectively. The average particle size (D[4,3]) for the different 0.5% w/w *A. vera* gel formulations were 952.615, 984.250 and 938.843 µm for the 20, 40 and 60% w/w micro-bead containing formulations respectively. Likewise, the median of the particle size distributions (d(0.5)) for these formulations were 927.430, 932.407 and 883.118 µm, respectively and the span values were 1.176, 1.002 and 1.069, respectively. It is evident from the particle size distribution histograms (Figure 4.3), as well as the (D[4,3]) and (d(0.5)) parameters that the 0.5% w/w *A. vera* gel formulations exhibited similar distributions, which was to be expected as the same method of preparation was followed for these formulations.

The particle size distributions of the bead-in-matrix formulations for the 1% w/w *A. vera* gel formulations (20, 40 and 60% w/w micro-bead containing formulations) are shown in Figure 4.4 A, B and C, respectively. The average particle size (D[4,3]) for the different 1% w/w *A. vera* gel formulations were 927.551, 948.240 and 991.497 µm for the 20, 40 and 60% w/w micro-bead containing formulations, respectively. Likewise, the median of the particle size distributions (d(0.5)) for these formulations were 883.552, 918.648 and 945.670 µm, respectively and the span values were1.117, 1.101 and 1.031, respectively. It is evident form the particle size distribution histograms, as well as the (D[4,3]) and (d(0.5)) parameters that the 1% w/w *A. vera* gel formulations exhibited similar distributions, which was to be expected as the same method of preparation was followed for these formulations.

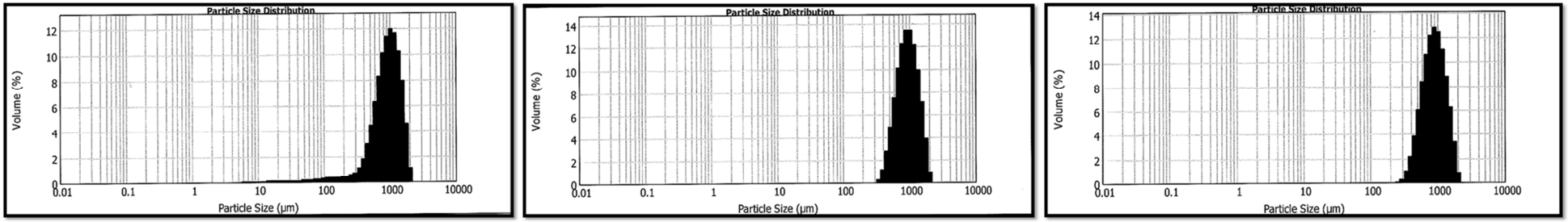

Figure 4.3: Particle size plot for the bead-in-matrix formulations containing 0.5% w/w *A. vera* gel **A:** Bead-in-matrix system, 20% w/w micro-beads (Formulation A) **B:** Bead-in-matrix system, 40% w/w micro-beads (Formulation G) **C:** Bead-in-matrix system, 60% w/w micro-beads (Formulation M)

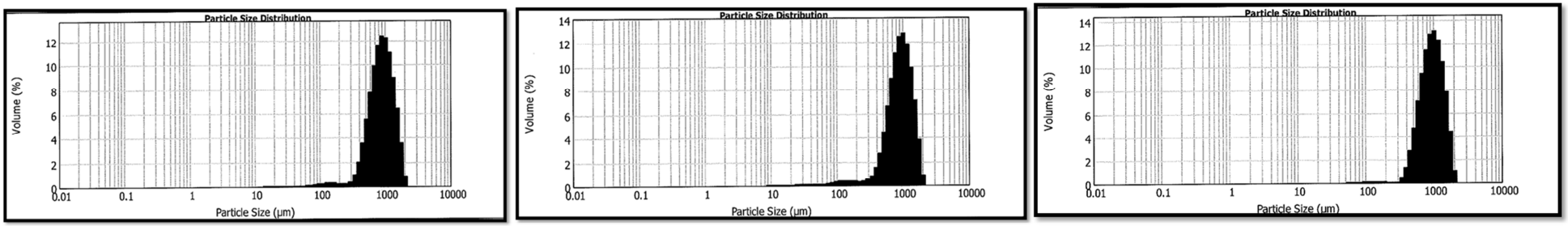

Figure 4.4: Particle size plot for the bead-in-matrix formulations containing 1% w/w *A. vera* gel. **A:** Bead-in-matrix system, 20% w/w micro-beads (Formulation B) **B:** Bead-in-matrix system, 40% w/w micro-beads (Formulation H) **C:** Bead-in-matrix system, 60% w/w micro-beads (Formulation N)

The particle size analysis data for the bead-in-matrix formulations containing *A. vera* gel as the absorption enhancing agent is summarized in Table 4.3.

Table 4.3: Summary of the particle size analysis data for absorption enhancer *A. vera* gel containing bead-in-matrix formulations

Formulation	Concentration absorption enhancer (% w/w)	Concentration micro-beads (% w/w)	Average median (d(0.5)) with standard deviation (µm)	Average volume weighed size distribution (D[4,3]) with standard deviation (µm)	Span with standard deviation
A	0.5	20	927.43 ± 53.69	952.62 ± 65.40	1.176 ± 0.21
G	0.5	40	932.41 ± 29.58	984.26 ± 27.97	1.002 ± 0.02
M	0.5	60	883.12 ± 66.41	938.84 ± 61.06	1.069 ± 0.05
B	1	20	883.55 ± 35.44	927.55 ± 31.69	1.117 ± 0.13
H	1	40	918.65 ± 98.14	948.24 ± 100.37	1.101 ± 0.22
N	1	60	945.67 ± 31.36	991.50 ± 34.06	1.031 ± 0.05

It is evident from the data in Table 4.3 that all the 0.5% and 1% w/w *A. vera* gel formulations exhibited a similar particle size distribution and that the particle size distribution parameters (D[4,3]) and (d(0.5)) were similar. The similarity for the distributions were also evident for the width of the distributions as characterized by the span value for the distributions. The span values indicated a relative narrow particle size distribution, which is characteristic of beads prepared by means of extrusion spheronisation.

4.3.3.2 Bead-in-matrix formulations of sodium deoxycholate

The particle size distributions of the bead-in-matrix formulations for the 0.5% w/w sodium deoxycholate formulations (i.e. 20, 40 and 60% w/w micro-bead containing formulations) are shown in Figure 4.5 A, B and C respectively. The average particle size (D[4,3]) for the different 0.5% w/w sodium deoxycholate formulations were 926.445, 1050.591 and 887.110 µm for the 20, 40 and 60% w/w micro-bead containing formulations, respectively. Likewise, the median of the particle size distributions (d(0.5)) for these formulations were 875.888, 1008.623 and 871.358 µm, respectively and the span values were 1.092, 0.923 and 1.409, respectively. It is evident form the particle size distribution histograms, as well as the (D[4,3]) and (d(0.5))

parameters that the 0.5% w/w sodium deoxycholate formulations exhibited similar particle size distributions, which was to be expected as the same method of preparation was followed for these formulations.

The particle size distributions of the bead-in-matrix formulations for the 1% w/w sodium deoxycholate formulations (20, 40 and 60% w/w micro-bead containing formulations) are shown in Figure 4.6 A, B and C, respectively. The average particle size (D[4,3]) for the different 1% w/w sodium deoxycholate formulations were 1029.134, 971.537 and 941.499 µm for the 20, 40 and 60% w/w micro-bead containing formulations, respectively. Likewise, the median of the particle size distributions (d(0.5)) for these formulations were 991.111, 944.077 and 920.021 µm, respectively and the span values were 0.933, 1.123 and 1.184, respectively. It is evident form the particle size distribution histograms, as well as the (D[4,3]) and (d(0.5)) parameters, that the 1% w/w sodium deoxycholate formulations exhibited similar particle size distributions, which was to be expected as the same method of preparation was followed for these formulations.

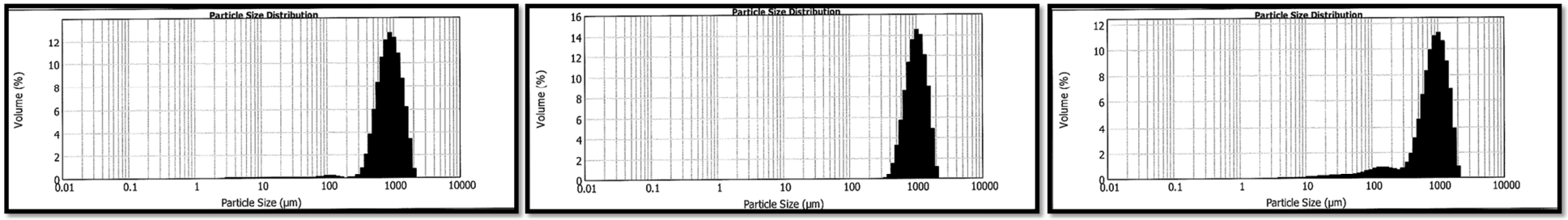

Figure 4.5: Particle size plot for the bead-in-matrix formulations containing 0.5% w/w sodium deoxycholate. **A:** Bead-in-matrix system, 20% w/w micro-beads (Formulation C) **B:** Bead-in-matrix system, 40% w/w micro-beads (Formulation I) **C:** Bead-in-matrix system, 60% w/w micro-beads (Formulation O)

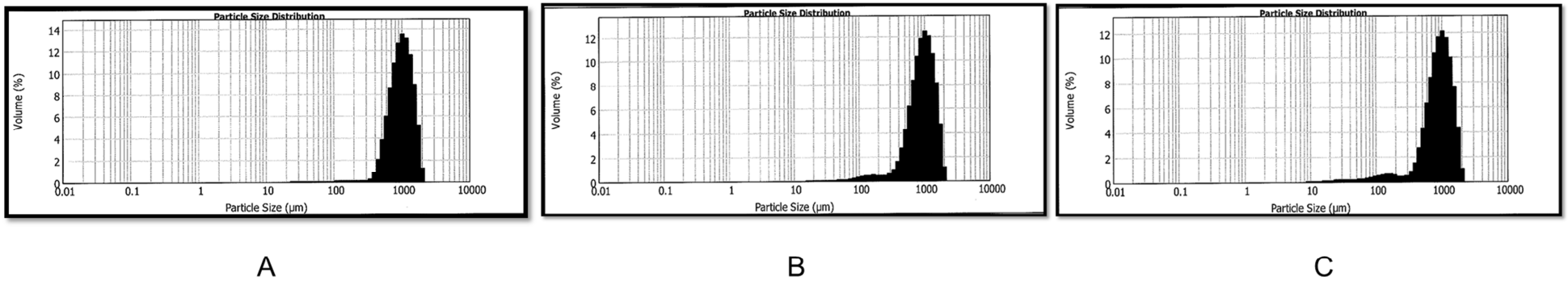

Figure 4.6: P Particle size plot for the bead-in-matrix formulations containing 1% w/w sodium deoxycholate. **A:** Bead-in-matrix system, 20% w/w micro-beads (Formulation D) **B:** Bead-in-matrix system, 40% w/w micro-beads (Formulation J) **C:** Bead-in-matrix system, 60% w/w micro-beads (Formulation P)

The particle size analysis data for the bead-in-matrix formulations containing sodium deoxycholate as the absorption enhancing agent is summarized in Table 4.4.

Table 4.4: Summary of the particle size analysis data for absorption enhancer sodium deoxycholate containing bead formulations

Formulation	Concentration absorption enhancer (% w/w)	Concentration micro-beads (% w/w)	Average median (d(0.5)) with standard deviation (µm)	Average volume weighed size distribution (D[4,3]) with standard deviation (µm)	Span with standard deviation
C	0.5	20	875.89 ± 101.94	926.45 ± 102.58	1.09 ± 0.11
I	0.5	40	1008.62 ± 35.46	1050.59 ± 43.39	0.92 ± 0.06
O	0.5	60	871.36 ± 22.66	887.11 ± 35.98	1.41 ± 0.14
D	1	20	991.11 ± 39.47	1029.13 ± 45.04	0.99 ± 0.08
J	1	40	944.08 ± 74.15	971.54 ± 70.39	1.12 ± 0.13
P	1	60	920.02 ± 49.11	941.50 ± 51.52	1.18 ± 0.12

Similar to the *A. vera* gel containing formulations, it is evident from the data in Table 4.4 that all the 0.5% and 1% w/w sodium deoxycholate formulations exhibited a similar particle size distribution and that the particle size distribution parameters (D[4,3]) and (d(0.5)) were also similar. The similarity for the distributions were also evident for the width of the distributions as characterized by the span value for the distributions, which indicated a relatively narrow particle size distribution.

4.3.3.3 Bead-in-matrix formulations for TMC

The particle size distributions of the bead-in-matrix formulations for the 0.5% w/w TMC formulations (20, 40 and 60% w/w micro-bead containing formulations) are shown in Figure 4.7 A, B and C, respectively. The average particle size (D[4,3]) for the different 0.5% w/w TMC formulations were 929.061, 928.172 and 972.393 µm for the 20, 40 and 60% w/w micro-bead containing formulations, respectively. Likewise, the median of the particle size distributions (d(0.5)) for these formulations were 888.518, 890.908 and 930.541 µm, respectively and the span values were 1.121, 1.188 and 1.080, respectively. It is evident form the particle size distribution histograms, as well as the (D[4,3]) and (d(0.5)) parameters that the 0.5% w/w TMC

formulations exhibited similar distributions, which was to be expected as the same method of preparation was followed for these formulations.

The particle size distributions of the bead-in-matrix formulations for the 1% w/w TMC formulations (20, 40 and 60% w/w micro-bead containing formulations) are shown in Figure 4.8 A, B and C, respectively. The average particle size (D[4,3]) for the different 1% w/w TMC formulations were 965.384, 948.997 and 1045.620 µm for the 20, 40 and 60% w/w micro-bead containing formulations, respectively. Likewise, the median of the particle size distributions (d(0.5)) for these formulations were 913.294, 900.647 and 1009.288 µm, respectively and the span values were 1.002, 1.064 and 0.950, respectively. It is evident form the particle size distribution histograms, as well as the (D[4,3]) and (d(0.5)) parameters that the 1% w/w TMC formulations exhibited similar distributions which was to be expected as the same method of preparation was followed for these formulations.

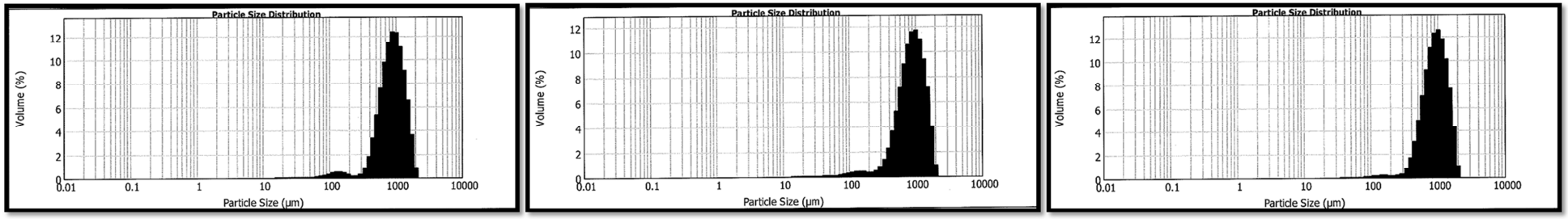

Figure 4.7: Particle size plot for the bead-in-matrix formulations containing 0.5% w/w TMC (Formulation E) **A:** Bead-in-matrix system, 20% w/w micro-beads (Formulation K) **B:** Bead-in-matrix system, 40% micro-beads. **C:** Bead-in-matrix system, 60% w/w micro-beads (Formulation Q)

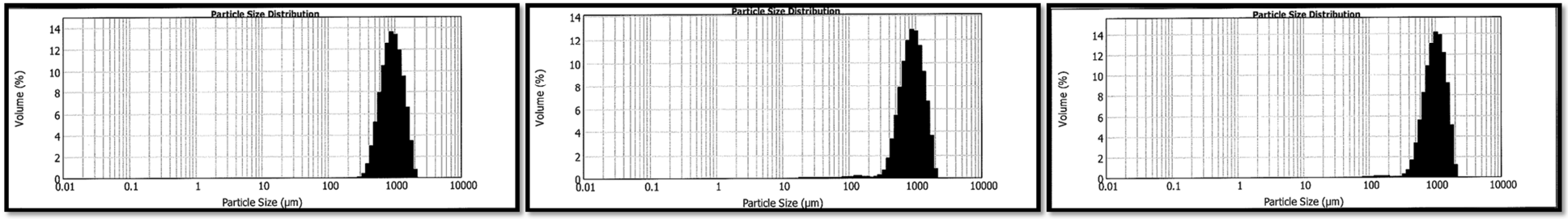

Figure 4.8: Particle size plot for the bead-in-matrix formulations containing 1% w/w TMC. **A:** Particle size distribution plot for the bead-in-matrix, 20% w/w micro-beads (Formulation F) **B:** Particle size distribution plot for the bead-in-matrix, 40% w/w micro-beads (Formulation L) **C:** Particle size distribution plot for the bead-in-matrix, 60% w/w micro-beads (Formulation R)

The particle size analysis data for the bead-in-matrix formulations containing TMC as the absorption enhancing agent is summarized in Table 4.5.

Table 4.5: Summary of the particle size analysis for absorption enhancer TMC containing bead formulations

Formulation	Concentration absorption enhancer (% w/w)	Concentration micro-beads (% w/w)	Average median (d(0.5)) with standard deviation (µm)	Average volume weighed size distribution (D[4,3]) with standard deviation (µm)	Span with standard deviation
E	0.5	20	88.51 ± 22.39	929.06 ± 24.34	1.12 ± 0.04
K	0.5	40	890.91 ± 93.32	928.17 ± 86.737	1.19 ± 0.16
Q	0.5	60	930.54 ± 39.89	972.39 ± 37.615	1.08 ± 0.08
F	1	20	913.29 ± 69.88	965.38 ± 63.023	1.00 ± 0.07
L	1	40	900.65 ± 32.13	949.00 ± 38.88	1.06 ± 0.07
R	1	60	1009.29 ± 39.93	1045.62 ± 39.51	0.95 ± 0.09

It is evident from the data in Table 4.5 that all the 0.5% and 1% w/w TMC formulations exhibited a similar particle size distribution and that the particle size distribution parameters (D[4,3]) and (d(0.5)) were also similar. The similarity for the distributions were also evident for the width of the distributions as characterized by the span value for the distributions.

4.3.3.4 Summary of particle size analysis

From the data obtained from the particle size analysis (Table 4.4 – 4.6), it is clear that there is a relatively small difference in terms of particle size between the 18 different bead-in-matrix formulations. This minimal difference between the particle sizes of the formulations was expected due to the fact that the same production procedures were followed with all 18 bead-in-matrix formulations. All the formulations were also passed through the same sieves (0.5 mm for the micro-beads and 2.5 mm for the macro-beads) during the extrusion step of the bead production process.

4.3.4 Drug release of the particle size analysis

The micro-beads (beads containing only insulin) inside the bead-in-matrix delivery system developed in this study should ideally have a delayed release. The rationale behind this is to allow time for the absorption enhancing agents (contained in the macro-bead) to move to the site of absorption and open the tight junctions prior to insulin release in an effort to improve insulin absorption. The insulin should therefore reach the site of absorption slightly later than the absorption enhancer. The delay in insulin release after the absorption enhancer was released, was ensured by incorporating the insulin in a second bead (i.e. the micro-bead) that was placed inside the macro-beads.

Furthermore, the enteric coating would protect the insulin against enzymatic and chemical degradation in the stomach (Maher *et al.,* 2016:3; Hamman *et al.,* 2005:166). The film coating solution used in this study was specifically formulated (a combination of 50% Eudragit®L100 and 50% Eudragit®S100) to dissolve above pH 6 (Zahirul *et al.,* 2000:550). According to the (BP, 2018:XII),the specifications for film coated, delayed release dosage forms specifythat no individual dosage form should release more than 10% of their drug content within 2 hours in an acidic dissolution medium.

4.3.4.1 Bead-in-matrix formulations for containing *A. vera* gel

The percentage insulin release from the coated bead-in-matrix formulations containing *A. vera* gel as absorption enhancer is depicted in Figure 4.9.

From Figure 4.9 it can be concluded that the drug releasing properties of all the *A. vera* gel bead-in-matrix formulations were similar. All of the *A. vera* gel bead-in-matrix formulations passed the BP criteria for film coated delayed release dosage forms since none of the formulations released more than 5% of their insulin content during the first 2 h of the dissolution study in an acidic medium (0.1 M HCl). The Eudragit® film coating applied to the bead-in-matrix systems effectively prevented the release of insulin in the acidic dissolution medium confirming its enteric coating properties, which are necessary to protect the insulin against chemical and enzymatic degradation in the stomach.

Within 10 min after increasing the pH from 1.2 to 6.8, a relatively high release rate of insulin was observed as indicated by the steep ascending slope of the release curves up to 155 min. A second phase of slightly slower insulin release followed, which can be observed from 155 min to 245 min. This could be explained by diffusion of insulin from the deeper layers of the micro-beads. However, it is important to mention that within 35 min after adjusting the pH, more than 50% of the insulin content was already released from all *A. vera* gel bead-in-matrix formulations. Furthermore, within 150 min after adjusting the pH, all of the *A. vera* gel bead-in-matrix

formulations released 100% of their insulin content. This indicated that the bead-in-matrix systems are capable of releasing the complete insulin dose within the period of movement through the small intestine which is approximately 3 h according to Davis, 2005:250.

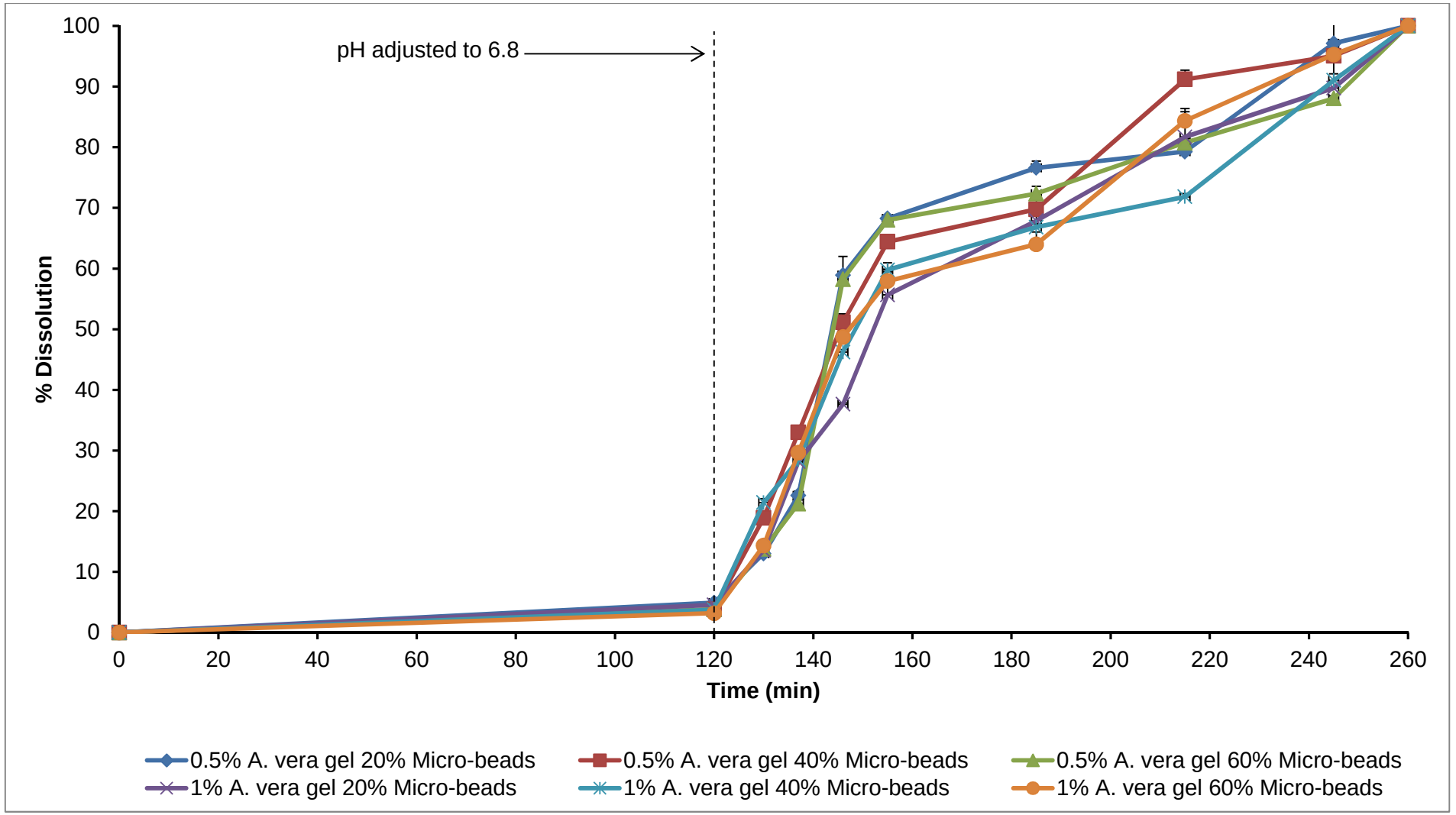

Figure 4.9: Percentage insulin release from the coated bead-in-matrix formulations for *A. vera* gel plotted as a function of time

4.3.4.2 Bead-in-matrix formulations for sodium deoxycholate

The percentage insulin release from the coated bead-in-matrix formulations containing sodium deoxycholate is depicted in Figure 4.10.

From Figure 4.10, it can be seen that the drug release profiles of all the sodium deoxycholate containing bead-in-matrix formulations followed similar trends, except for two formulations that showed slightly slower release during approximately the last third of the release period (i.e. from 155 to 245 min). All of the sodium deoxycholate bead-in-matrix formulations passed the BP criteria for film coated delayed release dosage forms and none of the formulations released more than 5% of the insulin content during the first 2 h of the dissolution study in an acidic medium (0.1 M HCl). Effective enteric coating of the bead-in-matrix systems was therefore achieved, indicating protection of the insulin against chemical and enzymatic degradation in the stomach.

Similar to the *A. vera* gel containing formulations, within 10 min after increasing the pH from 1.2 to 6.8, a relatively fast release of insulin was detected as observed by the steep dissolution curve slopes up to 155 min. Again, a second phase of slower release can be observed from 155 min to 245 min. After 35 min from the pH adjustment, more than 40% insulin was released from all sodium deoxycholate containing bead-in-matrix formulations, and within 150 min after adjusting the pH, all of the sodium deoxycholate bead-in-matrix formulations released 100% of the insulin content.

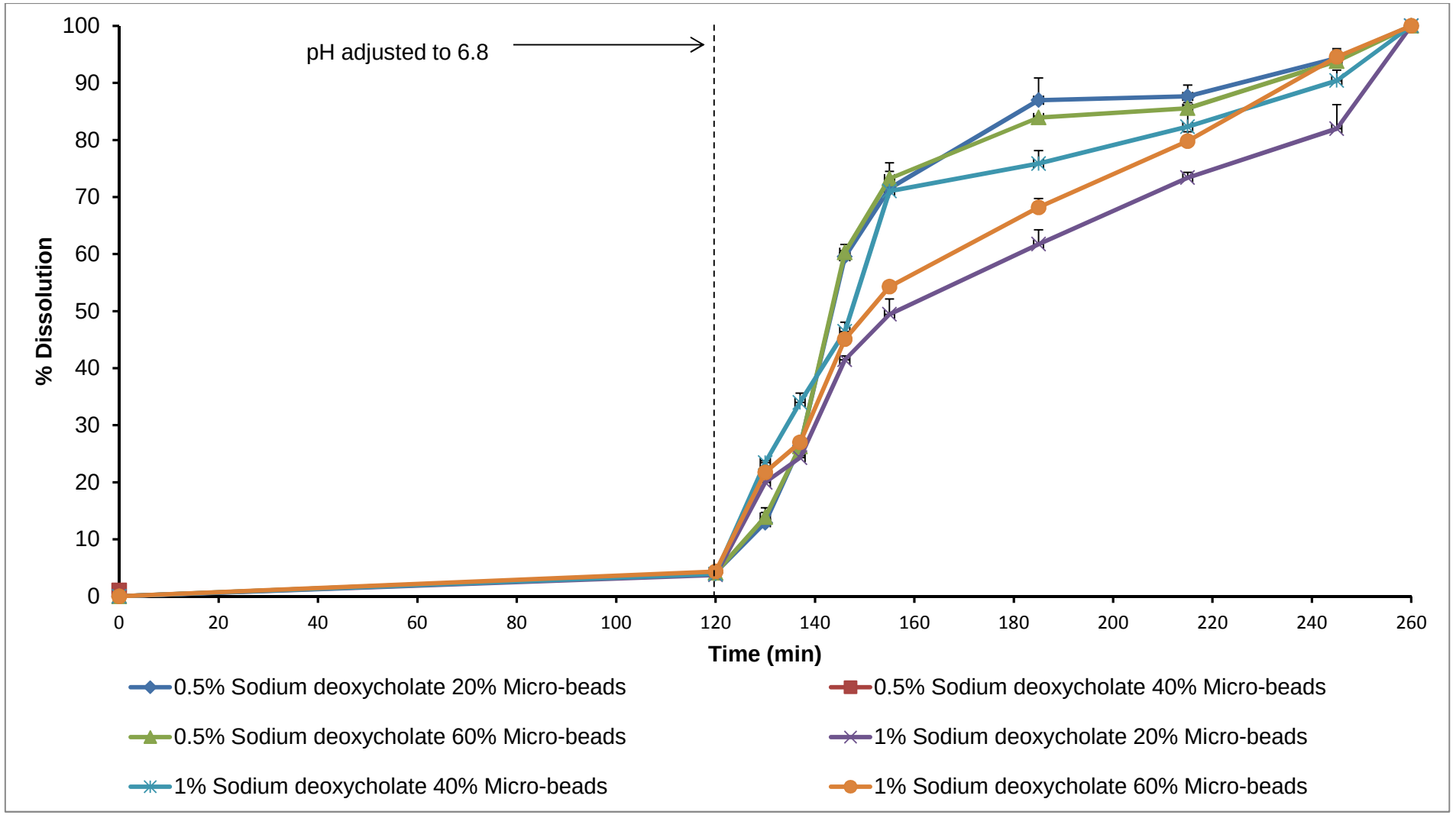

Figure 4.10: Percentage release of insulin as a function of time for sodium deoxycholate bead-in-matrix formulations

4.3.4.3 Bead-in-matrix formulations for TMC

The percentage insulin drug release from the coated bead-in-matrix formulations containing TMC is depicted in Figure 4.11.

From Figure 4.11, it can be concluded that the drug releasing properties of all the TMC containing bead-in-matrix formulations followed similar trends. All of the TMC containing bead-in-matrix formulations passed the BP criteria for film coated delayed dosage forms and none of the formulations released more than 5% of the insulin content during the first 2 h of the dissolution study in an acidic medium (0.1 M HCl). Once again, this indicated the dosage forms' ability to protect the insulin against the harsh environment in the stomach.

As with the previous formulations (both *A. vera* gel and sodium deoxycholate containing), within 10 min after increasing the pH from 1.2 to 6.8, a notable rate of insulin release was detected. Also, more than 50% of the insulin content was already released after 35 min from all TMC containing bead-in-matrix formulations and within 150 min after adjusting the pH all of the TMC containing bead-in-matrix formulations released 100% of the insulin content. The delivery system should therefore release the complete insulin dose during transit through the small intestine.

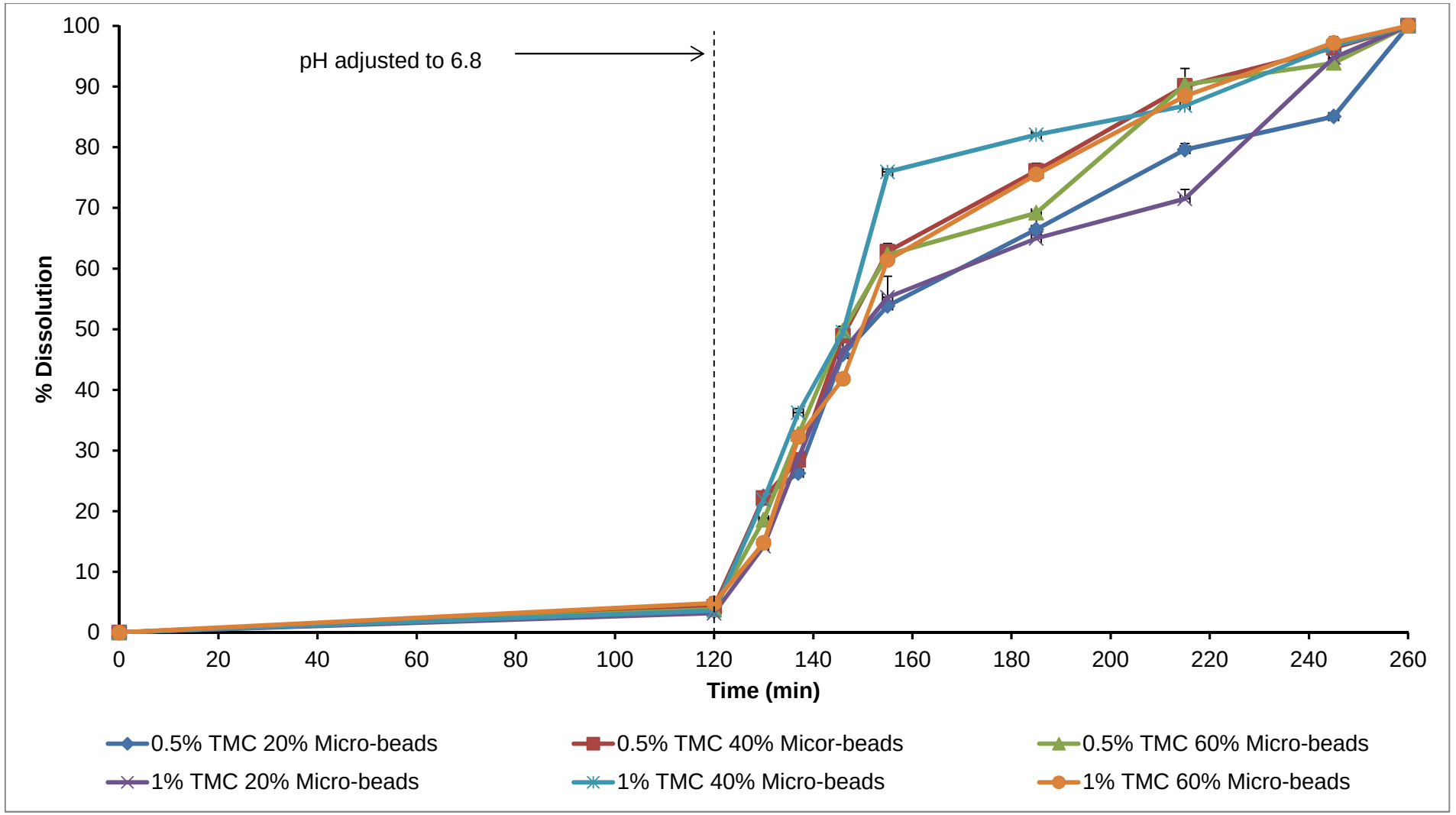

Figure 4.11: Percentage release of insulin as a function of time for TMC bead-in-matrix formulations

4.3.4.4 Summary of drug release studies

When comparing the results of the drug release studies (Figures 4.9 – 4.11), all 18 bead-in-matrix formulations exhibited similar release profiles. The similarity in drug release can be attributed to the same preparation method used to produce all 18 bead-in-matrix formulations. As mentioned in Section 4.2.3.4, all 18 bead-in-matrix formulations passed through the same size sieve during extrusion, followed by film coating the formulations in the same manner and for the same period of time. From the data obtained during the dissolution studies, it is clear that all 18 bead-in-matrix formulations complied with the BP criteria (<10% dissolution) for the drug release from film coated dosage forms. The compliance to the BP criteria indicated that the film coating effectively produced pH dependent delayed release properties known as enteric coating. The release of insulin was detected soon after the pH was adjusted to higher values within the dissolution vessels, which indicated that effective insulin release should be achieved in the small intestines once the beads are emptied from the stomach. Within 130 min after the pH was adjusted, 100% of the insulin content was released from all 18 bead-in-matrix formulations. This indicated that all the insulin should be completely released from the bead-in-matrix dosage form during movement through the small intestine before the colon is reached.

4.3.5 Insulin transport across excised porcine intestinal tissue

4.3.5.1 Control group

4.3.5.1.1 Lucifer yellow (LY)

The LY study was conducted to indicate that the mounting technique of the excised porcine intestinal tissue on the Sweetana-Grass diffusion chambers was not detrimental to tissue integrity and served as an indication of the viability of the porcine intestinal tissue for the duration of the transport study. The LY study therefore served to confirmthe tissue integrity over the entire transport period. According to Irvine *et al.* (1999:29), the normal range for LY permeability is between $1 – 7 \times 10^{-7}$ cm/s. During the LY control experiment an apparent permeability coefficient (P_{app}) value of 3.12×10^{-7} cm/s was obtained, which indicated that the tissues mounted in the diffusion chamber were intact. Figure 4.12 demonstrates the cumulative percentage LY transport obtained as a function of time when a LY solution with a concentration of 50 µg/ml was applied to the apical side of the excised porcine intestinal tissue in the Sweetana-Grass diffusion apparatus for a period of 120 min.

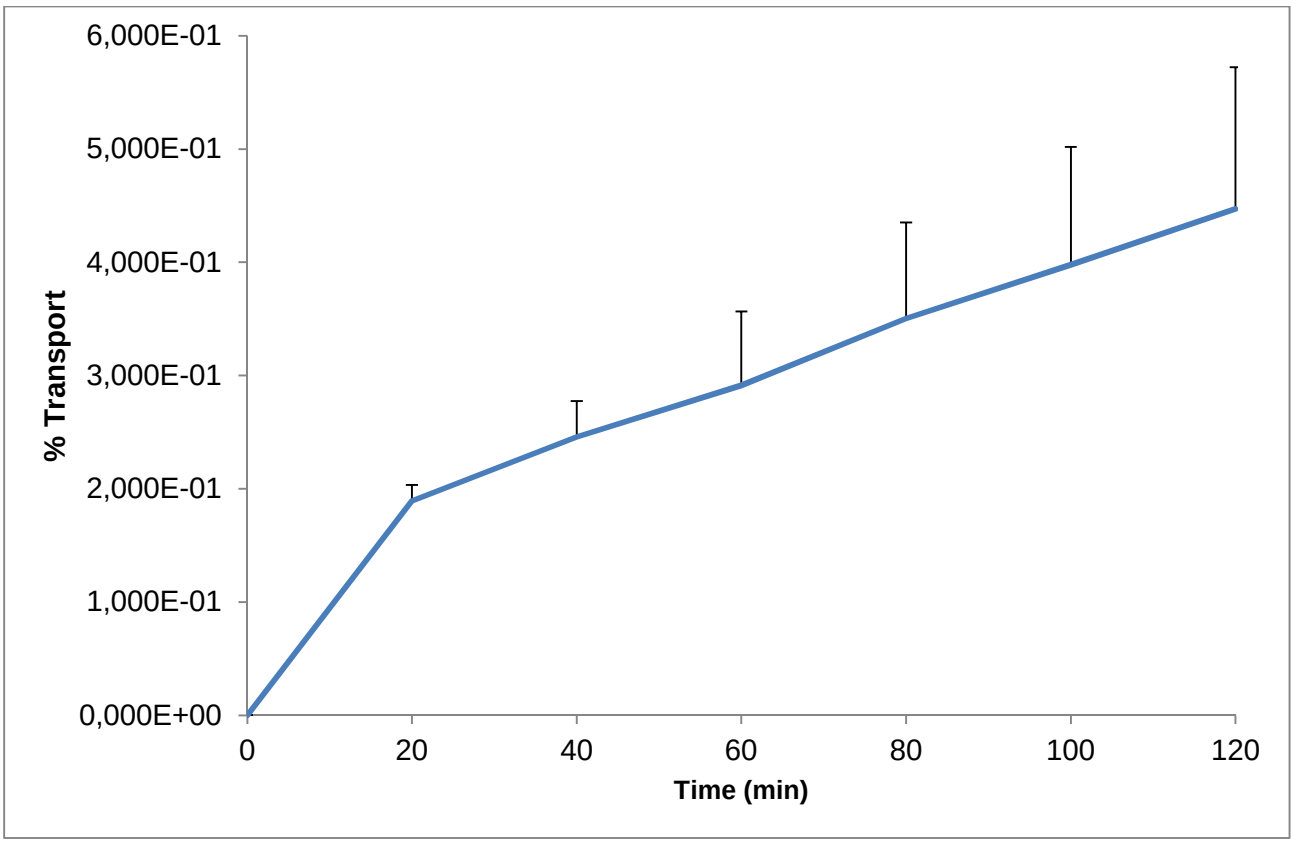

Figure 4.12: Percentage LY transport across excised porcine intestinal tissue plotted as a function of time for 50 µg/ml LY

The LY permeation study indicated that the porcine intestinal tissue remained viable for a period of 2 h – the duration and conditions of the transport experiments in this study.

4.3.5.1.2 Insulin beads (Micro-beads)

In Figure 4.13, the cumulative percentage insulin transport across the excised porcine intestinal tissue from the micro-beads containing only insulin (control group) for a period of 120 minutes is depicted. In this experimental control group, the excised porcine intestinal tissue was not exposed to any absorption enhancing agents.

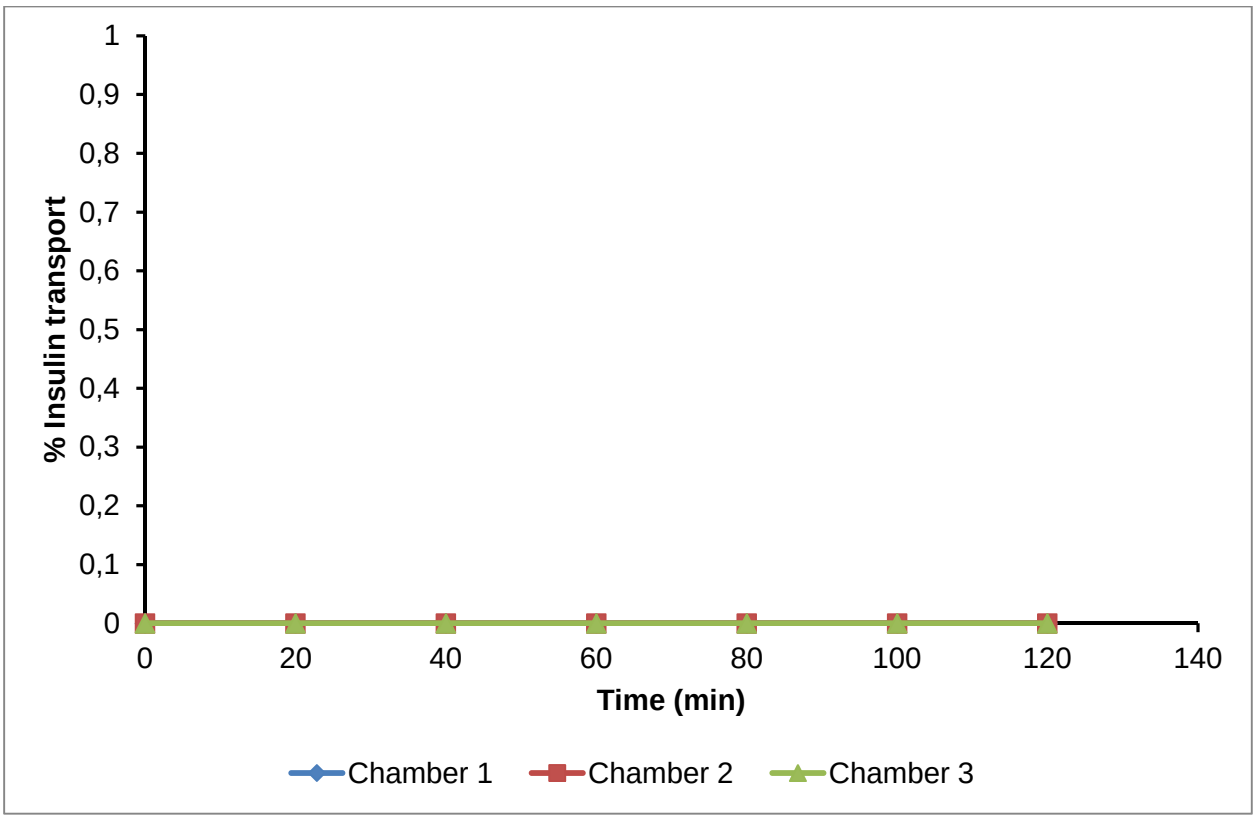

Figure 4.13: Percentage insulin transport across excised porcine intestinal tissue plotted as a function of time for insulin containing micro-beads without exposure to any absorption enhancing agents

Without the excised porcine intestinal tissue being exposed to any absorption enhancing agents, it is clear that insulin did not permeate the excised porcine intestinal tissue to any detectable extent (Figure 4.13) over a period of 120 min after the application of micro-beads. This can be attributed to the poor bioavailability, large size and hydrophilic properties of insulin (bioavailabilty after oral administration is typically <1% *in vivo*) (Maher *et al.,* 2016:2; Renukuntla *et al*., 2013:75).

4.3.5.2 Bead-in-matrix formulations containing *A. vera* gel

The cumulative percentage insulin absorptive transport obtained as a function of time for the bead-in-matrix formulations containing *A. vera* gel across porcine intestinal tissue for a period of 120 min is depicted in Figure 4.14. A summary of the average cumulative insulin transport for the different bead-in-matrix formulations containing *A. vera* gel is given in Table 4.6. In Figure 4.15, the data on the P_{app} values for insulin calculated from the transport data for insulin after application of the *A. vera* gel formulations to porcine intestinal tissue are given.

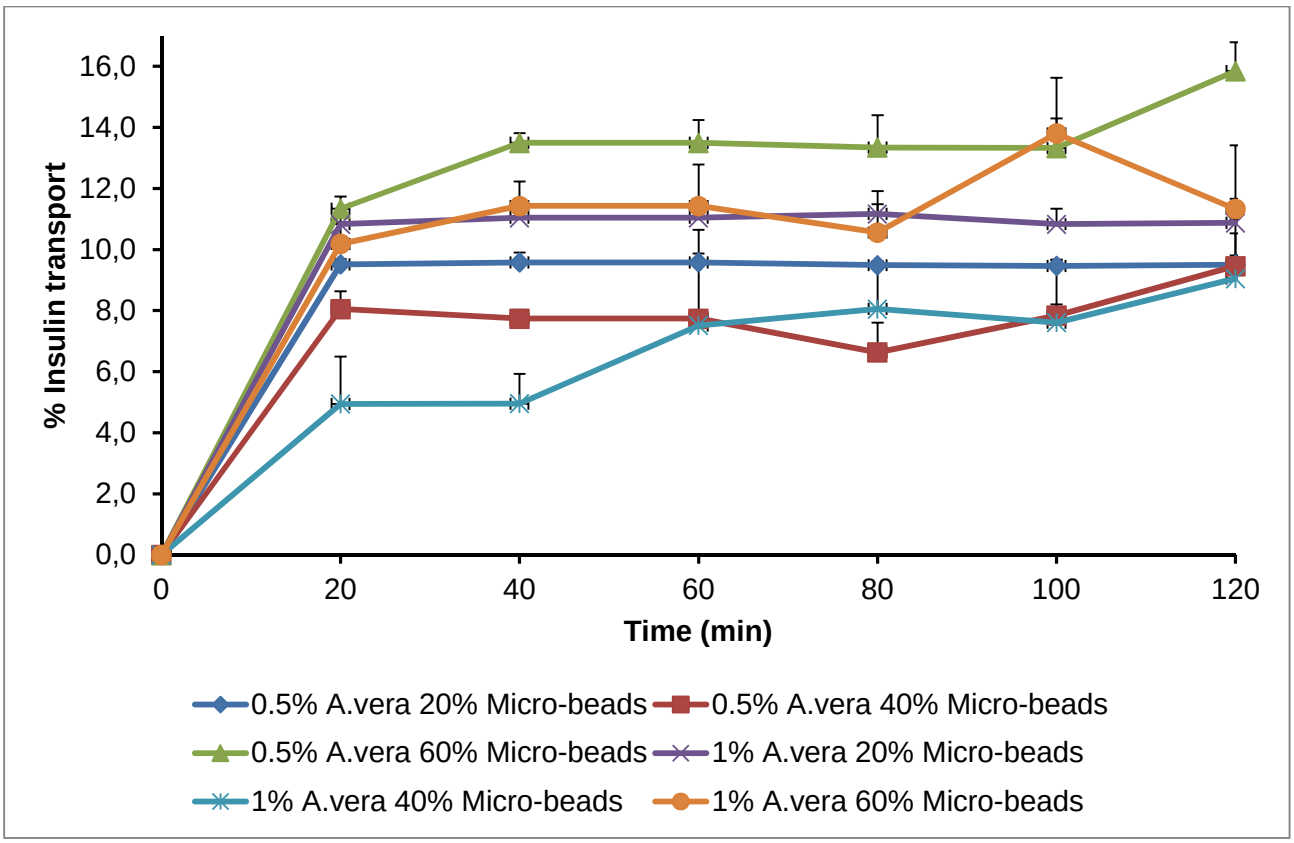

Figure 4.14: Percentage insulin transport across excised porcine intestinal tissue plotted as a function of time for bead-in-matrix formulations containing *A. vera* gel

The bead-in-matrix formulations containing *A. vera* gel as an absorption enhancer showed an average cumulative transport of between 7.90 ± 0.60 – 13.45 ± 0.95% over 2 h. Other *in vitro* studies have shown that *A. vera* gel has the ability to open tight junctions between adjacent cells across Caco-2 cell monolayers and excised rat intestinal tissue, consequently enhancing the transport of peptide drugs like insulin (Radha & Laxmipriya 2015:23; Beneke *et al.,* 2012:481; Chen *et al.,* 2009:591). In this *ex vivo* study, *A. vera* gel formulated into the bead-in-matrix delivery systems has shown the ability to enhance the intestinal transport of insulin when compared to the control group.

Table 4.6: Summary of the average cumulative insulin transport after application of the different bead-in-matrix formulations containing *A. vera* gel as absorption enhancer

Formulation	% Absorption enhancer (w/w)	% Micro-beads (w/w)	Average transport with standard deviation (%)
A	0.5	20	9.53 ± 0.23
G	0.5	40	7.90 ± 0.60
M	0.5	60	13.45 ± 0.95
B	1	20	10.95 ± 0.33
H	1	40	7.03 ± 2.25
N	1	60	11.45 ± 1.70

The lowest cumulative insulin transport was obtained from the 0.5% w/w *A. vera* gel and 40% w/w micro-bead containing formulation, while the highest cumulative insulin transport was obtained for the 0.5% w/w *A. vera* gel and 60% w/w containing micro-bead formulation. It is evident from the transport results that *A. vera* gel formulated into the bead-in-matrix dosage forms acted as an effective absorption enhancer for insulin across excised porcine intestinal tissues.

Both the 0.5% w/w and 1% w/w *A. vera* gel bead-in-matrix delivery systems (i.e. the 20, 40 and 60% micro-bead containing systems) exhibited inverse bell-shaped patterns in terms of insulin delivery across the excised porcine intestinal tissues. The insulin transport obtained by the 0.5% w/w *A. vera* gel formulation containing 60% w/w micro-beads was statistically significantly higher ($p<0.05$) to the 20% and 40% w/w micro-bead containing formulations. This may be explained by the higher amount of insulin available for transport across the intestinal tissues via the paracellular route in combination with the opening of the tight junctions by the *A. vera* gel. The higher insulin transport obtained with the 0.5% w/w *A. vera* gel, 60% w/w micro-bead formulation was also significantly higher in comparison to the 1% w/w *A. vera* gel, 20% and 40% w/w micro-bead containing formulations. The transport of insulin across porcine intestinal tissue was dependent on a complex interplay between the micro-bead loading as well as the *A. vera* gel concentration in the bead-in-matrix delivery systems.

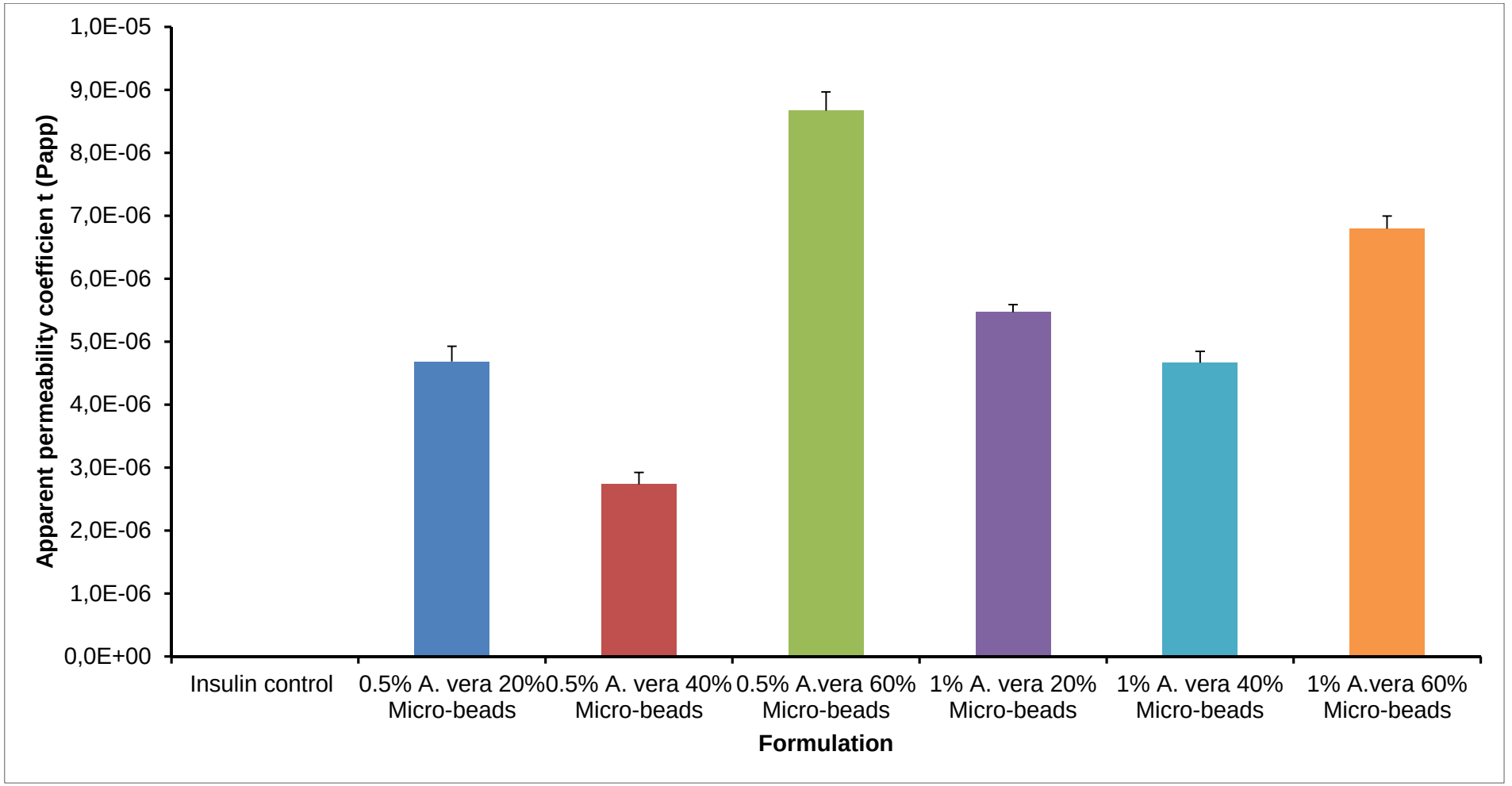

Figure 4.15: Apparent permeability coefficient (P_{app}) values for insulin after exposure to bead-in-matrix formulations containing *A.vera* gel as absorption enhancer

4.3.5.3 Bead-in-matrix formulations containing sodium deoxycholate

The cumulative percentage insulin transport obtained as a function of time after application of the bead-in-matrix formulations containing sodium deoxycholate across porcine intestinal tissue for a period of 120 min is depicted in Figure 4.16. A summary of the average cumulative insulin transport for the different bead-in-matrix formulations containing sodium deoxycholate is given in Table 4.7. In Figure 4.17, the P_{app} values for insulin calculated from the transport data for insulin after application of the sodium deoxycholate formulations to excised porcine intestinal tissues are given.

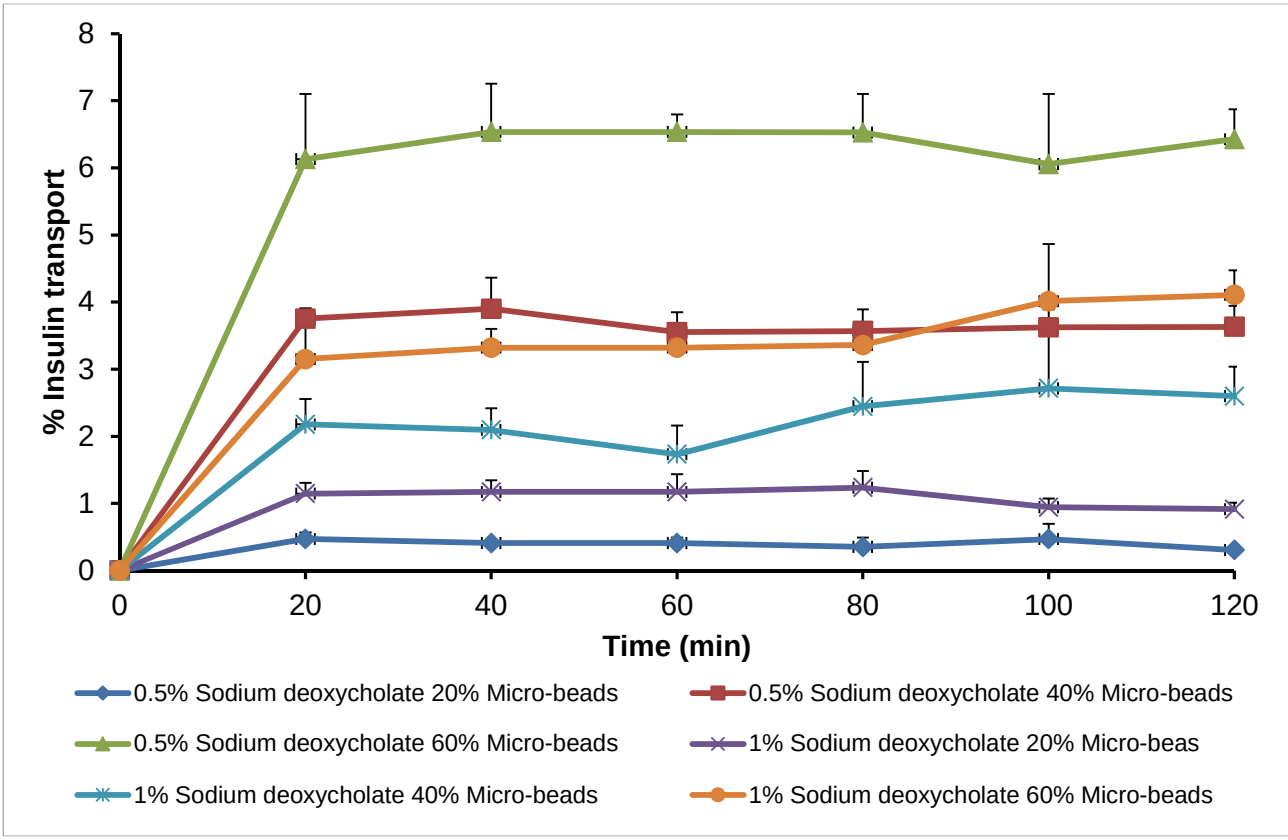

Figure 4.16: Percentage cumulative insulin transport across excised porcine intestinal tissue plotted as a function of time for bead-in-matrix formulations containing sodium deoxycholate as the absorption enhancing agent

It is evident from Figure 4.15 that sodium deoxycholate formulated into the bead-in-matrix delivery systems increased the intestinal transport of insulin form the apical to the basolateral direction compared to that of the control group (beads containing insulin only). The bead-in-matrix formulations containing sodium deoxycholate as an absorption enhancer showed an average cumulative transport of between 0.42 ± 0.10 – 6.35 ± 0.67% over a period of 2 h. Previous studies showed that sodium deoxycholate could successfully

enhance the transport of insulin across intestinal tissues (Sakai *et al.,* 1999:33; Uchiyama *et al.,* 1999:1248). In this *ex vivo* study, sodium deoxycholate formulated into novel bead-in-matrix dosage forms showed the ability to enhance the transport of insulin across excised porcine intestinal tissues.

Table 4.7: Summary of the average cumulative insulin transport after application of the different bead-in-matrix formulations containing sodium deoxycholate as absorption enhancer

Formulation	% Absorption enhancer (w/w)	% Micro-beads (w/w)	Average transport with standard deviation (%)
C	0.5	20	0.42 ± 0.10
I	0.5	40	3.68 ± 0.32
O	0.5	60	6.35 ± 0.67
D	1	20	1.08 ± 0.18
J	1	40	2.28 ± 0.34
P	1	60	3.55 ± 0.45

The lowest cumulative insulin transport was obtained for the 0.5% w/w sodium deoxycholate, 20% w/w micro-bead containing formulation, while the highest cumulative insulin transport was obtained for the 0.5% w/w sodium deoxycholate, 60% w/w containing micro-bead formulation. From the data in Table 4.7, an increase in insulin transport is noted with an increase in micro-bead content in both the 0.5% and 1% sodium deoxycholate containing bead-in-matrix delivery systems. It is evident from the transport results that *A. vera* gel was more effective as an absorption enhancer than sodium deoxycholate because higher cumulative transport of insulin was obtained with the former.

The increase in insulin transport observed for the 0.5% w/w sodium deoxycholate, 60% w/w micro-bead containing formulation was statistically significantly ($p < 0.05$) higher than the transport obtained for the 20 and 40% w/w micro-bead containing formulations with the same sodium deoxycholate concentration. It is evident from this data that an increase in micro-bead content resulted in a corresponding increase in insulin transport. This can be attributed to a higher total quantity of insulin available for transport (thus higher concentration gradient) with a higher micro-bead concentration for the 40 and 60% w/w

formulations, respectively. For the 1% w/w sodium deoxycholate formulations, an increase in insulin transport was also observed with an increase in micro-bead content. However, similar to the *A. vera* gel formulations, an increase in absorption enhancer concentration from 0.5 to 1% w/w was not associated with corresponding increase in insulin transport, specifically at the 60% w/w micro-bead concentration. The transport data therefore indicates that an increase in absorption enhancer concentration is not necessarily associated with an additional benefit in terms of insulin transport. Considering that bile salts are generally considered to act by destabilising membrane activities (Li *et al.,* 2016:2; Mukherjee *et al.,* 2016:495), the lower the concentration of the bile salt, the lower the potential for toxicity (i.e. cell damage) should be.

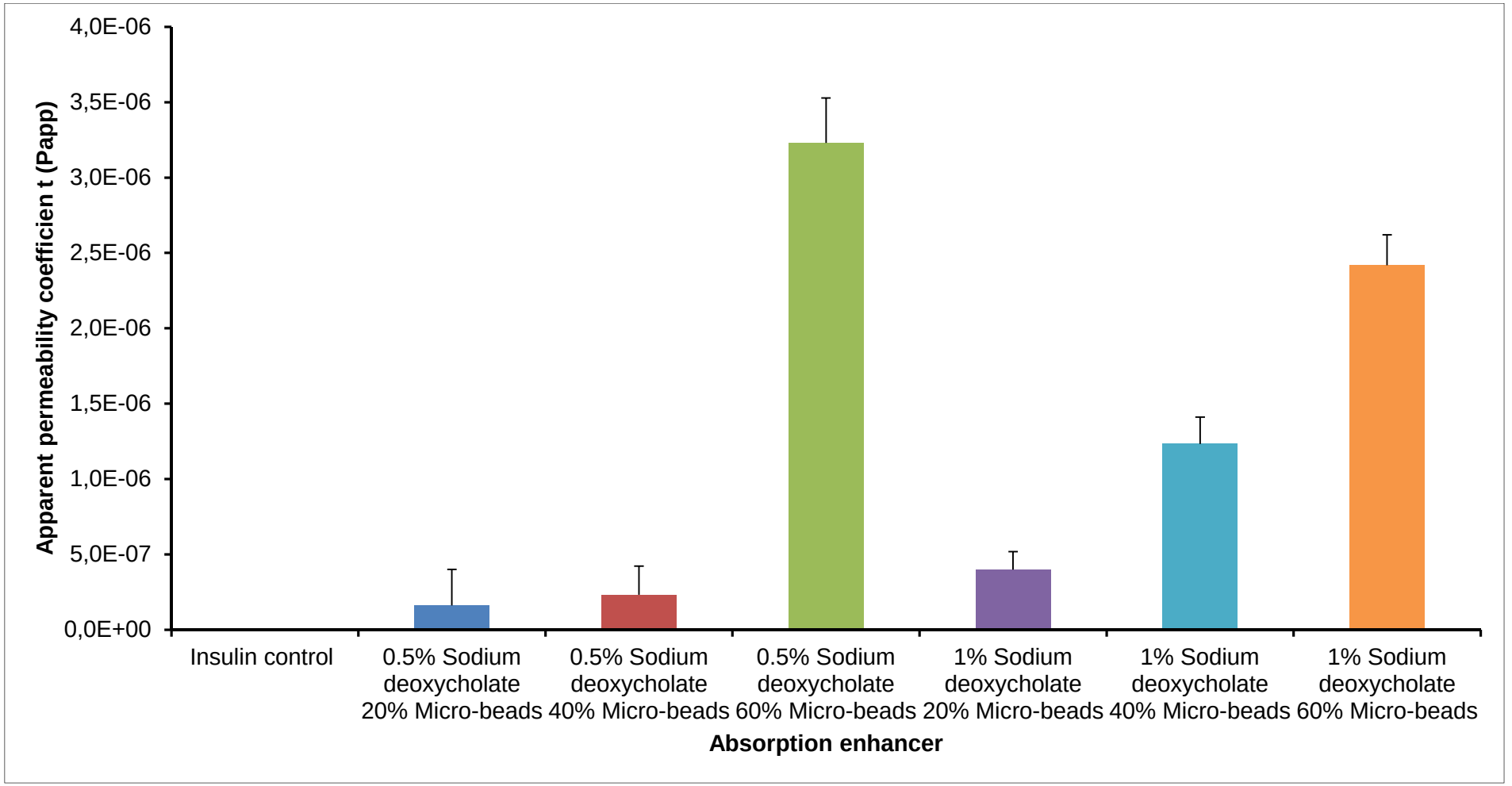

Figure 4.17: Apparent permeability coefficient (P_{app}) values for insulin after pre-exposure to bead-in-matrix formulations containing sodium deoxycholate as absorption enhancer

4.3.5.4 Bead-in-matrix formulations containing TMC

The cumulative percentage insulin absorptive transport obtained as a function of time for the bead-in-matrix formulation containing TMC across excised porcine intestinal tissue for a period of 120 min is depicted in Figure 4.18. A summary of the average cumulative insulin transport for the different bead-in-matrix formulations containing TMC is given in Table 4.8. In Figure 4.19, the data on the P_{app} values for insulin calculated from the transport data for insulin after application of the sodium deoxycholate formulations to porcine intestinal tissue are given.

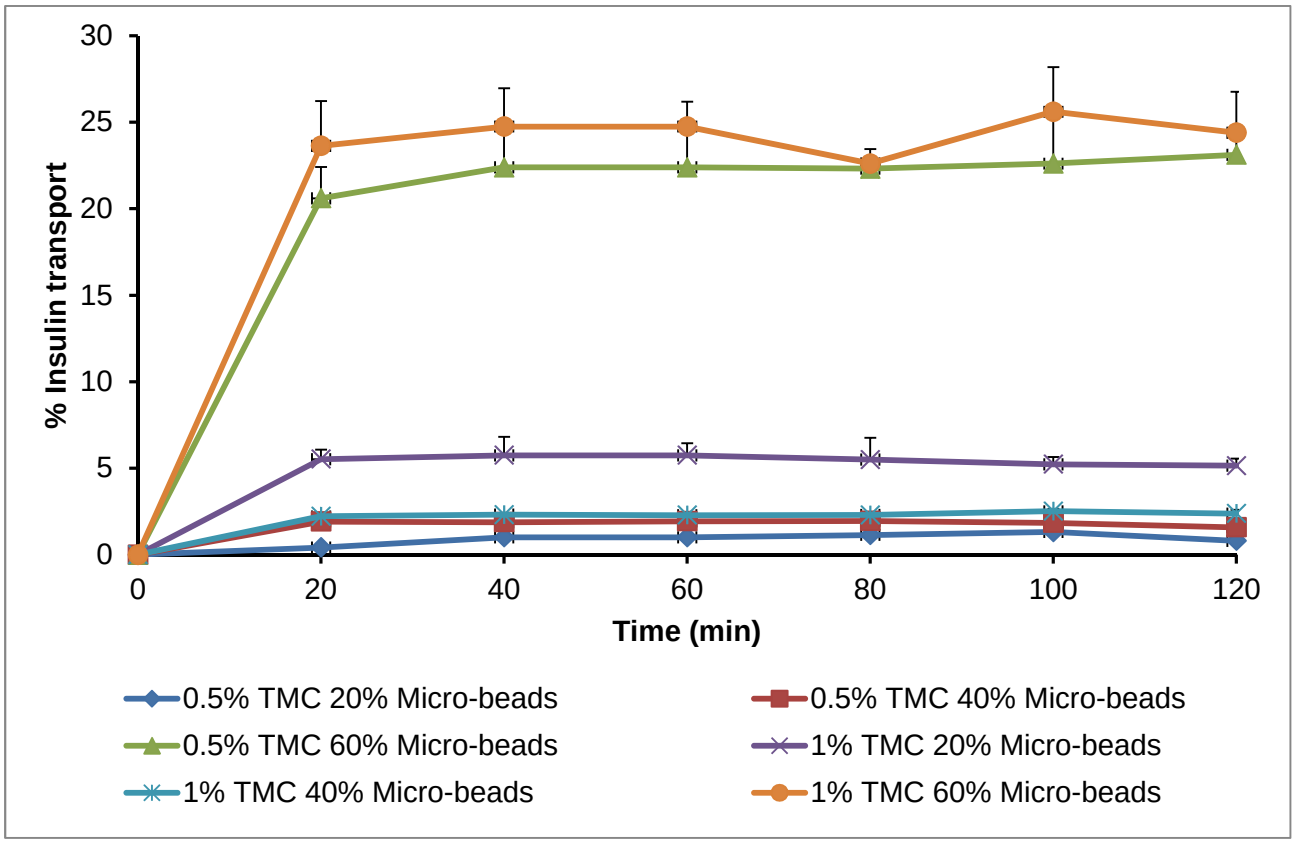

Figure 4.18: Cumulative percentage insulin transport across excised porcine intestinal tissue plotted as a function of time for bead-in-matrix formulations containing TMC

The bead-in-matrix formulations containing TMC as an absorption enhancer showed an average cumulative transport of between 0.93 ± 0.35 – 24.27 ± 2.00% after 2 h. In previous studies, it was concluded that TMC is a potent absorption enhancer, which was capable of increasing the intestinal absorption (paracellular transport) and consequently the bioavailability of peptide drugs by opening the tight junctions in rats and pigs (Van der Merwe *et al.,* 2004:90-91; Thanou *et al.,* 2001:S99). This *ex vivo* study showed that TMC

formulated into bead-in-matrix dosage forms was successful in opening the tight junctions in the excised porcine intestinal tissue to facilitate paracellular transport. From Figure 4.18 it can be seen that there is a pronounced difference in between the formulations containing 20 and 40% w/w micro-beads in comparison to the formulations containing 60% w/w micro-beads.

Table 4.8: Summary of the average cumulative insulin transport after application of the different bead-in-matrix formulations containing TMC as absorption enhancer

Formulation	% Absorption enhancer (w/w)	% Micro-beads (w/w)	Average transport with standard deviation (%)
E	0.5	20	0.93 ± 0.35
K	0.5	40	1.85 ± 0.25
P	0.5	60	22.23 ± 1.85
F	1	20	5.45 ± 0.75
L	1	40	2.33 ± 0.13
R	1	60	24.27 ± 2.00

The lowest cumulative insulin transport was obtained for the 0.5% w/w TMC, 20% w/w micro-bead containing formulation, while the highest cumulative insulin transport was obtained for the 1.0% w/w TMC, 60% w/w containing micro-bead formulation. It is evident from the transport results that for both the 0.5% and 1% w/w TMC containing formulations with a 60% w/w micro-bead content, that the highest average cumulative percentage insulin transport of 22.23 ±1.85 and 24.27 ±2.00%, respectively. It is clear from the data in Figure 4.16 and Table 4.8, that the increased insulin transport for both the 0.5% and 1.0% w/w TMC containing formulations, that the improved insulin transport was dependent on the micro-bead content. This trend was, however, only observed for the 60% w/w micro-bead containing formulations. The reason for this is not clear yet and should be investigated in future studies, but it may be explained by potential ionic complexation between the TMC and insulin due to opposite charges. This causes that a threshold concentration of insulin is needed to overcome the effect of the complexation and thereby the absorption enhancing effect of TMC is more clearly visible.

The insulin transport obtained with the 0.5% w/w TMC, 60% w/w micro-bead containing formulation is statistically significantly ($p<0.05$) higher than the insulin transport obtained with the 0.5% w/w TMC, 20% and 40% w/w micro-bead containing formulations. Furthermore, the insulin transport obtained with this formulation was also statistically significantly higher ($p < 0.05$) than the transport obtained for both the, 1% w/w TMC, 20% and 40% w/w micro-bead containing formulations as well. The 1% w/w TMC, 60% w/w micro-bead containing formulation also produced a statistically significantly higher insulin transport than both the 0.5% w/w TMC, 20% and 40% w/w, both the 1% w/w TMC, 20% and 40% w/w micro-bead containing formulations. The ability of TMC to open tight junctions can be attributed to the interaction of the protonated TMC with the anionic components of the glycoproteins found on the surface of the epithelial cells and the fixed negative charges of the interior of the tight junctions. TMC has been noted not to be absorbed itself and to have no acute cellular toxicity (Sandri *et al.,* 2010:363; van der Merwe *et al.,* 2004:86; Junginger & Verhoef, 1998:375).

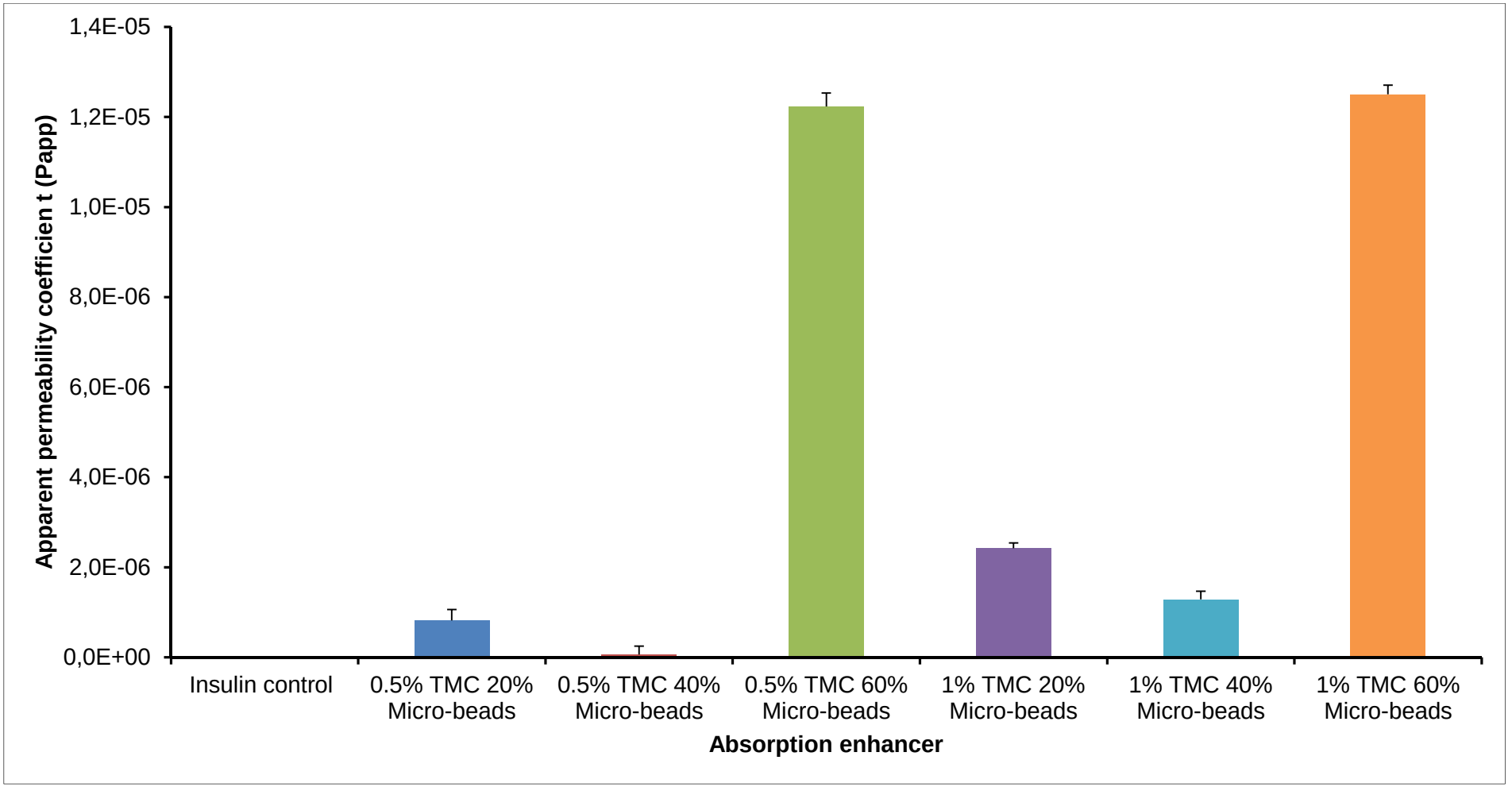

Figure 4.19: Apparent permeability coefficient (P_{app}) values for insulin after pre-exposure to bead-in-matrix formulations containing TMC as absorption enhancer

4.3.5.5 Summary of transport data

To summarise the transport results, the *A. vera* gel containing bead-in-matrix delivery systems showed in general to be the most effective in terms of insulin delivery across excised porcine intestinal tissues in comparison to the delivery systems containing sodium deoxycholate and TMC. However, the TMC containing bead-in-matrix formulations depicted the highest percentage of insulin transport at 60% w/w micro-bead concentration at both 0.5 and 1% w/w TMC.

4.4 Validation of HPLC analytical method

4.4.1 Linearity

An example of a typical standard curve obtained for instrument response (peak area) as function of insulin concentration is given in Figure 4.20.

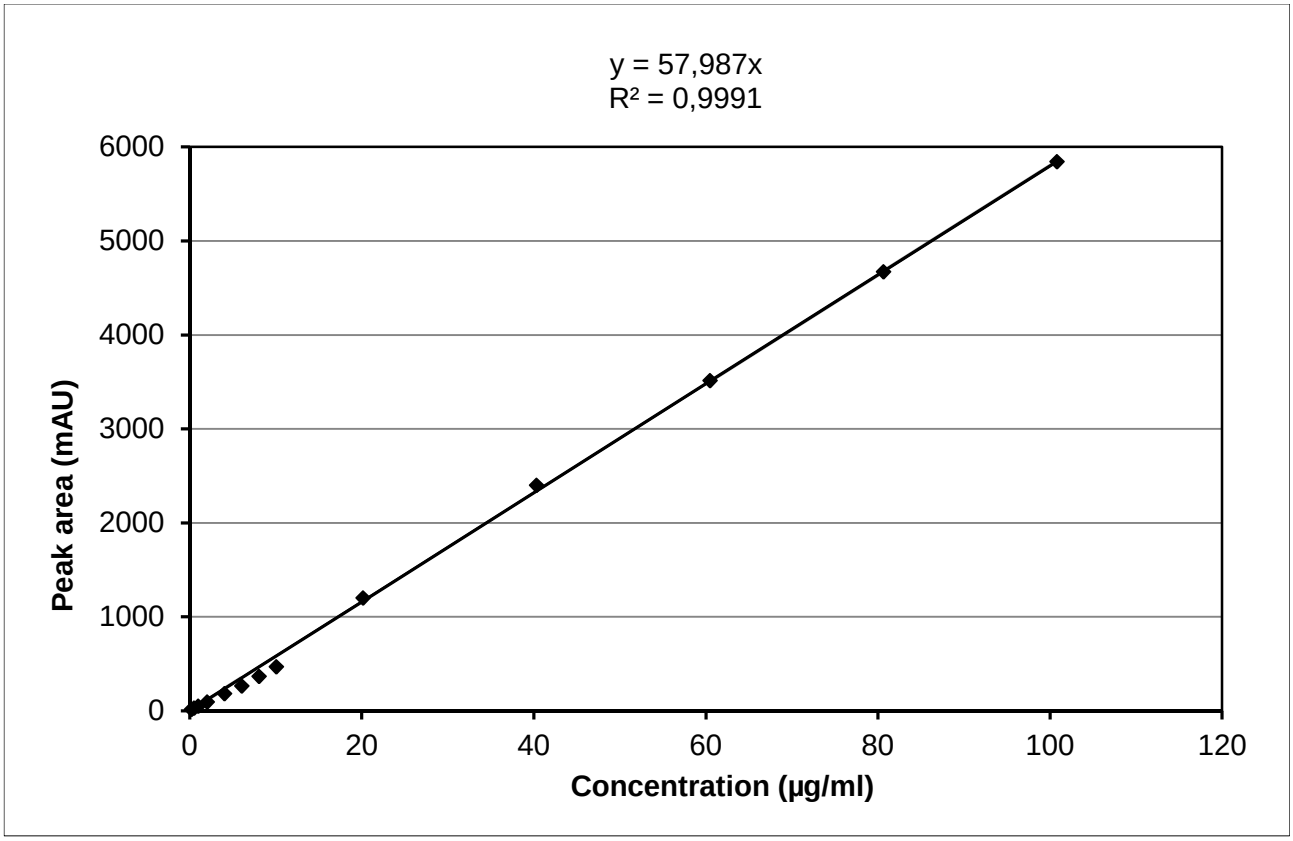

Figure 4.20: Example of a standard curve for insulin during validation

The regression coefficient (R^2) for this standard curve was 0.9991 for insulin, which complies with the requirements for the HPLC method (USP, 2017:783). The linearity data therefore indicate that a linear relationship existed between insulin concentration and instrument response (peak area).

4.4.2 Limit of detection (LOD) and limit of quantification (LOQ)

The HPLC method's LOD for insulin was determined as 0.02 µg/ml. The HPLC method's LOQ for insulin was determined as 0.2 µg/ml. The HPLC method was therefore sensitive enough to determine the insulin concentrations in the transport and dissolution samples.

4.4.3 Specificity

The chromatograms for insulin in the presence of the other compounds are illustrated in Figures 4.21 to 4.24. The different compounds used for the specificity testing included the absorption enhancers (i.e. *A. vera* gel, sodium deoxycholate and TMC), Pharmacel®, Ac-di-sol®, Kollidon®VA 64, ethanol and Krebs-Ringer Bicarbonate buffer (used as transport medium).

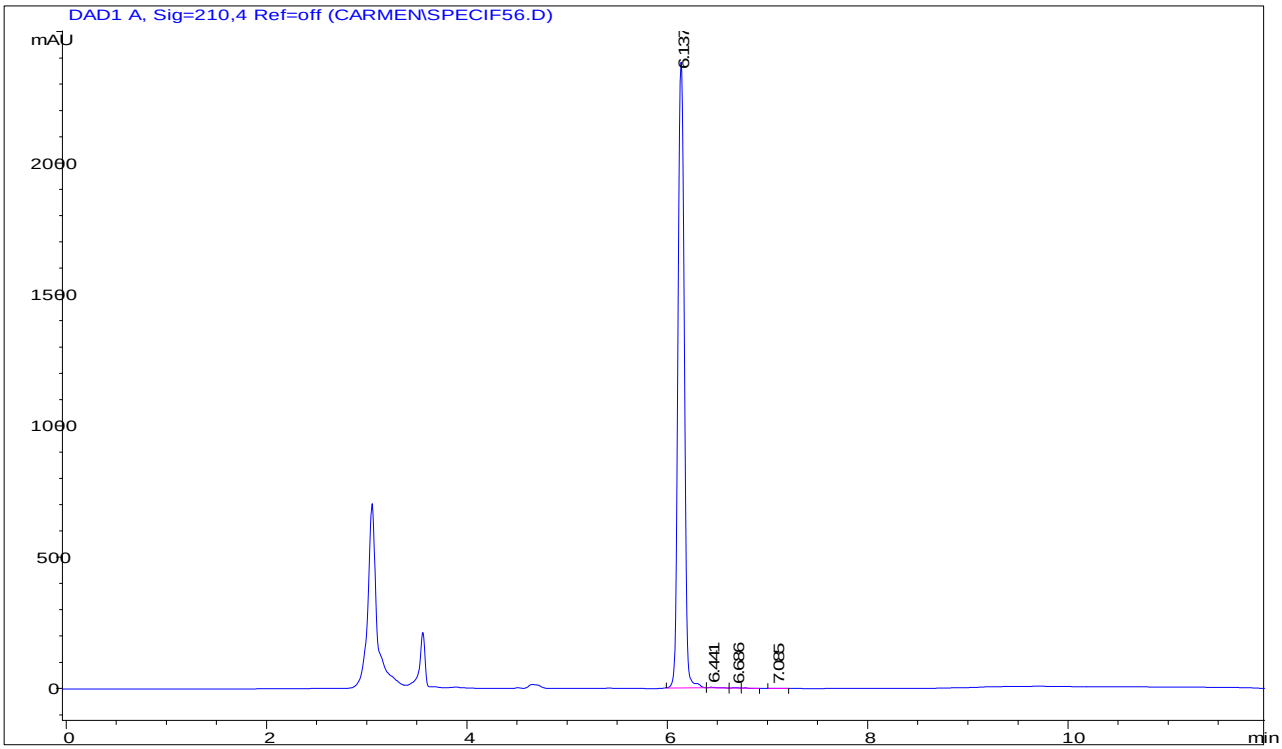

Figure 4.21: Chromatogram of insulin in the presence of *A. vera* gel

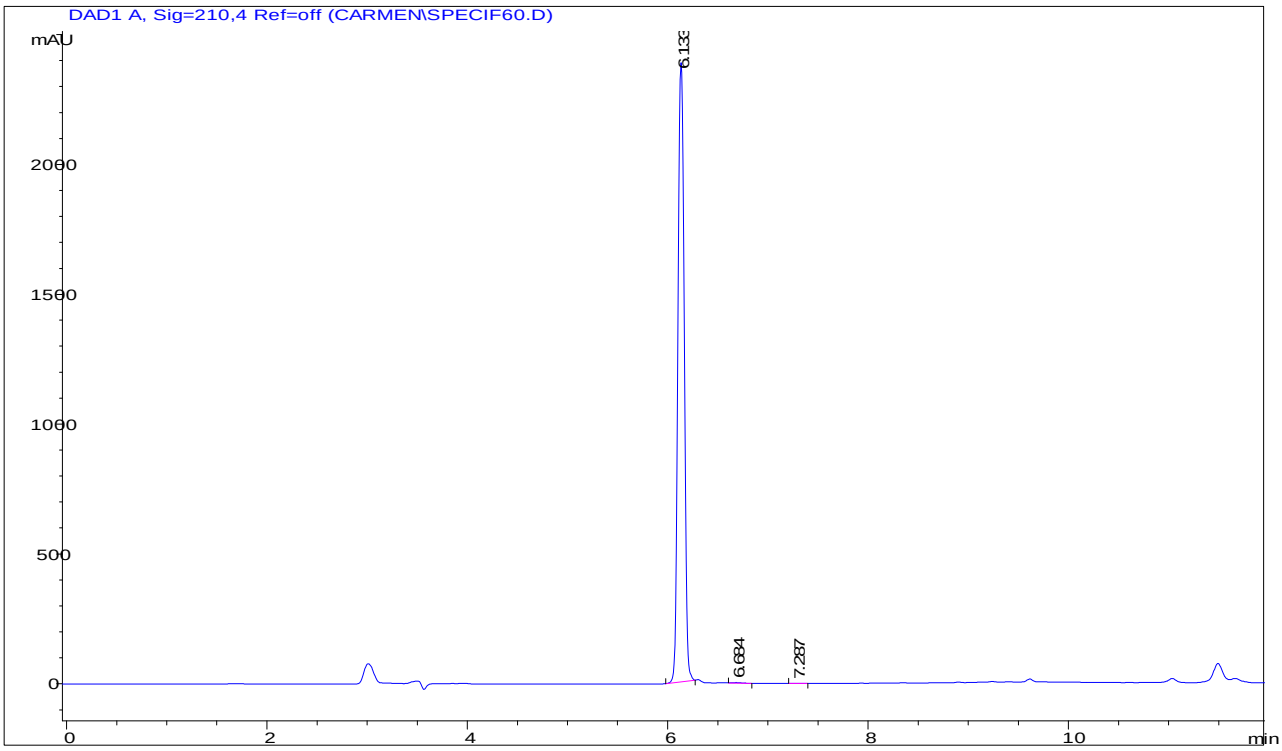

Figure 4.22: Chromatogram of insulin in the presence of sodium deoxycholate

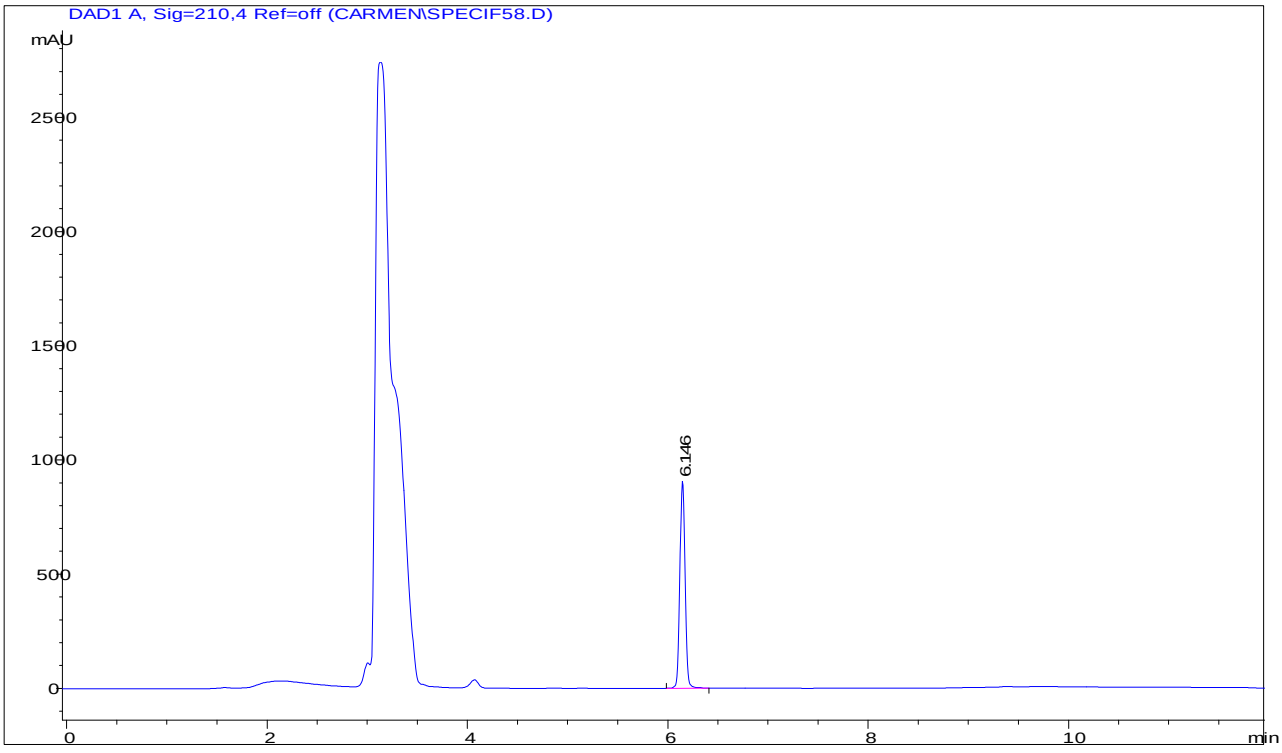

Figure 4.23: Chromatogram of insulin in the presence of TMC

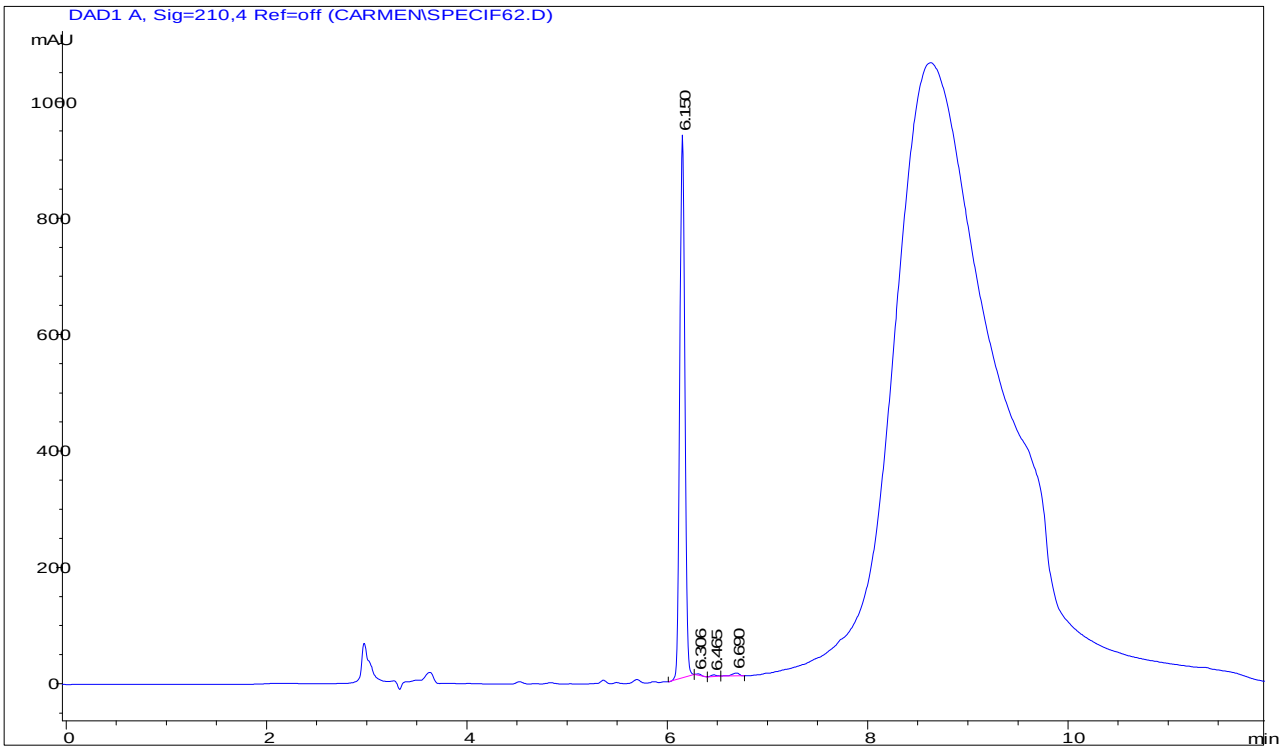

Figure 4.24: Chromatogram of insulin in the presence of Pharmacel®, Ac-di-sol®, Kollidon®VA 64, and Ethanol

It is clear form Figures 4.21 to 4.24, that the compounds used during the formulation processes or during the transport and dissolutions studies did not interfere with the HPLC insulin peak. Insulin exhibited a retention time of 6.142 min.

4.4.4 Summary of the HPLC method validation

The HPLC method was suitable to determine the insulin concentration in the dissolution and transport samples.

4.5 Fluorescence spectrometry method validation

The concentration of LY in samples withdrawn during the membrane integrity experiment were analysed by means of fluorescence spectrometry with the Spectramax Pradigm® plate reader. The excitation and emission wavelengths for LY were set at 485 nm and 520 nm respectively (reference). The analytic method was validated with regards to linearity, limit of detection, limit of quantification and precision.

4.5.1 Linearity

An example of a standard curve obtained for instrument response (fluorescent values) as function of LY concentration is given in Figure 4.25.

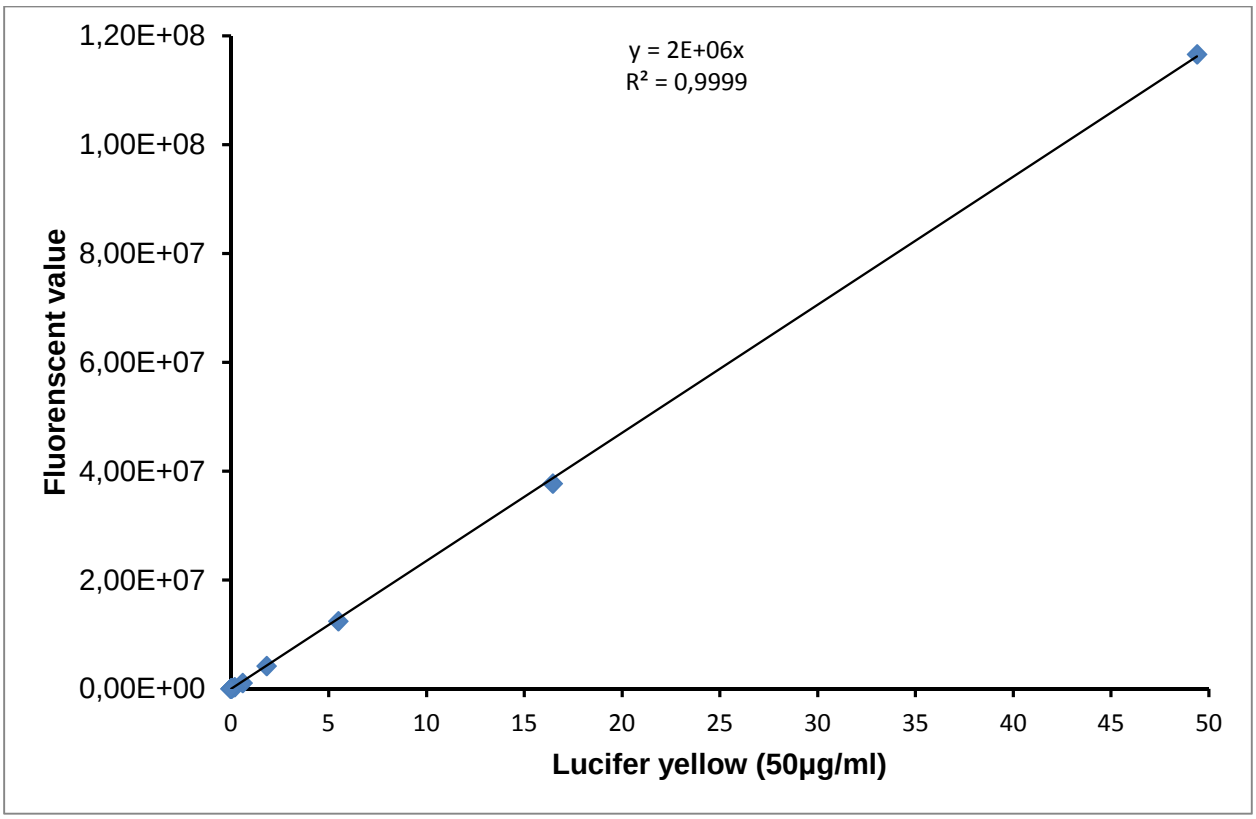

Figure 4.25: Standard curve for Lucifer yellow on which linear regression was applied

The regression coefficient (R^2) was 0.9999 for the LY standard curve, which complies with the requirements for the fluorescence spectrometry method (USP, 2017:783).

4.5.2 LOD and LOQ

The fluorescence spectrometry method's LOD for LY was determined as 1.75×10^{-3} nm/cm. The fluorescence spectrometry method's LOQ for LY was determined as 2.11×10^{-3} nm/cm.

4.5.3 Precision

4.5.3.1 Inter-day precision

Over a period of three days the three different concentrations of LY (50, 25 and 12.5 µg/ml) were used to calculate the average fluorescent value for each concentration. From the average fluorescent values the standard deviation and percentage relative standard deviation (% RSD) was calculated and these values are presented in Table 4.9.

Table 4.9: Data used to calculate inter-day precision of Lucifer yellow

	Concentration Lucifer yellow (µg/ml)		
	50	25	12.5
Day	Fluorescent value		
1	108211683.20	57785951.00	27496753.60
2	110514439.33	57647100.86	27560700.00
3	110859846.00	57959672.67	27766473.00
Standard deviation	1175431.73	127871.34	115074.96
% RSD	1.07	0.22	0.42

It is clear from Table 4.12 that the analytical method used complied with the precision specification of %RSD ≤ 2% (Shabir, 2003)

4.5.3.2 Intra-day precision

Three different concentrations of LY (50, 25 and 12.5 µg/ml) were used to acquire the standard deviation and % RSD. Table 4.10 summarised the data used to determine the intra-day precision.

Table 4.10: Data used to calculate intra-day precision of Lucifer yellow

	Concentration Lucifer yellow (µg/ml)		
	50	25	12.5
Repeat	Fluorescent value		
1	108211683.20	57785951.00	27496753.60
2	107644265.60	56594358.00	27039436.20
3	106498740.00	56418279.11	26825780.80
Standard deviation	712457.88	56932862.70	279879.41
% RSD	0.66	1.07	1.03

FSIt is clear from Table 4.13 that the analytical method used, complied with the precision specification of %RSD ≤ 2% (Shabir, 2003).

4.5.4 Summary of fluorescence spectrometry method validation results

The analysis method for LY on the Spectramax Pradigm® plate reader complied with all the indicated validation criteria as mentioned above

4.6 Summary

Novel bead-in-matrix (micro-bead in macro-bead) delivery systems containing insulin in the micro-bead and an absorption enhancing agent in the macro-bead was successfully prepared and characterised in terms of mass variation, particle size distribution and drug release. The enteric coating was able to limit insulin release (complying with pharmacopoeial specifications) in an acidic environment, while the insulin was released at a relatively high rate above a pH of 6. All the selected absorption enhancers (*A. vera* gel, sodium deoxycholate and TMC) formulated into the bead-in-matrix formulations were able to improve insulin delivery across excised porcine intestinal tissues using a Sweetana-Grass diffusion model. Transport results indicated that *A. vera* gel incorporated into the bead-in-mtarix delivery systems showed to be the most effective absorption enhancer in general, but TMC in these systems performed the best at the 60% micro-bead concentration.

CHAPTER 5: FINAL CONCLUSIONS AND FUTURE RECOMMENDATIONS

5.1 Final conclusion

The aim of this study was to prepare a bead-in-matrix delivery system comprising of micro-beads containing the peptide drug insulin loaded into a macro-bead containing an absorption enhancer. Three different absorption enhancers, namely *A. vera* gel, sodium deoxycholate and TMC at two different concentration levels (0.5% and 1% w/w) were investigated. Based on the experimental variables, 18 bead-in-matrix formulations were prepared in total. The bead-in-matrix delivery systems were designed in such a way that the absorption enhancer in the macro-beads could reach the site of absorption first, in order to open the tight junction to facilitate the paracellular transport of insulin (active ingredient) contained in the micro-beads.

From the results in Chapter 4 it can be concluded that bead-in-matrix delivery systems were successfully prepared. The bead-in-matrix delivery systems were characterised in terms of insulin content (assay), weight variation, particle size, dissolution behaviour and the ability to deliver insulin across porcine intestinal tissue. Electron microscopy indicated that micro-beads could be successfully enclosed within macro-beads resulting in a bead-in-matrix delivery system. In an effort to investigate the possibility to limit insulin release and in effect protect it from an acidic environment, the bead-in-matrix delivery systems were successfully coated with a mixture of Eudragit® L100 and Eudragit® S100 to produce enteric coated delivery systems. Dissolution studies indicated that the coating limited insulin release in 0.1 M HCl to less than 5% of the total dose. However, complete insulin release was illustrated at a pH of 6.8 within 150 min for all bead-in-matrix delivery systems. All the bead-in-matrix delivery systems exhibited similar drug release patterns, which can possibly be attributed to the same production method being used for all the bead-in-matrix formulations. All the bead-in-matrix formulations complied with the BP criteria for drug release from film coated dosage forms for delayed release.

Transport data indicated that the absorption enhancers (i.e. *A. vera* gel, sodium deoxycholate and TMC) in all bead-in-matrix formulations successfully facilitated the paracellular transport of insulin (active ingredient). The most effective absorption enhancer in this study was *A. vera* gel, which also exhibited relatively small variation in the average cumulative percentage insulin transport across the porcine intestinal tissue. Furthermore, from all the 20% w/w micro-bead containing formulations, the 0.5% *A. vera* gel containing formulation exhibited the highest P_{app} value. Sodium deoxycholate demonstrated to be the least effective absorption enhancer in this study, when compared to *A. vera* gel and TMC. The absorption enhancer, TMC yielded the highest cumulative percentage insulin transport for the 0.5% w/w TMC containing 60% w/w

micro-beads and the 1% w/w TMC containing 60% w/w micro-beads, when compared to the same concentrations of the other absorption enhancers (i.e. *A. vera* gel and sodium deoxycholate). However, comparison of the P_{app} values for TMC formulations (both 0.5 and 1% w/w) containing 20% and 40% w/w micro-beads with that of the *A. vera* gel formulations containing equivalent micro-bead loading, showed that these TMC containing delivery systems were capable of higher insulin delivery across porcine intestinal tissues.

This study forms part of a larger study involving beads (micro and macro) as a potential drug delivery system form protein/peptide drugs.

5.2 Recommendations for future studies

The bead-in-matrix delivery systems provided favourable results with regards to peptide drug delivery, which warrants further investigation as recommended below:

- There are variations between protein and peptide drugs, thus it would be recommended that different peptide drugs (e.g. vasopressin, somatostatin, calcitonin and growth factor) also be investigated in bead-in-matrix delivery systems. Other drug absorption enhancing agents (e.g. chitosan, sodium glycholate and *A. vera* whole leaf materials) should also be investigated in an effort to characterise the versatility of bead-in-matrix delivery systems for peptide delivery.
- To determine whether the bead-in-matrix drug delivery system with the selected absorption enhancing agents can provide clinically significant insulin bioavailability, *in vivo* studies should be conducted.
- The loss of the active ingredient during the preparation of the bead-in-matrix delivery systems should be investigated. Perhaps changes should be made to the production process in order to obtain higher percentage insulin content in the final bead-in-matrix formulation.

REFERENCES

Alpers, D.H. 1987. Digestion and absorption of carbohydrates and proteins. (*In* Johnson, L.R., *ed*. Physiology of the gastrointestinal tract. 2nd ed. *New York: Raven Press*, 1469-1487)

Anderle, P. 2009. Kinetics and pathways of intestinal absorption and enzymatic cleavage of therapeutic proteins upon peroral delivery. *Zürich: Swiss Federal Institute of Technology*, 1-30

Artursson, P. & Palm, K. 2012. Caco-2 monolayers in experimental and theoretical predictions of drug transport. *Advanced Drug Delivery Reviews*, 64:280-289

Ashford, M. 2007. Introduction to biopharmaceutics (In: Aulton, M.E., ed. Aulton's pharmaceutics. The design and manufacture of medicines, 3rd ed. *New York: Churchill Livingstone*, 266-269)

Atyabi, F., Majzoob, S., Iman, M., Salehi, M., Dorkoosh, F. 2005. In vitro evaluation and modification of pectinate gel beads containing trimethyl chitosan, as a multi-particulate system for delivery of water-soluble macromolecules to colon. *Carbohydrate polymers,*61:39-51

Aulton, M.E., 2007. Gastrointestinal tract – Physiology and drug absorption. (In: Aulton's pharmaceutics: The design and manufacture of medicines. 3rd ed. *Churchill Livingstone: Elsevier*, 270-285)

Backes, W.L., 2007. Passive diffusion of drugs across membranes. *New Orleans: Elsevier*, 1

Baker, J., Hidalgo, I.J. & Borchardt, R.T. 1991. Intestinal epithelial and vascular endothelial barriers to peptide and protein delivery. (*In* Lee, V.H.L. *ed.* Peptide and protein drug delivery. *New York: Marcel Dekker*, 359-390)

Ball, G.F.M. 2004. Vitamins Their Role in the Human Body. *USA: Wiley-Blackwell*, 12-93.

Banga, A.K. & Chien, Y.W. 1988. Systemic delivery of therapeutic peptides and proteins. *International journal of pharmaceutics,* 48:15-50

Basson, M.D., & Hong, F. 1996. Regulation of human Caco-2 intestinal epithelial brush border enzyme activity by cyclic nucleotides. *Cancer letters,* 99:155-160

Beneke, C., Viljoen, A. & Hamman, J. 2012. *In vitro* absorption enhancement effects of Aloe vera and Aloe ferox. *Scientia Pharmaceutica*, 80:475-486

Brady, M. E. 2006. Gastrointestinal drug absorption in rats exposed to ^{60}Co[gamma]-Radiation. *Journal of Pharmaceutical Science*, 66:361-365

Brayden, D.J. & Maher, S. 2010. Oral absorption enhancement: taking the next steps in therapeutic delivery. *Therapeutic Delivery*, 1:5-9

Brooker, C. 2010. Mosby's dictionary of medicine, nursing and health professions. UK ed. *London: Elsevier*

Boonyo, W., Junginger, H.E., Earanuch, N., Polnok, A. & Pitaksuteepong, T. 2007. Chitosan and trimethyl chitosan chloride (TMC) as adjuvants for inducing immune responses to ovalbumin in mice following nasal administration. *Journal of controlled release,* 121:168-175

Buchanan, A & Revell, J.D. 2015. Novel therapeutic proteins and peptides (In: Singh, M & Salnikova, M. 2014. Novel approaches and strategies for biologics, vaccines and cancer therapies, *London: Academic press*, 171-197

Burton, P.S., Goodwin, J.T., Conradi, R.A., Ho, N.F.H. & Hilgers, A.R. 1997. *In vitro* permeability of peptidomimetic drugs: the role of polarized efflux pathways as additional barriers to absorption. *Advanced drug delivery reviews*, 23:143-156

Caeamella, C., Ferrari, F., Bonfroni, M.C., Rossi, S & Sandri, G. 2010. Chitosan and its derivatives as drug penetration enhancers. *Journal of drug delivery of science technologies,* 20:5-13

Carino, G.P. & Matiowitz, E. 1999. Oral insulin delivery. *Advanced drug delivery reviews,* 35:249-257

Chen, F., Zhang, Z., Yuan, F., Qin, X., Wang, M. & Huang, Y. 2008. *In vitro* and *in vivo* study of *N*-trimethyl chitosan nanoparticles for oral protein delivery. *International journal of pharmaceutics,* 349:226-233

Chen, W., Lu, Z., Viljoen, A. & Hamman, H. 2009. Intestinal drug transport enhancement by Aloe vera. *Planta Medica*; 75:587-595.

Chitchumroonchokchai, C. 2004. Lutein and zeaxanthin use of in vitro models to examine digestive stability, absorption, and photoprotective activity in human lens epithelial cells. *Ohio State University: Human Nutrition and Food Management*, 1-65

Choonara, B.F., Choonara, Y.E., Kumar, P., Bijukumar, D., Du Toit, L.C., Pillay, V. 2014. A Review of advanced oral drug delivery technologies facilitating the protection and absorption of protein and peptide molecules. *Biotechnology advances*, 32:1269-1282

Dane, S. & Hänninen, O. 2015. Enzymes of digestion. (In: Encyclopedia of life support systems. 2nd ed. 45-50) http://www.eolss.net/sample-chapters/c03/e6-54-02-04.pdf

Daugherty, A.L. & Mrsny, R.J. *1999.* Transcellular uptake mechanisms of the intestinal epithelial barrier: part one. *Pharmaceutical Science and Technology Today, 2:*144-151

Davis, S. 2005. Formulation strategies for absorption windows. *Drug discovery today,* 10:249-257

Dey, N.S., Majumdar, S & Rao, M.E.B. 2008. Multiparticulate drug delivery systems for controlled release. *Tropical journal of pharmaceutical research,* 7:1067-1075

Di Paquale, G & Chiorini, J.A. 2006. AVV transcytosis through barrier epithelia and endothelium. *Molecular Therapy*, 13:506-515

Dorkoosh, F., Verhoef, J., Borchard, G., Rafiee-Tehrani, M., Junginger, H. 2001. Development and characterization of a novel peroral peptide drug delivery system. *Journal of Controlled Release,* 71:307-318

Ensign, L.M., Cone, R & Hanes, J. 2012. Oral drug delivery with polymeric nanoparticles: The gastrointestinal mucus barriers. *Advanced drug delivery reviews,* 64:557-570

Fasano, A. 1998. Novel approaches for oral delivery of macromolecules. *Journal of pharmaceutical sceineces,* 87:1351-1356

Fosgerau, K. & Hoffman, T. 2015. Peptide therapeutics: current status and future directions. *Drug Discovery Today*, 20:122-128

Gavhane, Y.N., & Yadav, A.V. 2012. Loss of orally administered drugs in GI tract. *Saudi pharmaceutical journal,* 20:331-344

Granger, D.N., Kvietys, P.R., Perry, M.A. & Barrowman, J.A. 1987. The microcirculation and intestinal transport. (*In* Johnson, L.R., *ed*. Physiology of the gastrointestinal tract. 2nd ed. *New York: Raven Press*. p. 1671-1697)

Grassl, S.M. 2012. Mechanisms of carrier-mediatedtransport. (In: Sperelakis, N., ed. Cell physiology: source book, 4th ed. *San Diego: CA Academic*, 153-165)

Günther, C., Buchen, B., Neurath, M.F. & Becker, C. 2014. Regulation and pathophysiological role of epithelial turnover in the gut. *Seminars in cell & developmental biology,* 35:40-50

Hamman, J.H. 2007. Drug absorption enhancement. (In: Oral drug delivery, biopharmaceutical principles, evaluation and optimization. Pretoria: Content solutions. 184-208).

Hamman, J.H. 2008. Composition and applications of Aloe vera leaf gel. *Molecules,* 13:1599-1616

Hamman, J.H., Enslin, G.M. & Kotze, A.F. 2005. Oral delivery of peptide drugs. *Biodrugs*, 19:165-177

Hamman, J.H & Steenekamps, J.H. 2011. Oral peptide drug delivery: Strategies to overcome challenges. (In: Peptide drug delivery and development. *Weinheim: Wiley-VCH Verlag & Co*, 71-90)

Hassani, L.N., Lewis, A & Richard, J. 2015. Oral peptide delivery: Technology landscape and current status. *Frederick furness publishing ltd,* 12-17

Hejazi, R. & Amiji, M. 2003. Chitosan-based gastrointestinal delivery systems. *Journal of controlled release*, 89:151-165.

Herkenne, C. 2005. Evaluation and optimization of topical drug bioavailability. *Genève: S.I*., 1-34

Hildalgo, I.J. 2001. Assessing the absorption of new pharmaceuticals. *Current Topics in Medicinal Chemistry*, 1:388

Hunter, J. & Hirst, B.H. 1997. Intestinal secretion of drugs. The role of P-glycoprotein and related drug efflux systems in limiting oral drug absorption. *Advanced drug delivery reviews*, 25:129-157

Ichikawa, H. & Peppas, N. 2003. Novel complexation hydrogeld for oral peptide drug delivery: in vitro evaluation of their cytocompatibility and insulin-transport enhancing effects using Caco-2 cell monolayers. *Journal of Biomedical Materials Research Part A*, 67:609-617

Jonker, C., Hamman, J.H. & Kotze, A.F. 2002. Intestinal paracellular enhancement with quaternised chitosan: in situ*. International journal of pharmaceutics,* 238:205-213

Kerns, E.H. & Di, L. 2008. Permeability. (In: Drug-like properties: concepts, structure design and methods from ADME to toxicity optimization, 2nd ed. *Amsterdam: Academic Press*, 86-99)

Krishna, R., & Yu, L. 2007. Biopharmaceutics applications in drug development. *New York: Springer,* 1-97

Kristensen, M., Foged, C., Berthelsen, J. & Morck Nielsen, H. 2013. Peptide-enhanced oral delivery of therapeutic peptides and proteins. *Journal of drug delivery science and technology,* 2013:365-373

Langguth, P., Bohner, V., Heizmann, J., Merkle, H.P., Wolffram, S., Amidon, G.L. & Yamashita, S. 1997. The challenge of proteolytic enzymes in intestinal peptide delivery. *Journal of controlled release,* 46:39-57

Lappierre, L.A. 2000. The molecular structure of the tight junction. *Advanced Drug Delivery Reviews,* 41:255-264

Lee, H.J. 2002. Protein drug oral delivery: The Recent Progress. *Archives of Pharmaceutical Research*, 25: 572-574

Lee, V.H.L. & Yamamoto, A. 1990. Penetration and enzymatic barriers to peptide and protein absorption. *Advanced drug delivery reviews,* 4:171-207

Legen, I., Salobir, M. & Kerč, J. 2005. Comparison of different intestinal epithelia as models for absorption enhancement studies. *International Journal of Pharmaceutics*, 291:183-188

Lemmer, H.J., & Hamman, J.H. 2013. Paracellular drug absorption enhancement through tight junction modulation. *Expert Opinion in Drug Delivery*, 10:103-114.

Lillienau, J., Schteingart, C.D., Hoffman, A.F. 1992. Physicochemical and physiological properties of cholylsarcosine. A Potential replacement detergent for bile acid deficiency states in the small intestine. *The Journal of clinical investigation*. 89:420-431

Liu. Z., Wang, S. & Hu, M. 2009. Oral absorption basics: pathways, physico-chemical and biological factors affecting. (In: Developing solid oral dosage forms: pharmaceutical theory and practise. *Massachusetts: Academic Press*, .265-287)

Loftsson, T. 2012. Drug permeation through biomembranes: cyclodextrins and the unstirred water layer. *Pharmazie,* 67:363-370

Madara, J.L. & Trier, J.S. 1987. Functional morphology of the mucosa of the small intestine. (*In* Johnson, L.R., *ed*. Physiology of the gastrointestinal tract. 2nd ed. *New York: Raven Press*, 1209-1249)

Majumdar, S., Duvvuri, S. & Mitra A.K. 2004. Membrane transporter/receptor-targeted prodrug design: Strategies for human and veterinary drug development. *Advance Drug Delivery Reviews*, 56:1437-1452

Mallipeddi, R., Saripella, K.K & Neau, S.H. 2010. Use of coarse ethylcellulose and PEO in beads produced by extrusion-spheronization. *International journal of pharmaceutics,* 385:53-65

Mansuri, S., Kesharwani, P., Jain, K., Tekade, R.K. & Jain, N.K. 2016. Mucoadhesion: a promising approach in drug delivery system. *Reactive and functional polymers,* 100:151-172

Mathiowitz, E., Chickering, D.E. & Lehr, C.M. 2009. Bioadhesive drug delivery systems fundamentals, novel approaches, and development. New York: Marcel Dekker, 1-63

Michael, S., Thöle, M., Dillman, R., Fahr, A., Drewe, J., Fricker, G. 2000. Improvement of intestinal peptide absorption by a synthetic bile acid derivative, cholylsarcosine. *European Journal of Pharmaceutical Sciences*, 10:133-140

Moghimipour, E., Ameri, A. & Handali, S. 2015. Absorption-enhancing effects of bile salts. *Molecules,* 20:14451-14473

Morishita, M. & Peppas, N.A. 2006. Is the oral route possible for peptide and protein drug delivery? *Drug discovery today,* 11:905-910

Mukhopadhyay, P., Mishra, R., Rana, D. & Kundu, P.P. 2012. Stategies for effective oral insulin delivery with modified chitosan nanoparticles: A review. *Progress in polymer science,* 37:1457-1475

Muranishi, S. 1990. Absorption enhancers. *Critical Reviews in Therapeutic Drug Carrier Systems,* 7:1-33

Náray-Szabó, G. 2014. Protein Modelling. *Cham: Springer International Publishing*, 1096-1121

Park, J.W., Kim, S.K., Al-hilal, T.A., Jeon, O.C., Moon, H.T. & Byuna, Y. 2010. Strategies for oral delivery of macromolecule drugs. *Biotechnology and bioprocess engineering,* 15:66-75

Park, K., & Mrsny, R. J. 2000. Controlled drug delivery: Designing technologies for the future. *Washington: American Chemical Society*, 459

Park, K., Kwon, I.C., & Park, K. 2011. Oral protein delivery: current status and future prospect. *Reactive & functional polymers,* 71:280-287

Patwekar, S.L. & Baramade, M.K. 2012. Controlled release approach to novel multiparticulate drug delivery system. *International journal of pharmacy and pharmaceutical sciences,* 4:757-763.

Pauletti, G.M., Gangwar, S., Knipp, G.T., Nerurkar, M.M., Okumu, F.W., Tamura, K., Siahaan., T.J. & Borchaedt, R.T. 1996. Structural requirements for *intestinal* absorption of peptide drugs. *Journal of controlled release,* 41:3-17

Peppas, N. 2004. Devices based on intelligent biopolymers. *International Journal of Pharmaceutics,* 277:11-17

Peppas, N., Bures, P., Leobandung, W. & Ichikawa, H. 2000. Hydrogels in pharmaceutical formulations. *European Journal of Pharmaceutics and Biopharmaceutics*, 50:27-46

Peppas, N.A., & Huang, Y. 2004. Nanoscale technology of mucoadhesive interactions. *Advanced drug delivery reviews,* 56:1675-1687

Pfister, D., & Morbidelli, M. 2014. Process for protei PEGylation. *Journal of Controlled Release,* 180:134-149

Radha, M.H. & Lamipriya, N.P. 2015. Evaluation of biological properties and clinical effectiveness of *Aloe vera*: a systematic review. *Journal of traditional and complementary medicine,* 5:21-26

Rekha, M.R. & Sharma, P. 2013. Oral delivery of therapeutic protein/peptide for diabetes. Future perspectives. *International journal of pharmaceutics,* 440:48-62

Renukuntla, J., Vadlapudi, A.D., Patel, A. Boddu, S.H.S. & Mitra, A.K. 2013. Approaches for enhancing oral bioavailability of peptides and proteins. *International journal of pharmaceutics*, 447:75-93

Salama, N.N., Eddington, N.D. & Fasano, A. 2006. Tight junction modulation and its relationship to drug delivery. *Advanced Drug Delivery Reviews*, 58:15-28

Salamat-Miller, N. & Johnston, T.P. 2005. Current strategies used to enhance the paracellular transport of therapeutic polypeptides across the intestinal epithelium. *International Journal of Pharmaceutics*, 294:201-216

Sato, H., Sugiyama, Y., Tsuji, A. & Horikoshi, I. 1996. Importance of receptor-mediated endocytosis in peptide delivery and targeting: kinetic aspects. *Advanced Drug Delivery Reviews*, 19:445-467

Shargel, L. & YU, A.B.C. 1999. Applied biopharmaceutics & pharmacokinetics. 4th ed. New *York: McGraw-Hill*, 768

Shargel, L., Wu-Pong, S & Yu, A.B.C. 2005. Hepatic elimination of drugs. (In: Shargel, L., Wu-Pong, S. & Yu, A.B.C. eds. Applied biopharmaceutics and pharmacokinetics, 5th ed. *New York: McGraw-Hill*, 303-353)

Shargel, L., Wu-Pong, S. & Yu, A.B.C. 2005. Physiologic factors related to drug absorption. (In: Shargel, L., Wu-Pong, S. & Yu, A.B.C. eds. Applied biopharmaceutics and pharmacokinetics, 5th ed. *New York: McGraw-Hill*, 371-408)

Silverstein, S.C., Steinman, R.M. & Cohn, Z.A. 1977. Endocytosis. *Annual Review of Biochemistry*, 46:669-772

Soarse, S., Costa, A. & Sarmento, B. 2012. Novel non-invasive methods of insulin delivery. *Expert opinion drug delivery,* 16:115-128

Takizawa, Y., Kishimoto, H., Kitazato, T., Ishizaka, H., Kamiya, N., Ito, Y., Tomita, M. & Hayashi, M. 2013. Characteristics of reversible absorption-enhancing effect of sodium nitroprusside in rat small intestine. *European journal of pharmaceutical sciences,* 49:664-670

Thanou, M., Verhoef, J.C. & Junginger, H.E. 2001. Chitosan and its derivatives as intestinal absorption enhancers. *Advanced drug delivery reviews,* 50:S91-S101

Thanou, M.M., Verhoef, J.C., Romeijn, S.G., Nagelkerke, J.F., Merkus, F.W.H.M. & Junginger, H.E. 1999. Effects of N-trimethyl chitosan chloride, a novel absorption enhancer on Caco-2 intestinal epithelia and the ciliary beat frequency of chicken embryo trachea. *International Journal of Pharmaceutics*, 185:73-82

Tillement, J.P. 2006. Protein binding and drug transport. *Symposia Medica Hoechst. Stuttgart: Schattauer*, 1-170

Tozaki, H., Komoike, J., Tada, C., Maruyama, T., Terabe, A., Suzuki, T., Yamamoto, A. & Muranishi, S. 1997. Chitosan capsules for colon-specific drug delivery: improvement of insulin absorption from the rat colon. *Journal of pharmaceutical sciences,* 86:1016-1021

Urbanska, A.M., Karagiannis, E.D., Au, A.S., Dai, S.Y., Mozafari, M. & Prakash, S. 2016. What's next for gastrointestinal disorders: No needles? *Journal of controlled release,* 221:48-61

Van Hoogdalem, E.J., De Boer, A.G. & Breimer, D.D. 1989. Intestinal drug absorption enhancement: an overview. *Pharmacology and therapeutics,* 44:407-443

Van Itallie, C.M. & Anderson, J.M. 2014. Architecture of tight junctions and principles of molecular composition. *Seminars in Cell Developmental Biology*, 36:157-165

Vinson, J.A., Al Kharrat, H. & Andreoli, L. 2005. Effect of Aloe vera preparations on the human bioavailability of vitamins C and E. *Phytomedicine*, 12:760-765

Vllasaliu, D., Illum, L. & Stolnik, S. 2010. Tight junction modulation by chitosan nanoparticles: Comparison with chitosan solution. *International journal of pharmaceutics,* 400:183-193

Wallis, L., Kleynhans, E., Du Toit, T., Gouws, C., Steyn, D., Steenekamp, J., Viljoen, J. & Hamman, J. 2014. Novel non-invasive protein and peptide drug delivery approaches. *Protein & peptide letters,* 31:1087-1101

Washington, N., Washington, C. & Wilson, C.G. 2001. Physiological pharmaceutics: barriers to drug absorption. 2nd ed. *New York: Taylor & Francis*, 312

Whitehead, K., Karr, N & Mitragotri, S. 2008. Discovery of synergistic permeation enhancers for oral drug delivery. *Journal of controlled release,* 128:128-133

Whitehead, K., Shen, Z. & Mitragotri S. 2004. Oral delivery of macromolecules using intestinal patches: applications for insulin delivery. *Journal of control release,* 98: 37-45

Widmaier, E.P., Raff, H., & Strang, K.T. 2008. Vander's human physiology: The mechanisms of body function. 11th ed. *New York: McGraw-Hill*, 114

Zhang, H., Alsarra, I.A. & Neau, S.H. 2002. An *in vitro* evaluation of a chitsoan-containing multiparticulate system for macromolecule delivery to the colon. *International journal of pharmaceutics,* 239:197-205

Zhang, X. & Wu, W. 2014. Ligand-mediated active targeting for enhanced oral absorption. *Drug discovery today,* 19:898-904

Zhou, X.H. & Li Wan Po, A. 1991. Peptide and protein drugs. I. Therapeutic applications, absorption and parenteral administration. *International journal of pharmaceutics,* 75:97-115

ADDENDUM A: PARTICLE SIZE ANALYSIS

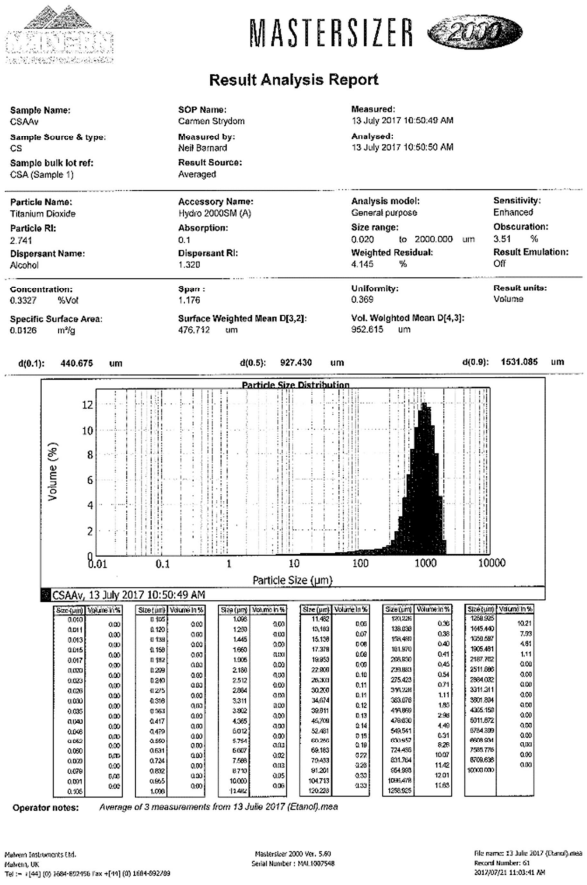

MASTERSIZER 2000

Result Analysis Report

Sample Name: CSAAv	**SOP Name:** Carmen Strydom	**Measured:** 13 July 2017 10:50:49 AM	
Sample Source & type: CS	**Measured by:** Neil Barnard	**Analysed:** 13 July 2017 10:50:50 AM	
Sample bulk lot ref: CSA (Sample 1)	**Result Source:** Averaged		
Particle Name: Titanium Dioxide	**Accessory Name:** Hydro 2000SM (A)	**Analysis model:** General purpose	**Sensitivity:** Enhanced
Particle RI: 2.741	**Absorption:** 0.1	**Size range:** 0.020 to 2000.000 um	**Obscuration:** 3.51 %
Dispersant Name: Alcohol	**Dispersant RI:** 1.320	**Weighted Residual:** 4.145 %	**Result Emulation:** Off
Concentration: 0.3327 %Vol	**Span :** 1.176	**Uniformity:** 0.369	**Result units:** Volume
Specific Surface Area: 0.0126 m²/g	**Surface Weighted Mean D[3,2]:** 476.712 um	**Vol. Weighted Mean D[4,3]:** 952.615 um	

d(0.1): 440.675 um d(0.5): 927.430 um d(0.9): 1531.085 um

Particle Size Distribution

CSAAv, 13 July 2017 10:50:49 AM

Operator notes: *Average of 3 measurements from 13 July 2017 (Etanol).mea*

Malvern Instruments Ltd.
Malvern, UK
Tel :- +[44] (0) 1684-892456 Fax +[44] (0) 1684-892789

Mastersizer 2000 Ver. 5.60
Serial Number : MAL1007548

File name: 13 July 2017 (Etanol).mea
Record Number: 61
2017/07/21 11:03:41 AM

Figure A.1: Mastersizer analysis report of 0.5% w/w *A. vera* gel, 20% w/w micro-beads (Formula A)

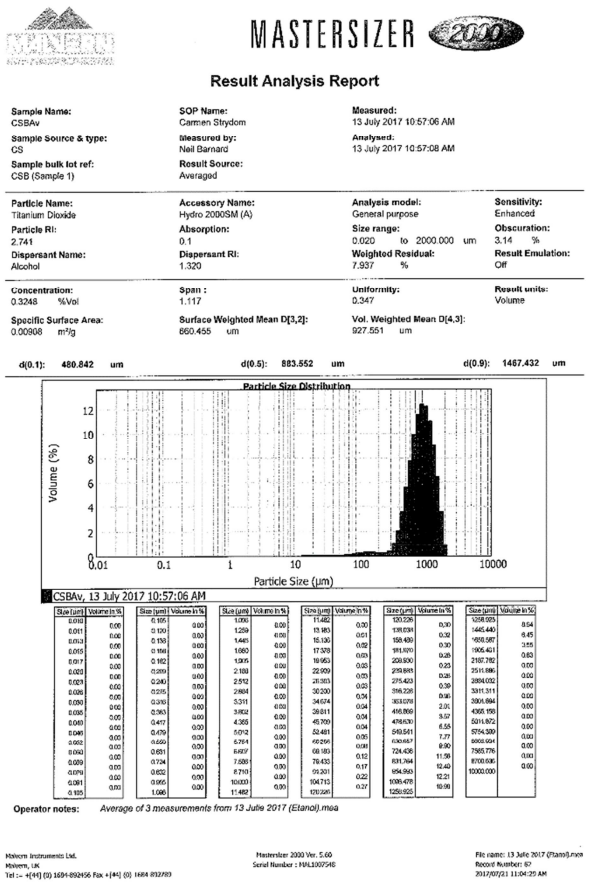

MASTERSIZER 2000

Result Analysis Report

Sample Name: CSBAv	**SOP Name:** Carmen Strydom	**Measured:** 13 July 2017 10:57:06 AM	
Sample Source & type: CS	**Measured by:** Neil Barnard	**Analysed:** 13 July 2017 10:57:08 AM	
Sample bulk lot ref: CSB (Sample 1)	**Result Source:** Averaged		
Particle Name: Titanium Dioxide	**Accessory Name:** Hydro 2000SM (A)	**Analysis model:** General purpose	**Sensitivity:** Enhanced
Particle RI: 2.741	**Absorption:** 0.1	**Size range:** 0.020 to 2000.000 um	**Obscuration:** 3.14 %
Dispersant Name: Alcohol	**Dispersant RI:** 1.320	**Weighted Residual:** 7.937 %	**Result Emulation:** Off
Concentration: 0.3248 %Vol	**Span :** 1.117	**Uniformity:** 0.347	**Result units:** Volume
Specific Surface Area: 0.00998 m²/g	**Surface Weighted Mean D[3,2]:** 600.455 um	**Vol. Weighted Mean D[4,3]:** 927.551 um	

d(0.1): 480.842 um d(0.5): 883.552 um d(0.9): 1467.432 um

Particle Size Distribution

CSBAv, 13 July 2017 10:57:06 AM

Operator notes: *Average of 3 measurements from 13 July 2017 (Etanol).mea*

Malvern Instruments Ltd.
Malvern, UK
Tel :- +[44] (0) 1684-892456 Fax +[44] (0) 1684-892789

Mastersizer 2000 Ver. 5.60
Serial Number : MAL1007548

File name: 13 July 2017 (Etanol).mea
Record Number: 67
2017/07/21 11:04:25 AM

Figure A.2: Mastersizer analysis report of 1% w/w *A. vera* gel, 20% micro-beads (Formula B)

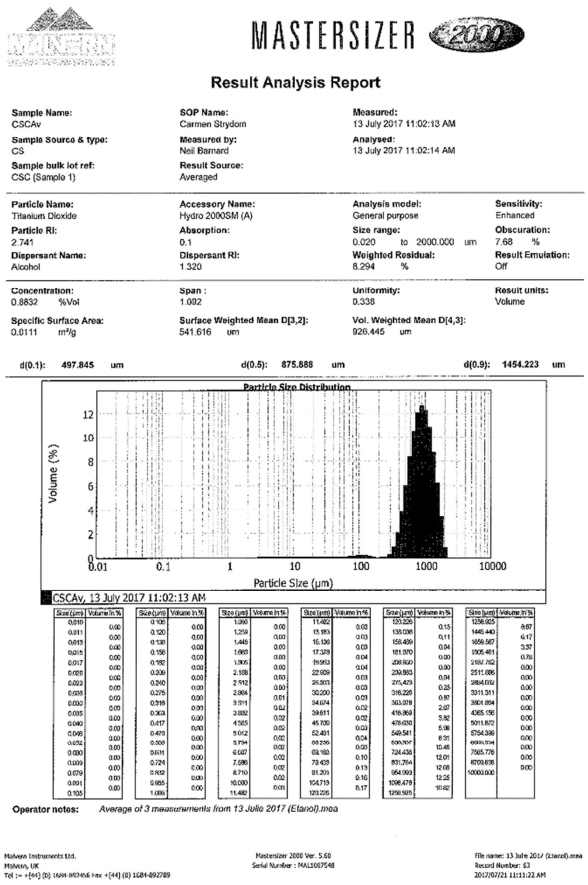

MASTERSIZER 2000

Result Analysis Report

Sample Name: CSCAv	**SOP Name:** Carmen Strydom	**Measured:** 13 July 2017 11:02:13 AM	
Sample Source & type: CS	**Measured by:** Neil Barnard	**Analysed:** 13 July 2017 11:02:14 AM	
Sample bulk lot ref: CSC (Sample 1)	**Result Source:** Averaged		
Particle Name: Titanium Dioxide	**Accessory Name:** Hydro 2000SM (A)	**Analysis model:** General purpose	**Sensitivity:** Enhanced
Particle RI: 2.741	**Absorption:** 0.1	**Size range:** 0.020 to 2000.000 um	**Obscuration:** 7.68 %
Dispersant Name: Alcohol	**Dispersant RI:** 1.320	**Weighted Residual:** 8.294 %	**Result Emulation:** Off
Concentration: 0.8832 %Vol	**Span :** 1.092	**Uniformity:** 0.338	**Result units:** Volume
Specific Surface Area: 0.0111 m²/g	**Surface Weighted Mean D[3,2]:** 541.616 um	**Vol. Weighted Mean D[4,3]:** 926.445 um	

d(0.1): 497.845 um **d(0.5): 875.888 um** **d(0.9): 1454.223 um**

Particle Size Distribution

Volume (%)

Particle Size (µm)

CSCAv, 13 July 2017 11:02:13 AM

Operator notes: *Average of 3 measurements from 13 July 2017 (Etanol).mea*

Malvern Instruments Ltd. Malvern, UK Tel := +[44] (0) 1684-892456 Fax +[44] (0) 1684-892789

Mastersizer 2000 Ver. 5.60 Serial Number : MAL1007548

File name: 13 July 2017 (Etanol).mea Record Number: 63 2017/07/21 11:11:22 AM

Figure A.3: Mastersizer analysis report of 0.5% w/w sodium deoxycholate, 20% w/w micro-beads (Formula C)

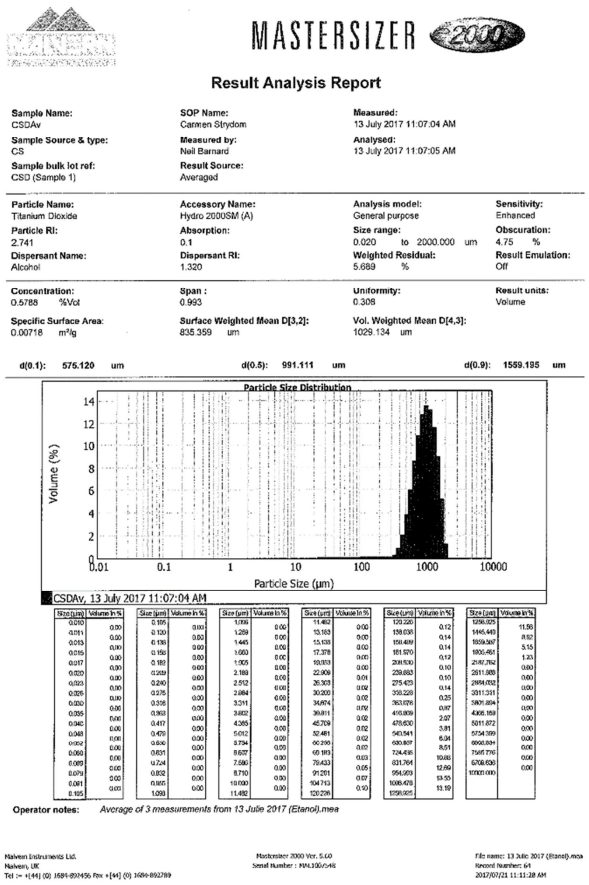

MASTERSIZER 2000

Result Analysis Report

Sample Name: CSDAv	**SOP Name:** Carmen Strydom	**Measured:** 13 July 2017 11:07:04 AM	
Sample Source & type: CS	**Measured by:** Neil Barnard	**Analysed:** 13 July 2017 11:07:05 AM	
Sample bulk lot ref: CSD (Sample 1)	**Result Source:** Averaged		
Particle Name: Titanium Dioxide	**Accessory Name:** Hydro 2000SM (A)	**Analysis model:** General purpose	**Sensitivity:** Enhanced
Particle RI: 2.741	**Absorption:** 0.1	**Size range:** 0.020 to 2000.000 um	**Obscuration:** 4.75 %
Dispersant Name: Alcohol	**Dispersant RI:** 1.320	**Weighted Residual:** 5.689 %	**Result Emulation:** Off
Concentration: 0.5788 %Vol	**Span :** 0.993	**Uniformity:** 0.308	**Result units:** Volume
Specific Surface Area: 0.00718 m²/g	**Surface Weighted Mean D[3,2]:** 835.359 um	**Vol. Weighted Mean D[4,3]:** 1029.134 um	

d(0.1): 575.120 um **d(0.5): 991.111 um** **d(0.9): 1559.195 um**

Particle Size Distribution

Volume (%)

Particle Size (µm)

CSDAv, 13 July 2017 11:07:04 AM

Operator notes: *Average of 3 measurements from 13 July 2017 (Etanol).mea*

Malvern Instruments Ltd. Malvern, UK Tel := +[44] (0) 1684-892456 Fax +[44] (0) 1684-892789

Mastersizer 2000 Ver. 5.60 Serial Number : MAL1007548

File name: 13 July 2017 (Etanol).mea Record Number: 64 2017/07/21 11:11:28 AM

Figure A.4: Mastersizer analysis report of 0.5% w/w sodium deoxycholate, 20% w/w micro-beads (Formula D)

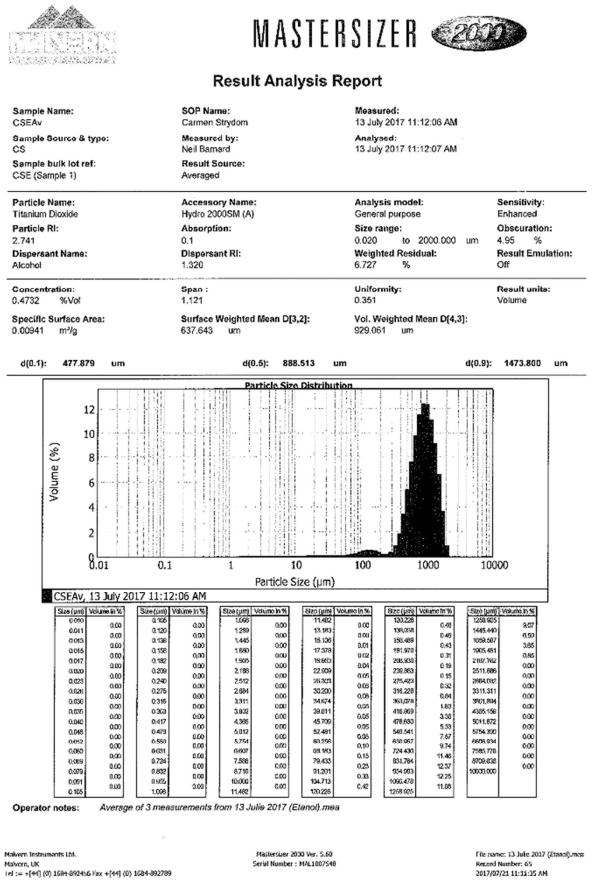

MASTERSIZER 2000

Result Analysis Report

Sample Name: CSEAv	**SOP Name:** Carmen Strydom	**Measured:** 13 July 2017 11:12:06 AM	
Sample Source & type: CS	**Measured by:** Neil Barnard	**Analysed:** 13 July 2017 11:12:07 AM	
Sample bulk lot ref: CSE (Sample 1)	**Result Source:** Averaged		
Particle Name: Titanium Dioxide	**Accessory Name:** Hydro 2000SM (A)	**Analysis model:** General purpose	**Sensitivity:** Enhanced
Particle RI: 2.741	**Absorption:** 0.1	**Size range:** 0.020 to 2000.000 um	**Obscuration:** 4.95 %
Dispersant Name: Alcohol	**Dispersant RI:** 1.320	**Weighted Residual:** 6.727 %	**Result Emulation:** Off
Concentration: 0.4732 %Vol	**Span :** 1.121	**Uniformity:** 0.351	**Result units:** Volume
Specific Surface Area: 0.00941 m²/g	**Surface Weighted Mean D[3,2]:** 637.643 um	**Vol. Weighted Mean D[4,3]:** 929.061 um	

d(0.1): 477.879 um **d(0.5):** 888.513 um **d(0.9):** 1473.800 um

Particle Size Distribution

Volume (%)

Particle Size (µm)

CSEAv, 13 July 2017 11:12:06 AM

Operator notes: *Average of 3 measurements from 13 Julie 2017 (Etanol).mea*

Malvern Instruments Ltd. Malvern, UK Tel :- +[44] (0) 1684-892456 Fax +[44] (0) 1684-892789

Mastersizer 2000 Ver. 5.60 Serial Number : MAL1007548

File name: 13 Julie 2017 (Etanol).mea Record Number: 65 2017/07/21 11:11:35 AM

Figure A.5: Mastersizer analysis report of 0.5% w/w TMC, 20% w/w micro-beads (Formula E)

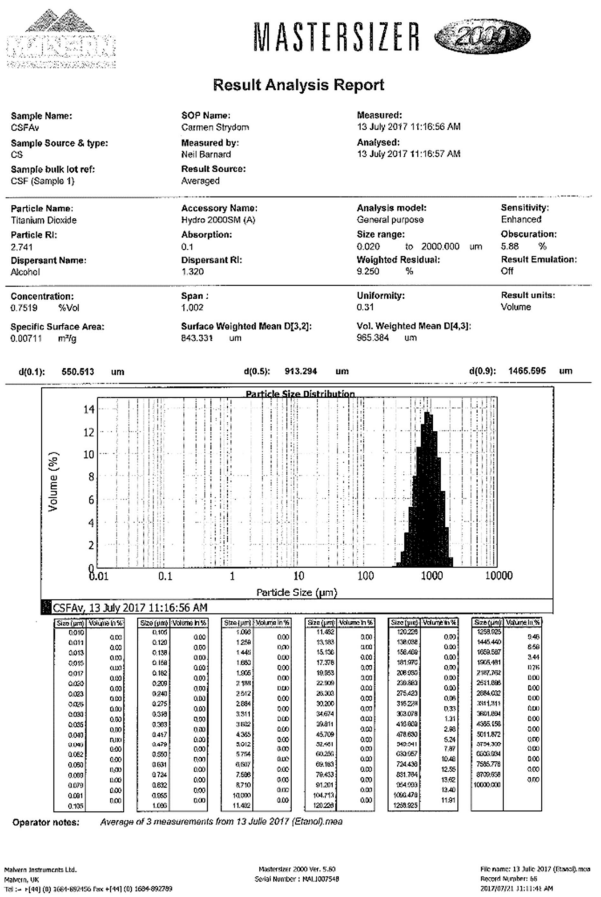

MASTERSIZER 2000

Result Analysis Report

Sample Name: CSFAv	**SOP Name:** Carmen Strydom	**Measured:** 13 July 2017 11:16:56 AM	
Sample Source & type: CS	**Measured by:** Neil Barnard	**Analysed:** 13 July 2017 11:16:57 AM	
Sample bulk lot ref: CSF (Sample 1)	**Result Source:** Averaged		
Particle Name: Titanium Dioxide	**Accessory Name:** Hydro 2000SM (A)	**Analysis model:** General purpose	**Sensitivity:** Enhanced
Particle RI: 2.741	**Absorption:** 0.1	**Size range:** 0.020 to 2000.000 um	**Obscuration:** 5.88 %
Dispersant Name: Alcohol	**Dispersant RI:** 1.320	**Weighted Residual:** 9.250 %	**Result Emulation:** Off
Concentration: 0.7519 %Vol	**Span :** 1.002	**Uniformity:** 0.31	**Result units:** Volume
Specific Surface Area: 0.00711 m²/g	**Surface Weighted Mean D[3,2]:** 843.331 um	**Vol. Weighted Mean D[4,3]:** 985.384 um	

d(0.1): 550.513 um **d(0.5):** 913.294 um **d(0.9):** 1465.595 um

Particle Size Distribution

Volume (%)

Particle Size (µm)

CSFAv, 13 July 2017 11:16:56 AM

Operator notes: *Average of 3 measurements from 13 Julie 2017 (Etanol).mea*

Malvern Instruments Ltd. Malvern, UK Tel :- +[44] (0) 1684-892456 Fax +[44] (0) 1684-892789

Mastersizer 2000 Ver. 5.60 Serial Number : MAL1007548

File name: 13 Julie 2017 (Etanol).mea Record Number: 66 2017/07/21 11:11:41 AM

Figure A.6: Mastersizer analysis report of 1% w/w TMC, 20% w/w micro-beads (Formula F)

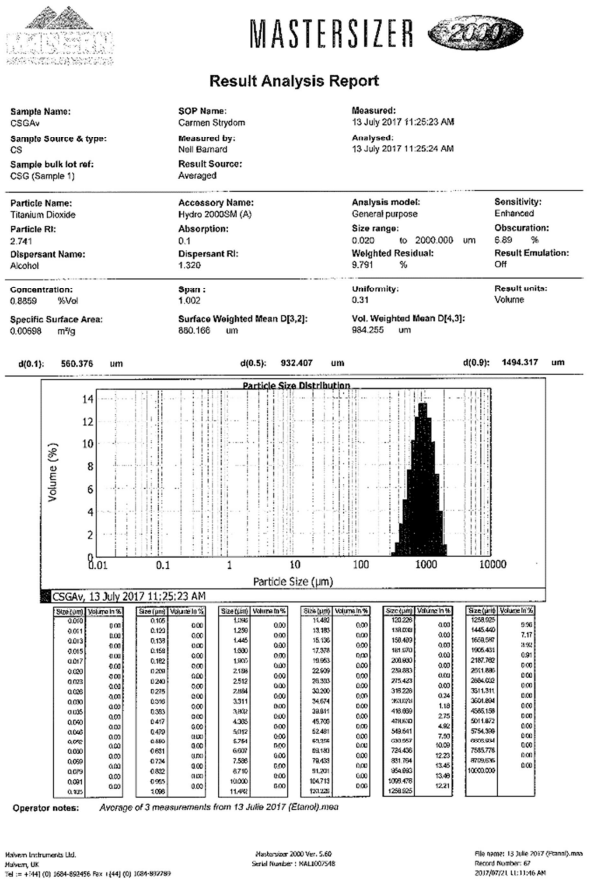

MASTERSIZER 2000

Result Analysis Report

Sample Name: CSGAv	**SOP Name:** Carmen Strydom	**Measured:** 13 July 2017 11:25:23 AM	
Sample Source & type: CS	**Measured by:** Neil Barnard	**Analysed:** 13 July 2017 11:25:24 AM	
Sample bulk lot ref: CSG (Sample 1)	**Result Source:** Averaged		
Particle Name: Titanium Dioxide	**Accessory Name:** Hydro 2000SM (A)	**Analysis model:** General purpose	**Sensitivity:** Enhanced
Particle RI: 2.741	**Absorption:** 0.1	**Size range:** 0.020 to 2000.000 um	**Obscuration:** 6.89 %
Dispersant Name: Alcohol	**Dispersant RI:** 1.320	**Weighted Residual:** 9.791 %	**Result Emulation:** Off
Concentration: 0.8859 %Vol	**Span :** 1.002	**Uniformity:** 0.31	**Result units:** Volume
Specific Surface Area: 0.00698 m²/g	**Surface Weighted Mean D[3,2]:** 860.166 um	**Vol. Weighted Mean D[4,3]:** 984.255 um	

d(0.1): 560.376 um **d(0.5):** 932.407 um **d(0.9):** 1494.317 um

Particle Size Distribution

Volume (%)

Particle Size (µm)

CSGAv, 13 July 2017 11:25:23 AM

Operator notes: *Average of 3 measurements from 13 Julie 2017 (Etanol).mea*

Malvern Instruments Ltd. Malvern, UK Tel := +[44] (0) 1684-892456 Fax :+[44] (0) 1684-892789

Mastersizer 2000 Ver. 5.60 Serial Number : MAL1007548

File name: 13 Julie 2017 (Etanol).mea Record Number: 67 2017/07/21 11:11:46 AM

Figure A.7: Mastersizer analysis report of 0.5% w/w *A. vera* gel, 40% w/w micro-beads (Formula G)

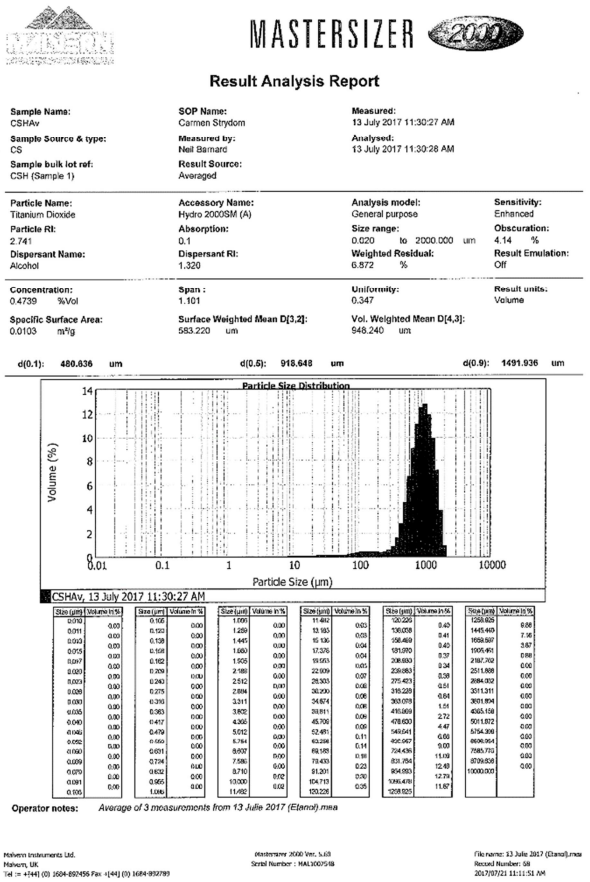

MASTERSIZER 2000

Result Analysis Report

Sample Name: CSHAv	**SOP Name:** Carmen Strydom	**Measured:** 13 July 2017 11:30:27 AM	
Sample Source & type: CS	**Measured by:** Neil Barnard	**Analysed:** 13 July 2017 11:30:28 AM	
Sample bulk lot ref: CSH (Sample 1)	**Result Source:** Averaged		
Particle Name: Titanium Dioxide	**Accessory Name:** Hydro 2000SM (A)	**Analysis model:** General purpose	**Sensitivity:** Enhanced
Particle RI: 2.741	**Absorption:** 0.1	**Size range:** 0.020 to 2000.000 um	**Obscuration:** 4.14 %
Dispersant Name: Alcohol	**Dispersant RI:** 1.320	**Weighted Residual:** 6.872 %	**Result Emulation:** Off
Concentration: 0.4739 %Vol	**Span :** 1.101	**Uniformity:** 0.347	**Result units:** Volume
Specific Surface Area: 0.0103 m²/g	**Surface Weighted Mean D[3,2]:** 583.220 um	**Vol. Weighted Mean D[4,3]:** 946.240 um	

d(0.1): 480.636 um **d(0.5):** 916.648 um **d(0.9):** 1491.936 um

Particle Size Distribution

Volume (%)

Particle Size (µm)

CSHAv, 13 July 2017 11:30:27 AM

Operator notes: *Average of 3 measurements from 13 Julie 2017 (Etanol).mea*

Malvern Instruments Ltd. Malvern, UK Tel := +[44] (0) 1684-892456 Fax :+[44] (0) 1684-892789

Mastersizer 2000 Ver. 5.60 Serial Number : MAL1007548

File name: 13 Julie 2017 (Etanol).mea Record Number: 68 2017/07/21 11:11:51 AM

Figure A.8: Mastersizer analysis report of 1% w/w *A. vera* gel, 40% w/w micro-beads (Formula H)

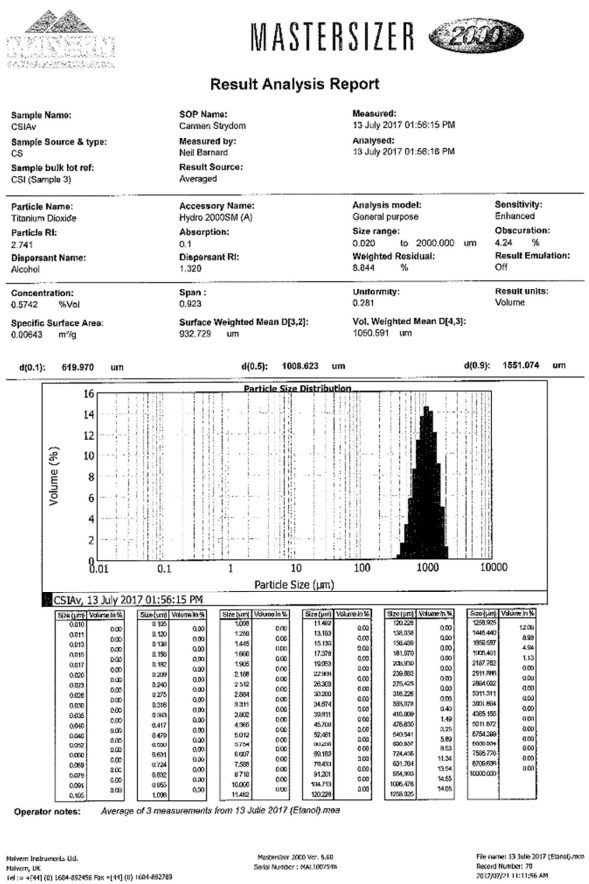

MASTERSIZER 2000

Result Analysis Report

Sample Name: CSIAv	**SOP Name:** Carmen Strydom	**Measured:** 13 July 2017 01:56:15 PM	
Sample Source & type: CS	**Measured by:** Neil Barnard	**Analysed:** 13 July 2017 01:56:16 PM	
Sample bulk lot ref: CSI (Sample 3)	**Result Source:** Averaged		
Particle Name: Titanium Dioxide	**Accessory Name:** Hydro 2000SM (A)	**Analysis model:** General purpose	**Sensitivity:** Enhanced
Particle RI: 2.741	**Absorption:** 0.1	**Size range:** 0.020 to 2000.000 um	**Obscuration:** 4.24 %
Dispersant Name: Alcohol	**Dispersant RI:** 1.320	**Weighted Residual:** 8.844 %	**Result Emulation:** Off
Concentration: 0.5742 %Vol	**Span :** 0.923	**Uniformity:** 0.281	**Result units:** Volume
Specific Surface Area: 0.00643 m²/g	**Surface Weighted Mean D[3,2]:** 932.729 um	**Vol. Weighted Mean D[4,3]:** 1060.591 um	

d(0.1): 619.970 um d(0.5): 1008.623 um d(0.9): 1551.074 um

Particle Size Distribution

CSIAv, 13 July 2017 01:56:15 PM

Size (µm)	Volume In %	Size (µm)	Volume In %	Size (µm)	Volume In %	Size (µm)	Volume In %	Size (µm)	Volume In %	Size (µm)	Volume In %
0.010	0.00	0.105	0.00	1.096	0.00	11.482	0.00	120.228	0.00	1258.925	12.06
0.011	0.00	0.120	0.00	1.259	0.00	13.183	0.00	136.038	0.00	1445.440	8.88
0.013	0.00	0.138	0.00	1.445	0.00	15.136	0.00	156.469	0.00	1658.587	4.56
0.015	0.00	0.158	0.00	1.660	0.00	17.378	0.00	181.970	0.00	1905.461	1.13
0.017	0.00	0.182	0.00	1.905	0.00	19.953	0.00	208.930	0.00	2187.762	0.00
0.020	0.00	0.209	0.00	2.188	0.00	22.909	0.00	239.883	0.00	2511.886	0.00
0.023	0.00	0.240	0.00	2.512	0.00	26.303	0.00	275.423	0.00	2884.032	0.00
0.026	0.00	0.275	0.00	2.884	0.00	30.200	0.00	316.228	0.00	3311.311	0.00
0.030	0.00	0.316	0.00	3.311	0.00	34.674	0.00	363.078	0.00	3801.894	0.00
0.035	0.00	0.363	0.00	3.802	0.00	39.811	0.00	416.869	0.40	4365.158	0.00
0.040	0.00	0.417	0.00	4.365	0.00	45.709	0.00	478.630	1.49	5011.872	0.00
0.046	0.00	0.479	0.00	5.012	0.00	52.481	0.00	549.541	3.25	5754.399	0.00
0.052	0.00	0.550	0.00	5.754	0.00	60.256	0.00	630.957	5.89	6606.934	0.00
0.060	0.00	0.631	0.00	6.607	0.00	69.183	0.00	724.436	9.53	7585.776	0.00
0.069	0.00	0.724	0.00	7.586	0.00	79.433	0.00	831.764	13.54	8709.636	0.00
0.079	0.00	0.832	0.00	8.710	0.00	91.201	0.00	954.993	16.55	10000.000	
0.091	0.00	0.955	0.00	10.000	0.00	104.713	0.00	1096.478	14.65		
0.105	0.00	1.096	0.00	11.482	0.00	120.228	0.00	1258.925	12.06		

Operator notes: *Average of 3 measurements from 13 July 2017 (Etanol).mea*

Malvern Instruments Ltd. Malvern, UK Tel:= +(44) (0) 1684 892456 Fax +(44) (0) 1684 892789

Mastersizer 2000 Ver. 5.60 Serial Number : MAL1007548

File name: 13 July 2017 (Etanol).mea Record Number: 78 2017/07/21 11:11:56 AM

Figure A.9: Mastersizer analysis report of 0.5% w/w sodium deoxycholate, 40% w/w micro-beads (Formula I)

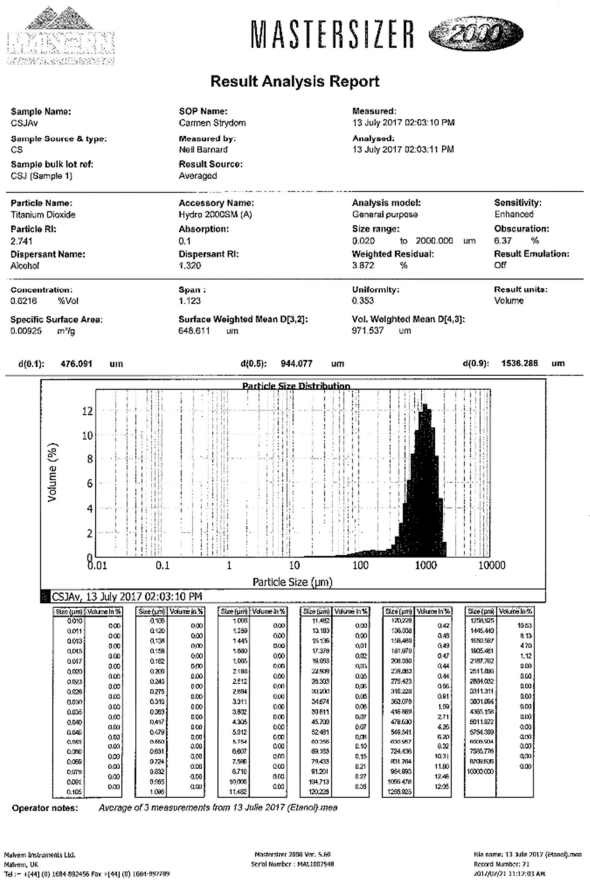

MASTERSIZER 2000

Result Analysis Report

Sample Name: CSJAv	**SOP Name:** Carmen Strydom	**Measured:** 13 July 2017 02:03:10 PM	
Sample Source & type: CS	**Measured by:** Neil Barnard	**Analysed:** 13 July 2017 02:03:11 PM	
Sample bulk lot ref: CSJ (Sample 1)	**Result Source:** Averaged		
Particle Name: Titanium Dioxide	**Accessory Name:** Hydro 2000SM (A)	**Analysis model:** General purpose	**Sensitivity:** Enhanced
Particle RI: 2.741	**Absorption:** 0.1	**Size range:** 0.020 to 2000.000 um	**Obscuration:** 6.37 %
Dispersant Name: Alcohol	**Dispersant RI:** 1.320	**Weighted Residual:** 3.872 %	**Result Emulation:** Off
Concentration: 0.6216 %Vol	**Span :** 1.123	**Uniformity:** 0.353	**Result units:** Volume
Specific Surface Area: 0.00925 m²/g	**Surface Weighted Mean D[3,2]:** 648.611 um	**Vol. Weighted Mean D[4,3]:** 971.537 um	

d(0.1): 476.091 um d(0.5): 944.077 um d(0.9): 1536.288 um

Particle Size Distribution

CSJAv, 13 July 2017 02:03:10 PM

Size (µm)	Volume In %	Size (µm)	Volume In %	Size (µm)	Volume In %	Size (µm)	Volume In %	Size (µm)	Volume In %	Size (µm)	Volume In %
0.010	0.00	0.105	0.00	1.096	0.00	11.482	0.00	120.228	0.42	1258.925	
0.011	0.00	0.120	0.00	1.259	0.00	13.183	0.00	136.038	0.48	1445.440	9.13
0.013	0.00	0.138	0.00	1.445	0.00	15.136	0.01	156.469	0.49	1658.587	4.70
0.015	0.00	0.158	0.00	1.660	0.00	17.378	0.02	181.970	0.47	1905.461	1.12
0.017	0.00	0.182	0.00	1.905	0.00	19.953	0.03	208.930	0.44	2187.762	0.00
0.020	0.00	0.209	0.00	2.188	0.00	22.909	0.05	239.883	0.44	2511.886	0.00
0.023	0.00	0.240	0.00	2.512	0.00	26.303	0.06	275.423	0.56	2884.032	0.00
0.026	0.00	0.275	0.00	2.884	0.00	30.200	0.06	316.228	0.81	3311.311	0.00
0.030	0.00	0.316	0.00	3.311	0.00	34.674	0.06	363.078	1.59	3801.894	0.00
0.035	0.00	0.363	0.00	3.802	0.00	39.811	0.06	416.869	2.71	4365.158	0.00
0.040	0.00	0.417	0.00	4.365	0.00	45.709	0.07	478.630	4.26	5011.872	0.00
0.046	0.00	0.479	0.00	5.012	0.00	52.481	0.08	549.541	6.20	5754.399	0.00
0.052	0.00	0.550	0.00	5.754	0.00	60.256	0.09	630.957	8.32	6606.934	0.00
0.060	0.00	0.631	0.00	6.607	0.00	69.183	0.10	724.436	10.31	7585.776	0.00
0.069	0.00	0.724	0.00	7.586	0.00	79.433	0.15	831.764	11.80	8709.636	0.00
0.079	0.00	0.832	0.00	8.710	0.00	91.201	0.21	954.993	12.46	10000.000	
0.091	0.00	0.955	0.00	10.000	0.00	104.713	0.27	1096.478	12.05		
0.105	0.00	1.096	0.00	11.482	0.00	120.228	0.26	1258.925	12.06		

Operator notes: *Average of 3 measurements from 13 July 2017 (Etanol).mea*

Malvern Instruments Ltd. Malvern, UK Tel:= +(44) (0) 1684 892456 Fax +(44) (0) 1684 892789

Mastersizer 2000 Ver. 5.60 Serial Number : MAL1007548

File name: 13 July 2017 (Etanol).mea Record Number: 71 2017/07/21 11:17:03 AM

Figure A.10: Mastersizer analysis report of 1% w/w sodium deoxycholate, 40% w/w micro-beads (Formula J)

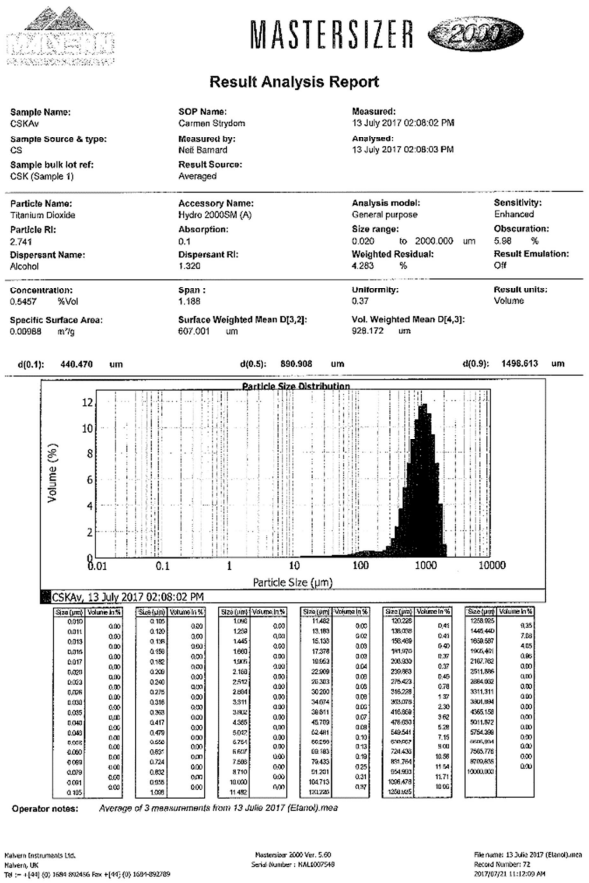

MASTERSIZER 2000

Result Analysis Report

Sample Name: CSKAv	**SOP Name:** Carmen Strydom	**Measured:** 13 July 2017 02:08:02 PM	
Sample Source & type: CS	**Measured by:** Neil Barnard	**Analysed:** 13 July 2017 02:08:03 PM	
Sample bulk lot ref: CSK (Sample 1)	**Result Source:** Averaged		
Particle Name: Titanium Dioxide	**Accessory Name:** Hydro 2000SM (A)	**Analysis model:** General purpose	**Sensitivity:** Enhanced
Particle RI: 2.741	**Absorption:** 0.1	**Size range:** 0.020 to 2000.000 um	**Obscuration:** 5.98 %
Dispersant Name: Alcohol	**Dispersant RI:** 1.320	**Weighted Residual:** 4.283 %	**Result Emulation:** Off
Concentration: 0.5457 %Vol	**Span :** 1.188	**Uniformity:** 0.37	**Result units:** Volume
Specific Surface Area: 0.00988 m²/g	**Surface Weighted Mean D[3,2]:** 607.001 um	**Vol. Weighted Mean D[4,3]:** 928.172 um	

d(0.1): 440.470 um **d(0.5):** 898.908 um **d(0.9):** 1498.613 um

Particle Size Distribution

Volume (%)

Particle Size (µm)

CSKAv, 13 July 2017 02:08:02 PM

Operator notes: *Average of 3 measurements from 13 July 2017 (Etanol).mea*

Malvern Instruments Ltd. Malvern, UK Tel :- +[44] (0) 1684 892456 Fax +[44] (0) 1684 892789

Mastersizer 2000 Ver. 5.60 Serial Number : MAL1007548

File name: 13 July 2017 (Etanol).mea Record Number: 72 2017/07/21 11:12:09 AM

Figure A.11: Mastersizer analysis report of 0.5% w/w TMC, 40% w/w micro-beads (Formula K)

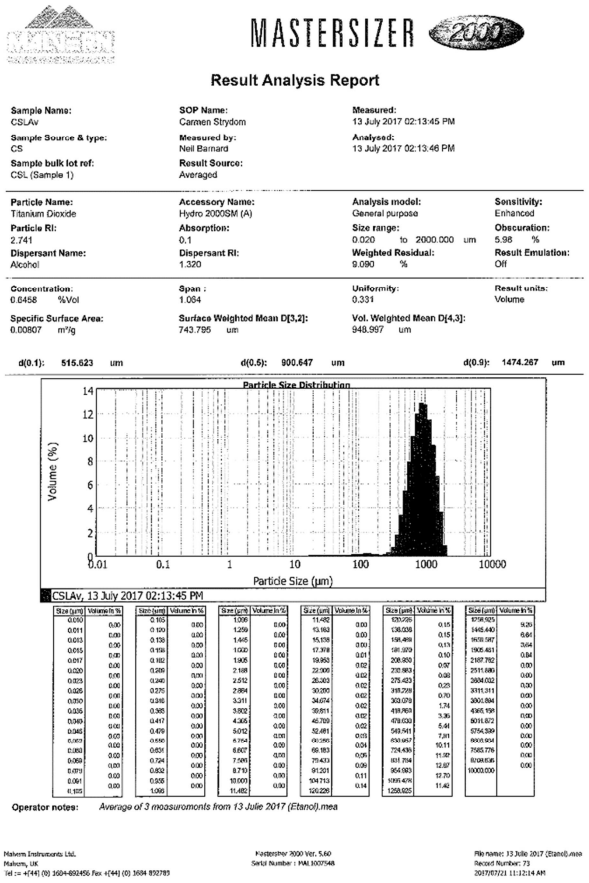

MASTERSIZER 2000

Result Analysis Report

Sample Name: CSLAv	**SOP Name:** Carmen Strydom	**Measured:** 13 July 2017 02:13:45 PM	
Sample Source & type: CS	**Measured by:** Neil Barnard	**Analysed:** 13 July 2017 02:13:46 PM	
Sample bulk lot ref: CSL (Sample 1)	**Result Source:** Averaged		
Particle Name: Titanium Dioxide	**Accessory Name:** Hydro 2000SM (A)	**Analysis model:** General purpose	**Sensitivity:** Enhanced
Particle RI: 2.741	**Absorption:** 0.1	**Size range:** 0.020 to 2000.000 um	**Obscuration:** 5.98 %
Dispersant Name: Alcohol	**Dispersant RI:** 1.320	**Weighted Residual:** 9.090 %	**Result Emulation:** Off
Concentration: 0.6458 %Vol	**Span :** 1.064	**Uniformity:** 0.331	**Result units:** Volume
Specific Surface Area: 0.00807 m²/g	**Surface Weighted Mean D[3,2]:** 743.795 um	**Vol. Weighted Mean D[4,3]:** 948.997 um	

d(0.1): 515.623 um **d(0.5):** 900.647 um **d(0.9):** 1474.267 um

Particle Size Distribution

Volume (%)

Particle Size (µm)

CSLAv, 13 July 2017 02:13:45 PM

Operator notes: *Average of 3 measurements from 13 July 2017 (Etanol).mea*

Malvern Instruments Ltd. Malvern, UK Tel :- +[44] (0) 1684 892456 Fax +[44] (0) 1684 892789

Mastersizer 2000 Ver. 5.60 Serial Number : MAL1007548

File name: 13 July 2017 (Etanol).mea Record Number: 73 2017/07/21 11:12:14 AM

Figure A.12: Mastersizer analysis report of 1% w/w TMC, 40% w/w micro-beads (Formula L)

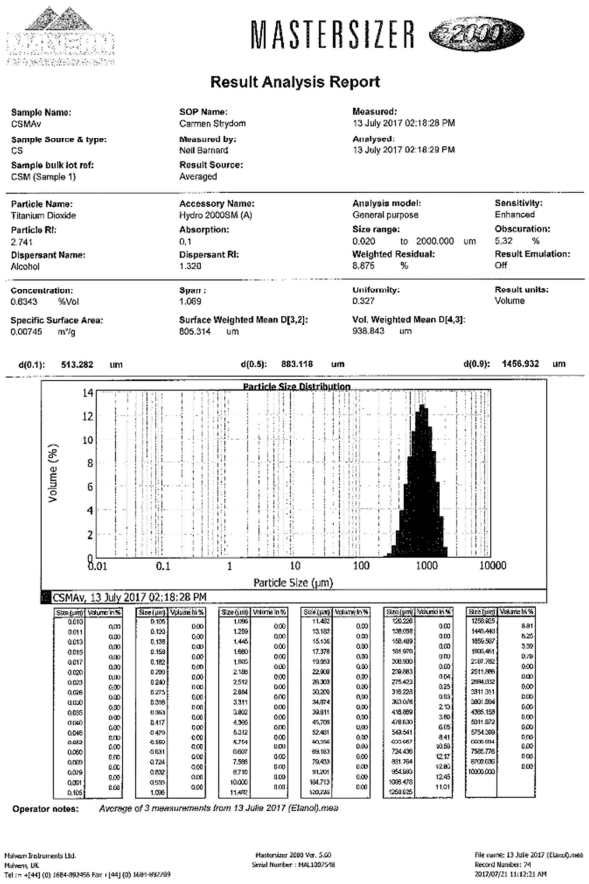

MASTERSIZER 2000

Result Analysis Report

Sample Name: CSMAv	**SOP Name:** Carmen Strydom	**Measured:** 13 July 2017 02:18:28 PM	
Sample Source & type: CS	**Measured by:** Neil Barnard	**Analysed:** 13 July 2017 02:18:29 PM	
Sample bulk lot ref: CSM (Sample 1)	**Result Source:** Averaged		
Particle Name: Titanium Dioxide	**Accessory Name:** Hydro 2000SM (A)	**Analysis model:** General purpose	**Sensitivity:** Enhanced
Particle RI: 2.741	**Absorption:** 0.1	**Size range:** 0.020 to 2000.000 um	**Obscuration:** 5.32 %
Dispersant Name: Alcohol	**Dispersant RI:** 1.320	**Weighted Residual:** 8.875 %	**Result Emulation:** Off
Concentration: 0.6343 %Vol	**Span :** 1.069	**Uniformity:** 0.327	**Result units:** Volume
Specific Surface Area: 0.00745 m²/g	**Surface Weighted Mean D[3,2]:** 805.314 um	**Vol. Weighted Mean D[4,3]:** 938.843 um	

d(0.1): 513.282 um **d(0.5):** 883.118 um **d(0.9):** 1456.932 um

Particle Size Distribution

Volume (%)

Particle Size (µm)

CSMAv, 13 July 2017 02:18:28 PM

Operator notes: *Average of 3 measurements from 13 July 2017 (Etanol).mea*

Malvern Instruments Ltd. Malvern, UK. Tel: +[44] (0) 1684-892456 Fax: +[44] (0) 1684-892789

Mastersizer 2000 Ver. 5.60 Serial Number : MAL1307518

File name: 13 July 2017 (Etanol).mea Record Number: 74 2017/07/21 11:12:21 AM

Figure A.13: Mastersizer analysis report of 0.5% w/w *A. vera* gel, 60% w/w micro-beads (Formula M)

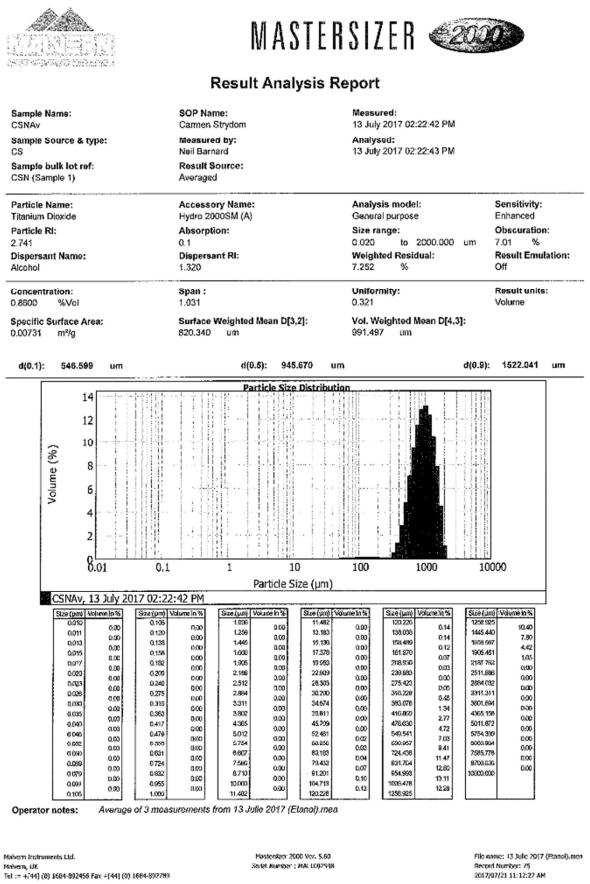

MASTERSIZER 2000

Result Analysis Report

Sample Name: CSNAv	**SOP Name:** Carmen Strydom	**Measured:** 13 July 2017 02:22:42 PM	
Sample Source & type: CS	**Measured by:** Neil Barnard	**Analysed:** 13 July 2017 02:22:43 PM	
Sample bulk lot ref: CSN (Sample 1)	**Result Source:** Averaged		
Particle Name: Titanium Dioxide	**Accessory Name:** Hydro 2000SM (A)	**Analysis model:** General purpose	**Sensitivity:** Enhanced
Particle RI: 2.741	**Absorption:** 0.1	**Size range:** 0.020 to 2000.000 um	**Obscuration:** 7.01 %
Dispersant Name: Alcohol	**Dispersant RI:** 1.320	**Weighted Residual:** 7.252 %	**Result Emulation:** Off
Concentration: 0.8600 %Vol	**Span :** 1.031	**Uniformity:** 0.321	**Result units:** Volume
Specific Surface Area: 0.00731 m²/g	**Surface Weighted Mean D[3,2]:** 820.340 um	**Vol. Weighted Mean D[4,3]:** 991.497 um	

d(0.1): 546.599 um **d(0.5):** 945.670 um **d(0.9):** 1522.041 um

Particle Size Distribution

Volume (%)

Particle Size (µm)

CSNAv, 13 July 2017 02:22:42 PM

Operator notes: *Average of 3 measurements from 13 July 2017 (Etanol).mea*

Malvern Instruments Ltd. Malvern, UK. Tel: +[44] (0) 1684-892456 Fax: +[44] (0) 1684-892789

Mastersizer 2000 Ver. 5.60 Serial Number : MAL1307518

File name: 13 July 2017 (Etanol).mea Record Number: 75 2017/07/21 11:12:27 AM

Figure A.14: Mastersizer analysis report of 1% w/w *A. vera* gel, 60% w/w micro-beads (Formula N)

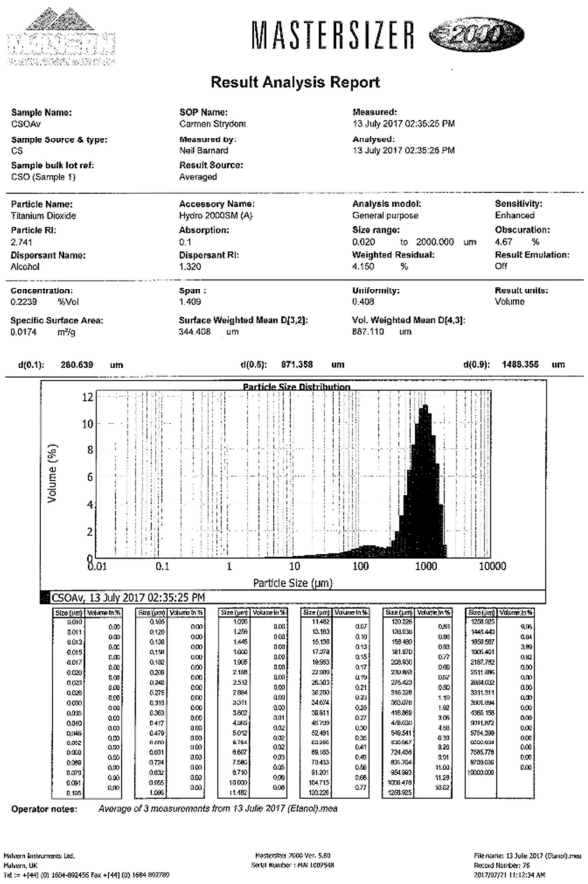

MASTERSIZER 2000

Result Analysis Report

Sample Name: CSOAv	**SOP Name:** Carmen Strydom	**Measured:** 13 July 2017 02:35:25 PM	
Sample Source & type: CS	**Measured by:** Neil Barnard	**Analysed:** 13 July 2017 02:35:26 PM	
Sample bulk lot ref: CSO (Sample 1)	**Result Source:** Averaged		
Particle Name: Titanium Dioxide	**Accessory Name:** Hydro 2000SM (A)	**Analysis model:** General purpose	**Sensitivity:** Enhanced
Particle RI: 2.741	**Absorption:** 0.1	**Size range:** 0.020 to 2000.000 um	**Obscuration:** 4.67 %
Dispersant Name: Alcohol	**Dispersant RI:** 1.320	**Weighted Residual:** 4.150 %	**Result Emulation:** Off
Concentration: 0.2239 %Vol	**Span :** 1.409	**Uniformity:** 0.408	**Result units:** Volume
Specific Surface Area: 0.0174 m²/g	**Surface Weighted Mean D[3,2]:** 344.408 um	**Vol. Weighted Mean D[4,3]:** 887.110 um	

d(0.1): 260.639 um **d(0.5): 871.358 um** **d(0.9): 1488.355 um**

Particle Size Distribution

Volume (%)

Particle Size (µm)

CSOAv, 13 July 2017 02:35:25 PM

Operator notes: *Average of 3 measurements from 13 July 2017 (Etanol).mea*

Malvern Instruments Ltd. Malvern, UK Tel:= +[44] (0) 1684-892456 Fax +[44] (0) 1684 892789

Mastersizer 2000 Ver. 5.60 Serial Number : MAL1007548

File name: 13 July 2017 (Etanol).mea Record Number: 76 2017/07/21 11:12:34 AM

Figure A.15: Mastersizer analysis report of 0.5% w/w sodium deoxycholate, 60% w/w micro-beads (Formula O)

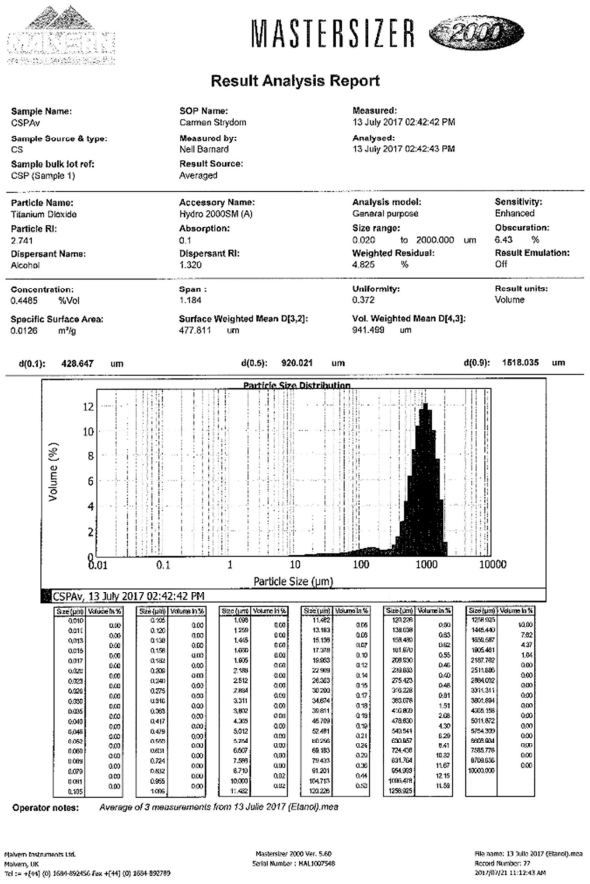

MASTERSIZER 2000

Result Analysis Report

Sample Name: CSPAv	**SOP Name:** Carmen Strydom	**Measured:** 13 July 2017 02:42:42 PM	
Sample Source & type: CS	**Measured by:** Neil Barnard	**Analysed:** 13 July 2017 02:42:43 PM	
Sample bulk lot ref: CSP (Sample 1)	**Result Source:** Averaged		
Particle Name: Titanium Dioxide	**Accessory Name:** Hydro 2000SM (A)	**Analysis model:** General purpose	**Sensitivity:** Enhanced
Particle RI: 2.741	**Absorption:** 0.1	**Size range:** 0.020 to 2000.000 um	**Obscuration:** 6.43 %
Dispersant Name: Alcohol	**Dispersant RI:** 1.320	**Weighted Residual:** 4.825 %	**Result Emulation:** Off
Concentration: 0.4485 %Vol	**Span :** 1.184	**Uniformity:** 0.372	**Result units:** Volume
Specific Surface Area: 0.0126 m²/g	**Surface Weighted Mean D[3,2]:** 477.611 um	**Vol. Weighted Mean D[4,3]:** 941.469 um	

d(0.1): 428.647 um **d(0.5): 920.021 um** **d(0.9): 1518.035 um**

Particle Size Distribution

Volume (%)

Particle Size (µm)

CSPAv, 13 July 2017 02:42:42 PM

Operator notes: *Average of 3 measurements from 13 July 2017 (Etanol).mea*

Malvern Instruments Ltd. Malvern, UK Tel:= +[44] (0) 1684-892456 Fax +[44] (0) 1684 892789

Mastersizer 2000 Ver. 5.60 Serial Number : MAL1007548

File name: 13 July 2017 (Etanol).mea Record Number: 77 2017/07/21 11:12:43 AM

Figure A.16: Mastersizer analysis report of 1% w/w sodium deoxycholate, 60% w/w micro-beads (Formula P)

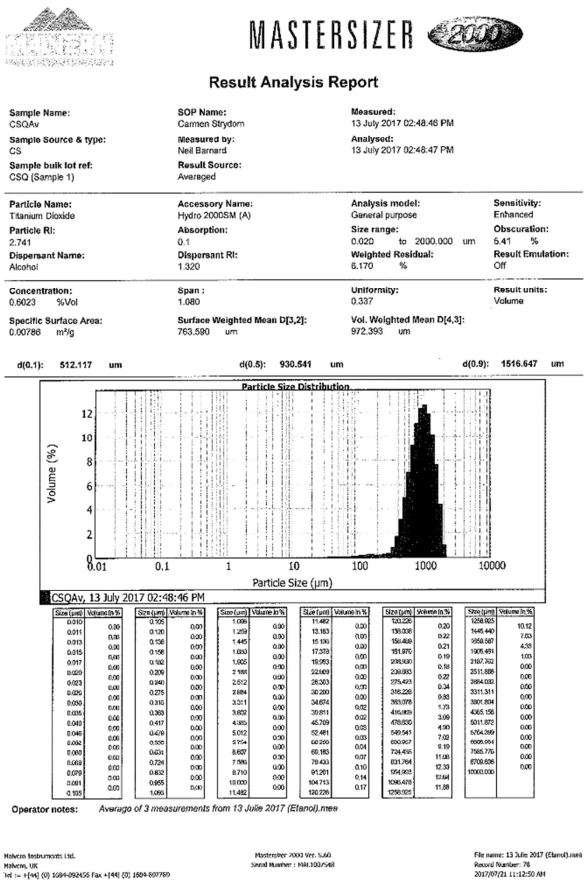

MASTERSIZER 2000

Result Analysis Report

Sample Name: CSQAv	**SOP Name:** Carmen Strydom	**Measured:** 13 July 2017 02:48:46 PM	
Sample Source & type: CS	**Measured by:** Neil Barnard	**Analysed:** 13 July 2017 02:48:47 PM	
Sample bulk lot ref: CSQ (Sample 1)	**Result Source:** Averaged		
Particle Name: Titanium Dioxide	**Accessory Name:** Hydro 2000SM (A)	**Analysis model:** General purpose	**Sensitivity:** Enhanced
Particle RI: 2.741	**Absorption:** 0.1	**Size range:** 0.020 to 2000.000 um	**Obscuration:** 5.41 %
Dispersant Name: Alcohol	**Dispersant RI:** 1.320	**Weighted Residual:** 6.170 %	**Result Emulation:** Off
Concentration: 0.6023 %Vol	**Span :** 1.080	**Uniformity:** 0.337	**Result units:** Volume
Specific Surface Area: 0.00788 m²/g	**Surface Weighted Mean D[3,2]:** 763.590 um	**Vol. Weighted Mean D[4,3]:** 972.393 um	

d(0.1): 512.117 um **d(0.5):** 930.541 um **d(0.9):** 1516.647 um

Particle Size Distribution

Volume (%)

Particle Size (µm)

CSQAv, 13 July 2017 02:48:46 PM

Size (µm)	Volume In %	Size (µm)	Volume In %	Size (µm)	Volume In %	Size (µm)	Volume In %	Size (µm)	Volume In %	Size (µm)	Volume In %
0.010	0.00	0.105	0.00	1.096	0.00	11.482	0.00	120.226	0.20	1258.925	0.00
0.011	0.00	0.120	0.00	1.259	0.00	13.183	0.00	138.038	0.22	1445.440	10.12
0.013	0.00	0.138	0.00	1.445	0.00	15.136	0.00	158.489	0.22	1659.587	7.63
0.015	0.00	0.158	0.00	1.660	0.00	17.378	0.00	181.970	0.21	1905.461	4.33
0.017	0.00	0.182	0.00	1.905	0.00	19.953	0.00	208.930	0.19	2187.762	1.03
0.020	0.00	0.209	0.00	2.188	0.00	22.909	0.00	239.883	0.18	2511.886	0.00
0.023	0.00	0.240	0.00	2.512	0.00	26.303	0.00	275.423	0.34	2884.032	0.00
0.026	0.00	0.275	0.00	2.884	0.00	30.200	0.00	316.228	0.83	3311.311	0.00
0.030	0.00	0.316	0.00	3.311	0.00	34.674	0.00	363.078	1.73	3801.894	0.00
0.035	0.00	0.363	0.00	3.802	0.00	39.811	0.02	416.869	3.09	4365.158	0.00
0.040	0.00	0.417	0.00	4.365	0.00	45.709	0.05	478.630	4.90	5011.872	0.00
0.046	0.00	0.479	0.00	5.012	0.00	52.481	0.03	549.541	6.39	5754.399	0.00
0.052	0.00	0.550	0.00	5.754	0.00	60.256	0.04	630.957	7.02	6606.934	0.00
0.060	0.00	0.631	0.00	6.607	0.00	69.183	0.07	724.436	6.19	7585.776	0.00
0.069	0.00	0.724	0.00	7.586	0.00	79.433	0.10	831.764	11.08	8709.636	0.00
0.079	0.00	0.832	0.00	8.710	0.00	91.201	0.14	954.993	12.33	10000.000	
0.091	0.00	0.955	0.00	10.000	0.00	104.713	0.17	1096.478	12.64		
0.105	0.00	1.096	0.00	11.482	0.00	120.226	0.17	1258.925	11.08		

Operator notes: *Average of 3 measurements from 13 July 2017 (Etanol).mea*

Malvern Instruments Ltd.
Malvern, UK
Tel :+ +[44] (0) 1684-892455 Fax +[44] (0) 1684-892789

Mastersizer 2000 Ver. 5.60
Serial Number : MAL1007548

File name: 13 July 2017 (Etanol).mea
Record Number: 76
2017/07/21 11:12:50 AM

Figure A.17: Mastersizer analysis report of 0.5% w/w TMC, 60% w/w micro-beads (Formula Q)

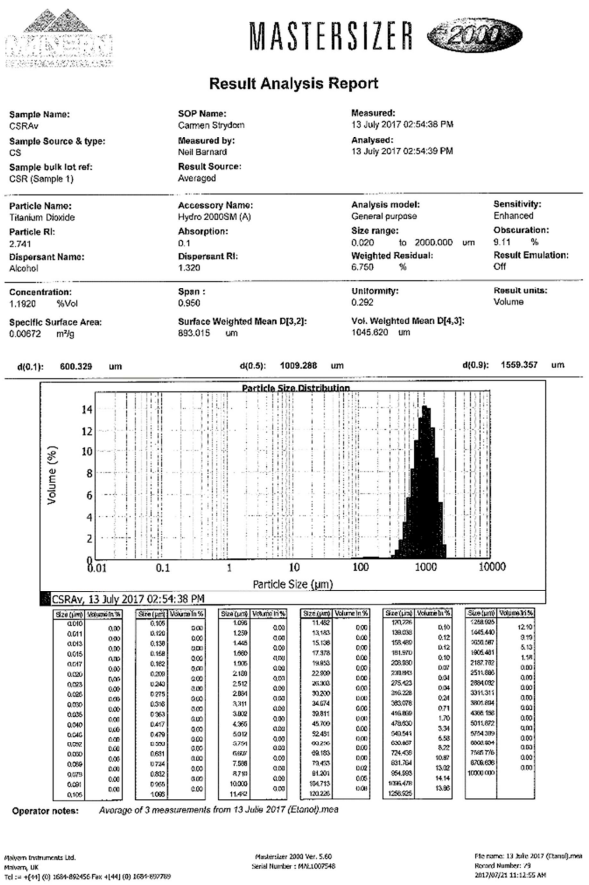

MASTERSIZER 2000

Result Analysis Report

Sample Name: CSRAv	**SOP Name:** Carmen Strydom	**Measured:** 13 July 2017 02:54:38 PM	
Sample Source & type: CS	**Measured by:** Neil Barnard	**Analysed:** 13 July 2017 02:54:39 PM	
Sample bulk lot ref: CSR (Sample 1)	**Result Source:** Averaged		
Particle Name: Titanium Dioxide	**Accessory Name:** Hydro 2000SM (A)	**Analysis model:** General purpose	**Sensitivity:** Enhanced
Particle RI: 2.741	**Absorption:** 0.1	**Size range:** 0.020 to 2000.000 um	**Obscuration:** 9.11 %
Dispersant Name: Alcohol	**Dispersant RI:** 1.320	**Weighted Residual:** 6.750 %	**Result Emulation:** Off
Concentration: 1.1920 %Vol	**Span :** 0.950	**Uniformity:** 0.292	**Result units:** Volume
Specific Surface Area: 0.00572 m²/g	**Surface Weighted Mean D[3,2]:** 893.015 um	**Vol. Weighted Mean D[4,3]:** 1045.620 um	

d(0.1): 600.329 um **d(0.5):** 1009.288 um **d(0.9):** 1559.357 um

Particle Size Distribution

Volume (%)

Particle Size (µm)

CSRAv, 13 July 2017 02:54:38 PM

Size (µm)	Volume In %	Size (µm)	Volume In %	Size (µm)	Volume In %	Size (µm)	Volume In %	Size (µm)	Volume In %	Size (µm)	Volume In %
0.010	0.00	0.105	0.00	1.096	0.00	11.482	0.00	120.226	0.10	1258.925	12.10
0.011	0.00	0.120	0.00	1.259	0.00	13.183	0.00	138.038	0.12	1445.440	9.15
0.013	0.00	0.138	0.00	1.445	0.00	15.136	0.00	158.489	0.12	1659.587	5.13
0.015	0.00	0.158	0.00	1.660	0.00	17.378	0.00	181.970	0.10	1905.461	1.58
0.017	0.00	0.182	0.00	1.905	0.00	19.953	0.00	208.930	0.07	2187.762	0.00
0.020	0.00	0.209	0.00	2.188	0.00	22.909	0.00	239.883	0.04	2511.886	0.00
0.023	0.00	0.240	0.00	2.512	0.00	26.303	0.00	275.423	0.04	2884.032	0.00
0.026	0.00	0.275	0.00	2.884	0.00	30.200	0.00	316.228	0.24	3311.311	0.00
0.030	0.00	0.316	0.00	3.311	0.00	34.674	0.00	363.078	0.68	3801.894	0.00
0.035	0.00	0.363	0.00	3.802	0.00	39.811	0.00	416.869	0.71	4365.158	0.00
0.040	0.00	0.417	0.00	4.365	0.00	45.709	0.00	478.630	1.70	5011.872	0.00
0.046	0.00	0.479	0.00	5.012	0.00	52.481	0.00	549.541	3.34	5754.399	0.00
0.052	0.00	0.550	0.00	5.754	0.00	60.256	0.00	630.957	5.58	6606.934	0.00
0.060	0.00	0.631	0.00	6.607	0.00	69.183	0.00	724.436	8.22	7585.776	0.00
0.069	0.00	0.724	0.00	7.586	0.00	79.433	0.02	831.764	10.87	8709.636	0.00
0.079	0.00	0.832	0.00	8.710	0.00	91.201	0.05	954.993	13.02	10000.000	
0.091	0.00	0.955	0.00	10.000	0.00	104.713	0.05	1096.478	14.14		
0.105	0.00	1.096	0.00	11.482	0.00	120.226	0.00	1258.925	13.80		

Operator notes: *Average of 3 measurements from 13 July 2017 (Etanol).mea*

Malvern Instruments Ltd.
Malvern, UK
Tel :+ +[44] (0) 1684-892456 Fax +[44] (0) 1684-892789

Mastersizer 2000 Ver. 5.60
Serial Number : MAL1007548

File name: 13 July 2017 (Etanol).mea
Record Number: 79
2017/07/21 11:12:55 AM

Figure A.188: Mastersizer analysis report of 1% TMC, 60% micro-beads (Formula R)

ADDENDUM B: DISSOLUTION DATA

Table B.1: Dissolution data of insulin of 0.5% w/w *A. vera* gel, 20% w/w micro-beads (Formulation A)

Time (min)	Average Peak Area			Corrected Average Peak Area			Average Concentration (ug/ml)			Dissolution (%)			Average Dissolution (%)	Standard deviation	% RSD
	SAMPLE 1	SAMPLE 2	SAMPLE 3	SAMPLE 1	SAMPLE 2	SAMPLE 3	SAMPLE 1	SAMPLE 2	SAMPLE 3	SAMPLE 1	SAMPLE 2	SAMPLE 3			
0	0.00	0.00	0.00	0.00	0.00	0.00	0.00	0.00	0.00	0.00	0.00	0.00	0.00	0.00	0.00
120	12.70	12.85	12.85	12.70	12.85	12.85	0.16	0.16	0.16	5.14	4.86	4.79	4.93	0.19	3.76
130	36.80	32.70	31.55	36.83	32.73	31.58	0.47	0.42	0.40	14.91	12.37	11.78	13.02	1.66	12.77
137	57.65	58.05	59.95	57.76	58.15	60.05	0.74	0.74	0.77	23.38	21.97	22.41	22.59	0.72	3.20
146	152.50	156.45	148.90	152.74	156.68	149.13	1.95	2.00	1.91	61.83	59.20	55.64	58.89	3.11	5.27
155	167.55	181.75	181.20	168.13	182.33	181.76	2.15	2.33	2.33	68.06	68.89	67.82	68.26	0.56	0.82
185	190.40	202.80	200.90	191.35	203.78	201.87	2.45	2.61	2.58	77.46	77.00	75.32	76.59	1.13	1.47
215	196.00	213.15	204.58	197.38	214.59	205.99	2.53	2.75	2.64	79.90	81.08	76.86	79.28	2.18	2.75
245	224.55	265.25	262.85	226.37	267.16	264.72	2.90	3.42	3.39	91.64	100.95	98.77	97.12	4.87	5.01
260	244.70	262.15	265.55	247.02	264.66	268.01	3.16	3.39	3.43	100.00	100.00	100.00	100.00	0.00	0.00